

SIBYLLE DUERI

**ÉVALUATION DE L'EFFICACITÉ D'UNE COUCHE  
DE RECOUVREMENT PAR MODÉLISATION  
NUMÉRIQUE: APPLICATION AU CAS DU FJORD  
DU SAGUENAY**

Thèse  
présentée  
à la Faculté des études supérieures  
de l'Université Laval  
pour l'obtention  
du grade de Philosophiae Doctor (Ph.D.)

Département de géologie et génie géologique  
FACULTÉ DE SCIENCES ET GÉNIE  
UNIVERSITÉ LAVAL  
QUÉBEC

JUIN 2003

## RÉSUMÉ

Suite au délugé qui a marqué la région du Saguenay en 1996, une couche de nouveaux sédiments a recouvert les sédiments du secteur amont du fjord du Saguenay. Avant le délugé cette zone était caractérisée par la présence de sédiments contaminés, associés au déversement incontrôlé d'effluents liquides, pratiqué dans le passé par les industries de la région. La couche de sédiments déposés en 1996 a enfoui les sédiments contaminés et constitue donc une barrière isolante composée de matériaux plus propres.

Afin d'estimer l'efficacité à long terme de la couche, un nouveau modèle numérique (TRANSCAP-1D) a été développé. Ce modèle simule la migration de composantes dissoutes dans une colonne de sédiments et considère l'advection, la diffusion/dispersion, et l'effet de la bio-irrigation. La formulation mathématique représente un milieu à double porosité, composé de pores et de trous ou tubes de vers.

Le modèle a été calé avec les profils de concentration de l'arsenic dissous qui ont été mesurés à deux stations du fjord du Saguenay, après la déposition de la couche de recouvrement naturelle. Par la suite, une analyse de sensibilité a été réalisée afin d'évaluer l'impact de certains paramètres caractérisés par une variabilité ou incertitude importante aux sites à l'étude. Les résultats montrent que les paramètres associés à la bio-irrigation ont un impact significatif sur la migration des contaminants dissous vers la colonne d'eau.

Par la suite, nous avons réalisé une analyse d'incertitude en utilisant la méthode Monte Carlo et les résultats ont été intégrés dans une analyse de décision pour le design d'une couche de recouvrement potentielle. Le cas présenté est hypothétique et concerne la réhabilitation d'un site contaminé qui est fréquenté régulièrement par la population de bélugas du Saint Laurent. L'exemple illustre les avantages de l'application de l'analyse de décision pour trouver l'alternative correspondante au coût total plus bas, en considérant les coûts et les risques d'échec associés au projet de réhabilitation.

## ABSTRACT

In 1996 two days of intense rainfalls caused severe flooding in the Saguenay region and a new sediment layer was deposited on the upstream area of the Saguenay fjord. In the past, this area was exposed to the uncontrolled discharge of industrial effluents and the sediments were contaminated. The new sediment layer buried the contaminated sediments and constitutes a natural barrier of cleaner material, which isolates the contaminants from the water column.

A new numerical model (TRANSCAP-1D) was developed in order to estimate the effectiveness of the natural barrier in isolating the contaminated sediments from the overlying water column. The model simulates the migration of dissolved compounds in a sediment column and includes advection, diffusion/dispersion and the effect of bio-irrigation. The mathematical formulation represents a double porosity medium, composed of sediment pores and tubes or burrows dug by worms.

The model was calibrated using the concentration profiles of dissolved arsenic measured at two stations of the Saguenay fjord, after the capping event. Thereafter, a sensitivity analysis was performed in order to evaluate the impact of certain parameters showing a great variability and uncertainty at the studied sites. The results indicate that the parameters associated to bio-irrigation have a significant impact on the migration of dissolved contaminants towards the water column.

Thereafter, we performed an uncertainty analysis, using the Monte Carlo method. The results were integrated in a decision analysis for the design of a capping layer in a hypothetical case of sediment remediation. The presented case considers a contaminated site regularly frequented by the beluga population of the St. Lawrence Estuary. The example illustrates the advantages of the application of the decision analysis method, which is used to find the least cost option, considering the costs and failure risks associated to the remediation project.

## AVANT-PROPOS

Trois des quatre chapitres de cette thèse ont été ou seront soumis prochainement pour publication dans des revues scientifiques. Les articles vont paraître sous le titre:

*Chapitre 2:*

**Dueri, S.**, Therrien, R. et Locat, J. Numerical modeling of the migration of dissolved contaminants through a subaqueous capping layer.

*Chapitre 3:*

**Dueri, S.** et Therrien, R. Factors controlling contaminant transport through the flood sediments of the Saguenay Fjord: numerical sensitivity analysis.

*Chapitre 4:*

**Dueri, S.**, Therrien, R. et Locat, J. Decision analysis: Application to the design of a subaqueous capping layer.

Le premier article a été accepté pour publication dans la Revue du Génie et de la Science de l'Environnement. L'article présente un nouveau modèle numérique (TRANSCAP-1D) et son calage. Les travaux de modélisation et de rédaction ont été réalisés par S. Dueri sous la supervision de R. Therrien et les corrections de J. Locat. Les données utilisées pour le calage ont été acquises lors des nombreuses missions en mer du Projet Saguenay Post Déluge par différents groupes de recherches de l'université Laval, de l'université McGill et de l'université du Québec à Rimouski. Les travaux de terrain et de laboratoire ont été accomplis par les étudiants, les stagiaires et les techniciens des trois universités, sous la supervision de J. Locat, professeur au département de géologie et génie géologique de l'université Laval, R. Galvez-Cloutier, professeure au département de génie civil de l'université Laval, S. Leroueil, professeur au département de génie civil de l'université Laval, A. Mucci, professeur au département des Sciences de la Terre et des planètes de l'université McGill et G. Desrosiers, professeur à l'institut des sciences de la

mer de l'université du Québec à Rimouski. Lors des missions en mer les sédiments ont été échantillonnés avec l'aide très précieuse de l'équipage de l'Alcide C. Horth.

Le deuxième article présente une analyse de sensibilité réalisée avec le modèle numérique TRANSCAP-1D. Cet article a été accepté pour publication dans "*Contaminated Sediments: Characterization, Evaluation, Mitigation/Restoration, and Management Strategy Performance, ASTM STP 1442, J. Locat, R. Galvez-Cloutier, R.C. Chaney, and K. Demars, Eds., ASTM International, West Conshohocken, PA, 2003*", un recueil d'articles, publié par l'ASTM suite au deuxième symposium international sur les sédiments contaminés. L'analyse de sensibilité ainsi que la rédaction ont été réalisés par S. Dueri sous la supervision de R. Therrien.

Le troisième article présente les résultats d'une analyse d'incertitude et l'application de l'analyse de décision pour le design d'une couche de recouvrement. Cet article n'a pas encore été soumis. L'analyse d'incertitude, l'analyse de décision et la rédaction ont été réalisés par S. Dueri sous la supervision de R. Therrien et avec les corrections de J. Locat.

Je tiens à remercier particulièrement mon directeur de thèse René Therrien pour ses précieux conseils, sa disponibilité et pour m'avoir toujours encouragé et aidé dans mes recherches. Je voudrais remercier également mon codirecteur Jacques Locat, pour son soutien et pour m'avoir donné l'opportunité de travailler dans un projet d'une grande envergure, tel le Projet Saguenay Post-Déluge. Un gros merci aussi à Rosa Galvez-Cloutier, René Lefebvre et Pierre Gelinas pour leurs commentaires qui ont considérablement amélioré la qualité de la thèse.

Je voudrais aussi remercier mes collègues et amis à l'Université Laval. J'ai vraiment apprécié le travail à l'intérieur d'une équipe aussi dynamique que celle du Projet Saguenay Post-Déluge, ainsi que les échanges avec des personnes externes au projet, qui m'ont apporté des nouvelles idées et perspectives. Grâce à vous les années passées à l'Université Laval ont été très riches, autant d'un côté scientifique que d'un côté humain.

Un gros merci à mes parents pour leur soutien et pour m'avoir transmis la confiance dans mes moyens et dans la vie qui est fort utile pour aboutir un projet à long terme tel un doctorat. Je remercie également mes amis à l'extérieur de l'Université Laval ainsi que ma famille, pour leur support dans les périodes difficiles et pour avoir partagé avec moi les beaux moments de mes années au Québec.

Enfin je voudrais remercier sincèrement le Conseil Canadien de Recherche en Science Naturelle et en Génie (CRSNG), le Fonds pour la Formation de Chercheurs et l'Aide à la Recherche (FCAR) et Alcan (Canada Ltd) pour leur support financier, sans lequel le projet n'aurait pas vu le jour.

# TABLE DES MATIÈRES

RÉSUMÉ .....	I
ABSTRACT .....	II
AVANT-PROPOS .....	III
INTRODUCTION .....	1
<b>CHAPITRE 1 HISTORIQUE DE LA CONTAMINATION DU FJORD ET PROPRIÉTÉS DES SÉDIMENTS .....</b>	<b>5</b>
1.1 CONTAMINATION DES SÉDIMENTS DU FJORD DU SAGUENAY.....	6
1.2 PROPRIÉTÉS DES SÉDIMENTS CONTAMINÉS .....	8
1.2.1 <i>Granulométrie et minéralogie</i> .....	8
1.2.2 <i>Propriétés géotechniques</i> .....	8
1.2.3 <i>Géochimie des sédiments et des contaminants</i> .....	9
1.3 PROPRIÉTÉS DES SÉDIMENTS DILUVIENS .....	9
1.3.1 <i>Granulométrie et minéralogie</i> .....	10
1.3.2 <i>Géochimie des sédiments</i> .....	10
1.4 CONSOLIDATION ET ADVECTION SUITE AU DÉLUGE .....	11
1.4.1 <i>Consolidation de la couche contaminée</i> .....	14
1.4.2 <i>Consolidation de la couche de turbidite</i> .....	14
<b>CHAPITRE 2 SIMULATION OF THE MIGRATION OF DISSOLVED CONTAMINANTS THROUGH A SUBAQUEOUS CAPPING LAYER: MODEL DEVELOPMENT AND APPLICATION FOR ARSENIC MIGRATION .....</b>	<b>16</b>
RÉSUMÉ .....	17
ABSTRACT .....	17
2.1 INTRODUCTION .....	18
2.2 MATHEMATICAL FORMULATION AND NUMERICAL SOLUTION .....	22
2.3 VERIFICATION.....	25
2.4 APPLICATION OF THE MODEL TO THE FLOOD SEDIMENTS OF THE SAGUENAY FJORD.....	27
2.4.1 <i>Input parameters for the numerical model</i> .....	31
2.4.2 <i>Simulations</i> .....	36
2.5 EFFECT OF VARIABLE INPUT PARAMETERS ON THE RESPONSE OF THE MODEL .....	39
2.6 SUMMARY AND CONCLUSION.....	45

2.7 REFERENCES .....	47
<b>CHAPITRE 3 FACTORS CONTROLLING CONTAMINANT TRANSPORT THROUGH THE FLOOD SEDIMENTS OF THE SAGUENAY FJORD: NUMERICAL SENSITIVITY ANALYSIS</b>	
RÉSUMÉ .....	54
ABSTRACT.....	54
3.1 INTRODUCTION .....	55
3.2 MODEL EQUATIONS AND PARAMETERS.....	57
3.3 DESIGN OF THE SENSITIVITY ANALYSIS.....	61
3.4 RESULTS .....	65
3.4.1 <i>Total mass released from the sediment to the water column after 10 years</i> .....	67
3.4.2 <i>Final concentration at the top of the sediment column after 10 years</i> .....	70
3.5 CONCLUSIONS.....	74
3.6 REFERENCES .....	74
<b>CHAPITRE 4 DECISION ANALYSIS: APPLICATION TO THE DESIGN OF A SUBAQUEOUS CAPPING LAYER.....</b>	
RÉSUMÉ .....	78
ABSTRACT.....	78
4.1 INTRODUCTION .....	80
4.2 DECISION ANALYSIS METHOD .....	85
4.3 SITE DESCRIPTION .....	87
4.4 COST ESTIMATES .....	89
4.5 NUMERICAL MODEL .....	91
4.6 UNCERTAINTY ANALYSIS.....	94
4.6.1 <i>Input distributions</i> .....	95
4.6.2 <i>Shape, stability and accuracy of the output distribution</i> .....	98
4.7 MOBILITY OF LOW SOLUBILITY CONTAMINANT .....	100
4.8 RESULTS OF THE DECISION ANALYSIS .....	101
4.8.1 <i>Trace metals</i> .....	102
4.8.2 <i>Organic contaminants</i> .....	104
4.8.3 <i>Evaluation of the influence of the cost of failure</i> .....	105
4.9 DISCUSSION AND CONCLUSION.....	106
4.10 REFERENCES .....	107
<b>CONCLUSION .....</b>	<b>113</b>

# LISTE DES TABLEAUX

TABLE 1.1: <i>CHARACTÉRISTIQUES PHYSIQUES DÉTERMINÉS EN LABORATOIRE.</i>	13
TABLE 2.1: <i>INPUT PARAMETERS FOR THE SEMI-ANALYTICAL SOLUTION OF NEVILLE ET AL. (2000).</i>	26
TABLE 2.2: <i>COEFFICIENTS FOR THE DISSOLUTION TERM, DERIVED FROM CONCENTRATIONS OF DISSOLVED AS AND SOLID FES MEASURED IN THE SAGUENAY FJORD.....</i>	33
TABLE 2.3: <i>BIO-IRRIGATION PARAMETERS FOUND IN THE LITERATURE FOR SEDIMENTS BIOTURBATED BY POLYCHAETES AND OLIGOCHAETES WORMS.....</i>	35
TABLE 2.4: <i>INPUT PARAMETERS OF THE NUMERICAL MODEL.</i>	37
TABLE 2.5: <i>SPECIFIC CHARACTERISTICS OF THE SIMULATIONS AND TOTAL MASS OF CONTAMINANT RELEASED FROM THE UPPER BOUNDARY OF THE SYSTEM 5 YEARS AFTER THE CAPPING EVENT.</i>	40
TABLE 3.1: <i>MINIMUM AND MAXIMUM VALUES FOR THE TESTED FACTORS.....</i>	62
TABLE 3.2: <i>DESCRIPTION OF THE SERIES OF SIMULATIONS FOR THE SENSITIVITY ANALYSIS .....</i>	65
TABLE 3.3: <i>SIMULATION PROTOCOL FOR THE FACTORIAL DESIGN OF FOUR TESTED FACTORS: VARIABLE INPUT VALUES USED FOR A SET OF 16 SIMULATIONS .....</i>	66
TABLE 3.4: <i>SUMS OF SQUARES FOR A REACTIVE COMPOUND MIGRATING THROUGH A CAP OF 0.2 M (SERIES 1, ILLUSTRATED IN FIGURE 3.1) AND A CAP OF 0.1 M (SERIES 2, NOT ILLUSTRATED).</i>	68
TABLE 3.5: <i>REVIEW OF THE FACTORS HAVING A SIGNIFICANT EFFECT ON THE OUTPUT OF THE MODEL .....</i>	73
TABLE 4.1: <i>COSTS OF COMPONENTS USED FOR THE CAPPING MANAGEMENT OPTIONS (IN \$ CAD).</i>	90
TABLE 4.2: <i>CAPPING OPTIONS AND CONSTRUCTION COST TO CAP AN AREA OF 4 KM<sup>2</sup>.</i>	91
TABLE 4.3: <i>INPUT PARAMETERS OF THE NUMERICAL MODEL.</i>	93
TABLE 4.4: <i>DEFINITION OF UNIFORM AND NORMAL PDFS DESCRIBING THE VARIABLE PARAMETERS.</i>	96

# LISTE DES FIGURES

FIGURE I.1: SCHÉMA GÉNÉRAL DU SYSTÈME À L'ÉTUDE .....	2
FIGURE 1.1 : PROFIL DE CONTAMINATION DES SÉDIMENTS DU FJORD, À LA JONCTION DE LA BAIE DES HA! HA! ET DU BRAS NORD, AVANT LE RECOUVREMENT DE 1996 (D'APRÈS GAGNON ET AL. 1993). .....	7
FIGURE 1.2: CONSOLIDATION SUITE À LA DÉPOSITION RAPIDE D'UNE NOUVELLE COUCHE DE SÉDIMENTS. ....	12
FIGURE 1.3: MONTAGE DE L'ESSAI OEDOMÉTRIQUE AVEC MESURE DE LA PERMÉABILITÉ. ....	13
FIGURE 2.1: SCHEMATIC DIAGRAM ILLUSTRATING THE SIMPLIFIED GEOMETRY OF A TUBE/BURROW AND THE BIO-IRRIGATED LAYER, APPROXIMATED BY PACKED CYLINDERS, AFTER ALLER (1980). ( $R_1$ = INNER RADIUS OF CYLINDERS, $R_2$ = HALF DISTANCE BETWEEN TWO CYLINDERS, $A$ = DISTANCE TO THE POINT WHERE THE CONCENTRATION IN THE SEDIMENTS EQUALS THE HORIZONTALLY INTEGRATED VALUE) .....	21
FIGURE 2.2: DIAGRAM REPRESENTING THE SEDIMENT COLUMN, THE MAIN TRANSPORT PROCESSES IN THE DUAL POROSITY SYSTEM (SEDIMENT PORES AND TUBES), THE INITIAL CONCENTRATION AND THE VARIATION OF TUBE POROSITY WITH DEPTH. ....	23
FIGURE 2.3: VERIFICATION OF THE MODEL RESULTS WITH THE SEMI-ANALYTICAL SOLUTION OF NEVILLE ET AL. (2000).....	27
FIGURE 2.4: MAP OF THE SAGUENAY FJORD SHOWING THE TWO STATIONS THAT WERE USED TO TEST THE MODEL. ....	28
FIGURE 2.5: REMOBILIZATION OF AS AFTER OXIDATION OF FES AROUND THE TUBE WALLS. ....	30
FIGURE 2.6 (A) AND (B): RESPONSE OF THE NUMERICAL MODEL FOR A SIMULATION TIME OF 2 YEARS (DASHED LINE) COMPARED TO THE CONCENTRATIONS MEASURED IN 1998 (SYMBOLS) AT STATION 1 (A) AND AT STATION 2 (B). THE INITIAL CONCENTRATION OF AS IS REPRESENTED BY THE SOLID LINE. ....	39
FIGURE 2.7 (A) AND (B): EVOLUTION OF CONTAMINATION AFTER THE DEPOSITION OF A CAPPING LAYER OF 0.2 M. THE BIO-IRRIGATION DEPTH (B. D.) ATTAINS 0.2 M IN SIMULATION 1 (A) AND 0.1 M IN SIMULATION 2 (B). 41	41
FIGURE 2.8 (A) AND (B): EVOLUTION OF CONTAMINATION AFTER THE DEPOSITION OF A CAPPING LAYER OF 0.1 M. THE BIO-IRRIGATION DEPTH ATTAINS 0.2 M IN SIM. 3 (A) AND 0.1 M IN SIM. 4 (B). ....	42

FIGURE 2.9 (A) AND (B): <i>EVOLUTION OF CONTAMINATION FOR A NON-REACTIVE CONTAMINANT AFTER THE DEPOSITION OF A CAPPING LAYER OF 0.14 M. THE BIO-IRRIGATION DEPTH ATTAINS 0.2 M IN SIM. 5 (A) AND 0.1 M IN SIM. 6 (B).</i> .....	43
FIGURE 2.10: <i>PREDICTED CONTAMINANT RELEASE FROM THE SEDIMENTS TO THE WATER COLUMN, OVER PERIOD OF 5 YEARS, FOR A CONTAMINANT UNDERGOING DISSOLUTION (SIM. 1 AND 2) AND FOR A NON-REACTIVE CONTAMINANT (SIM. 5 AND 6).</i> .....	45
FIGURE 3.1: <i>EFFECT OF TESTED FACTORS ON THE MASS RELEASE OF A REACTIVE COMPOUND. CAP THICKNESS OF 0.2 M. SIGNIFICANT EFFECTS ARE IDENTIFIED BY THE VARIABLE NAME.</i> .....	67
FIGURE 3.2: <i>EFFECT OF TESTED FACTORS ON THE MASS RELEASE OF A NON-REACTIVE COMPOUND. CAP THICKNESS OF 0.2 M. SIGNIFICANT EFFECTS ARE IDENTIFIED BY THE VARIABLE NAME.</i> .....	69
FIGURE 3.3: <i>EFFECT OF TESTED FACTORS ON THE MASS RELEASE OF A NON-REACTIVE COMPOUND. CAP THICKNESS OF 0.1 M. SIGNIFICANT EFFECT IS IDENTIFIED BY THE VARIABLE NAME.</i> .....	69
FIGURE 3.4: <i>EFFECT OF TESTED FACTORS ON THE SURFACE CONCENTRATION OF A REACTIVE CONTAMINANT. CAP THICKNESS OF 0.2 M. SIGNIFICANT EFFECTS ARE LISTED.</i> .....	70
FIGURE 3.5: <i>EFFECT OF TESTED FACTORS ON THE SURFACE CONCENTRATION OF A REACTIVE CONTAMINANT. CAP THICKNESS OF 0.1 M. SIGNIFICANT EFFECTS ARE LISTED.</i> .....	71
FIGURE 3.6: <i>EFFECT OF TESTED FACTORS ON THE SURFACE CONCENTRATION OF A NON-REACTIVE CONTAMINANT. CAP THICKNESS OF 0.2 M.</i> .....	72
FIGURE 3.7: <i>EFFECTS OF TESTED FACTORS ON THE SURFACE CONCENTRATION OF A NON-REACTIVE CONTAMINANT. CAP THICKNESS OF 0.1 M.</i> .....	72
FIGURE 4.1: <i>DECISION ANALYSIS FRAMEWORK (ADAPTED, AFTER FREEZE ET AL. 1990).</i> .....	81
FIGURE 4.2: <i>PROGRESSIVE INVESTIGATION OF UNCERTAINTY. THE GRAPH ON THE RIGHT ILLUSTRATES THE TYPICAL OUTPUT FOR EACH ANALYSIS.</i> .....	82
FIGURE 4.3: <i>LOCALIZATION MAP OF THE STUDY SITE.</i> .....	84
FIGURE 4.4: <i>DEFINITION OF THE PROBABILITY OF FAILURE (SHADOWED AREA) FOR A NORMAL DISTRIBUTION.</i> ...	86

FIGURE 4.5: CONCEPTUAL MODEL: DISCRETIZATION OF THE SEDIMENT COLUMN AND INITIAL CONTAMINANT CONCENTRATION.....	92
FIGURE 4.6: RESULTS OF THE KOLMOGOROV-SMIRNOV TEST FOR NORMALITY, FOR DIFFERENT MODEL RESPONSES AND DIFFERENT MONTE CARLO SERIES. SQUARES CORRESPOND TO A 0.1 M CAP, TRIANGLES A 0.2 M CAP AND THE STRAIGHT LINE REPRESENTS THE CRITICAL VALUE OF THE TEST.....	98
FIGURE 4.7: MEAN DEVIATION OF THE MEAN ( $MD\mu$ ) AND OF THE STANDARD DEVIATION ( $MD\sigma$ ) FOR DIFFERENT MONTE CARLO SERIES. ....	100
FIGURE 4.8: COSTS OF DIFFERENT MANAGEMENT OPTIONS, CONSIDERING A DISSOLVED CONTAMINANT AND A FINE-GRAINED CAP (R: COST ASSOCIATED TO THE RISK OF FAILURE; C: COST OF CONSTRUCTION; $\Phi$ : TOTAL COST). .....	103
FIGURE 4.9: COSTS OF DIFFERENT MANAGEMENT OPTIONS, CONSIDERING A DISSOLVED CONTAMINANT AND A SANDY CAP (R: COST ASSOCIATED TO THE RISK OF FAILURE; C: COST OF CONSTRUCTION; $\Phi$ : TOTAL COST). .....	104
FIGURE 4.10: COSTS OF DIFFERENT MANAGEMENT OPTIONS, FOR A LOW SOLUBILITY CONTAMINANT (R: COST ASSOCIATED TO THE RISK OF FAILURE; C: COST OF CONSTRUCTION; $\Phi$ : TOTAL COST). .....	105
FIGURE 4.11: TOTAL COST FOR DIFFERENT CAPPING OPTIONS, CONSIDERING VARIOUS COSTS OF FAILURE.....	106

## LISTE DES ABRÉVIATIONS

$\alpha_L$  : Dispersivité des sédiments [L]

$\beta$  : Coefficient de transfert de masse du soluté (premier ordre) [ $T^{-1}$ ]

$\beta_1$  [ $T^{-1}$ ] et  $\beta_2$  [ $L^{-1}$ ] : Coefficients empiriques pour la variation spatiale des tubes

$\gamma$  : Facteur cinétique

$\gamma_w$  : Poids spécifique de l'eau [ $kN\ L^{-3}$ ]

$\delta$  : Distance entre l'axe du tube et le point où la concentration est égale à la valeur de l'intégral horizontal [L]

$\sigma'_p$  : Contrainte de préconsolidation [kPa]

$\sigma'_v$  : poids des terres [kPa]

$\Phi$  : Fonction objectif [\$]

B : Bénéfice [\$]

Biox : Profondeur de bio-irrigation [L]

C : Coût [\$]

Cc : Indice de compression [-]

$C_{DTD}$  : Coût de dragage, transport et recouvrement [\$]

$C_E$  : Coût technique [\$]

$C_f$  : Coût d'échec [\$]

$C_{FeS}$  : Concentration de FeS solide dans les sédiments [ $M/L^3$ ]

$C_M$  : Coût de mobilisation du matériel [\$]

$C_S$  : Concentration du soluté dans l'eau des pores des sédiments [ $ML^{-3}$ ]

$C_T$  : Concentration du soluté dans les tubes de vers [ $ML^{-3}$ ]

$C_u$  : Résistance au cisaillement [kPa]

$c_v$  : Coefficient de consolidation [ $L^2\ T^{-1}$ ]

$D_d$  : Coefficient de diffusion effectif [ $L^2T^{-1}$ ]

$D_m$  : Coefficient de diffusion/dispersion dans les tubes [ $L^2T^{-1}$ ]

$D_s$  : Coefficient de diffusion/dispersion du soluté dans les sédiments [ $L^2T^{-1}$ ]

$e_0$  : Indice des vides initial [-]

$K$  : Conductivité hydraulique [ $L T^{-1}$ ]

$k_1 [g^2 mol^{-1} l^{-1}]$  et  $k_2 [\mu g l^{-1}]$  : Coefficients de dissolution

$m$  : Nombre de tubes par aire unitaire [ $L^{-2}$ ]

MO : Pourcentage de matière organique [%]

$n_s$  : Porosité des sédiments [-]

$n_t$  : Porosité des tubes [-]

$n_t^\circ$  : Porosité des tubes à la surface de la colonne de sédiments [-]

$P_f$  : Probabilité d'échec [-]

R : Risque [\$]

$R_t$  : Facteur de retard [-]

$r_1$  : Rayon interne des tubes [L]

$r_2$  : Demi-distance entre deux tubes [L]

$v_s$  : Vitesse du fluide dans les sédiments [ $LT^{-1}$ ]

$v_t$  : Vitesse de bio-irrigation [ $LT^{-1}$ ]

## INTRODUCTION

Le fjord du Saguenay est situé à environ 200 km au nord-est de la ville de Québec, entre Saint Fulgence et Tadoussac. Il s'étend sur une longueur de 90 km et sa largeur varie entre 1 et 6 km. La partie en amont du fjord se divise en deux secteurs : la Baie des Ha! Ha! et le Bras Nord, dans lequel se déverse la rivière Saguenay, qui contribue à 90% de l'apport d'eau douce dans le fjord. La profondeur dans ces deux secteurs varie entre 100 et 200 m. Le maximum est atteint dans le bassin central avec une profondeur de 275 m. La confluence du fjord et de l'estuaire du Saint Laurent, située à Tadoussac, est caractérisée par un seuil d'environ 20 m de profondeur. La colonne d'eau du fjord est stratifiée en deux couches: une mince couche d'eau plutôt douce en surface, suivi d'une couche plus épaisse d'eau salée en provenance de l'estuaire du Saint Laurent. Dans les eaux plus profondes la salinité peut atteindre 31‰ (g/kg) et la température est d'environ 1 °C. Grâce à la bonne circulation des eaux profondes, celles-ci sont toujours bien oxygénées (Syvitski 1987, Schafer et al. 1990). Le taux de sédimentation dans le Bras Nord varie en moyenne entre  $0.35 \text{ cm an}^{-1}$  et  $0.7 \text{ cm an}^{-1}$ , avec un pic de plus que 1  $\text{cm an}^{-1}$  à l'embouchure de la rivière Saguenay, tandis que dans la Baie des Ha! Ha! le taux de sédimentation est plus faible et varie autour de  $0.1 \text{ cm an}^{-1}$  (Barbeau et al. 1981a).

En juillet 1996, la région du Saguenay a été marquée par un déluge avec des conséquences graves. Des pluies extrêmes se sont déversées durant une période de 48 heures sur la partie en amont du fjord. La crue des rivières a entraîné une érosion massive et l'apport de plusieurs millions de mètres cubes de nouveaux sédiments dans la Baie des Ha! Ha! et le Bras Nord (Lapointe et al. 1998). Cette couche d'origine terrestre et non-contaminée est composée principalement d'argile et de silt et a une épaisseur moyenne de 0.2 m. Elle recouvre des sédiments contaminés par des métaux lourds et des HAP et constitue une barrière naturelle pour la migration des contaminants (Figure I.1).

Le Projet Saguenay Post-Déluge est un projet de recherche multidisciplinaire, qui regroupe des chercheurs de plusieurs domaines et différentes universités, afin d'étudier les caractéristiques physiques, chimiques et biologiques de la nouvelle couche de

sédiments. Le projet vise à mieux comprendre le fonctionnement et l'évolution dans le temps d'une couche de recouvrement, afin d'évaluer l'efficacité de cette couche comme barrière pour isoler les contaminants dans les sédiments sous-jacents. Un des objectifs principaux du Projet Saguenay Post-Déluge est le développement technologique, qui pourra ensuite être appliqué à la planification ainsi qu'à la réalisation des couches de recouvrement.

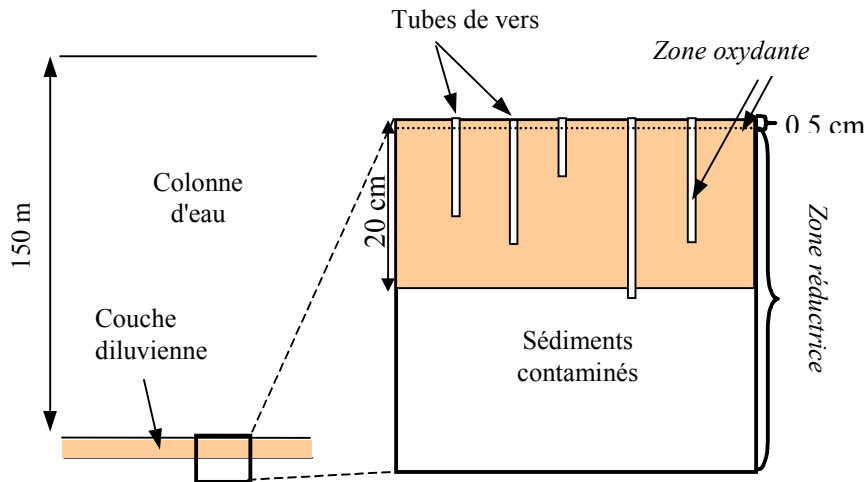


Figure I.1: Schéma général du système à l'étude

Face aux problèmes de pollution des fonds marins, le recouvrement des sites contaminés avec des sédiments propres est une option intéressante, parce qu'elle représente une façon efficace et potentiellement économique d'isoler les contaminants de l'environnement externe (USEPA 1994, Palermo et al. 1999). Une couche de recouvrement a pour objectif d'isoler physiquement les contaminants de la faune benthique, de stabiliser les sédiments et de réduire le flux des contaminants vers la colonne d'eau. Le design d'une telle couche doit considérer tous les facteurs qui peuvent affecter l'efficacité, la stabilité et la pérennité du recouvrement, tels que la consolidation, la migration de contaminant par advection ou diffusion, la bioturbation et l'érosion.

La migration de contaminants dissous à travers une couche de recouvrement composée principalement de matériaux fins est déterminée par la diffusion, l'advection associée à la consolidation, les réactions géochimiques des contaminants avec les

sédiments et la bio-irrigation qui a lieu dans les tubes de vers. À l'intérieur du recouvrement, les contaminants peuvent être retenus par adsorption, ce qui cause un retard dans la migration du front de contaminant et une atténuation la concentration maximale. La capacité d'atténuation dépend surtout de la composition de la couche de recouvrement, plus particulièrement de son pourcentage de particules fines et de matière organique. Il faut aussi considérer les changements de Eh et pH à proximité des tubes de vers qui peuvent être causés par la bio-irrigation et qui peuvent remobiliser certains métaux (Figure I.1).

Les objectifs particuliers de cette étude se situent dans le cadre global du Projet Saguenay Post-Déluge et visent à approfondir la compréhension du fonctionnement d'une couche de recouvrement et à fournir un outil pour le design d'une couche de recouvrement. Plus spécifiquement l'étude est subdivisée en trois volets:

- 1) Le développement et le calage d'un modèle numérique capable de décrire la migration verticale de contaminants dissous à travers une couche de recouvrement.
- 2) L'identification des paramètres avec un impact important sur le transport à l'intérieur de la couche.
- 3) L'évaluation de l'efficacité à long terme de la barrière vis à vis du transport de contaminants et l'utilisation du modèle pour le design d'un recouvrement.

Ces trois parties correspondent à trois articles qui constituent les chapitres 2, 3 et 4 de la thèse.

L'approche numérique est choisie parce que, pour les conditions à l'étude, il n'y a pas de solution analytique pour résoudre le système d'équations différentielles partielles qui représentent le transport. En outre, malgré les simplifications nécessaires pour représenter un système complexe comme les sédiments bio-irrigués, l'approche nous permet de calculer les flux de masse à l'intérieur d'une couche de recouvrement et d'identifier les paramètres qui ont une influence significative sur l'efficacité de la barrière.

Les données recueillies sur les sédiments du fjord du Saguenay suite au délugé de 1996 et à la déposition de la nouvelle couche, constituent une opportunité unique pour étudier le fonctionnement d'une couche de recouvrement. Une très grande quantité d'analyses chimiques, physiques et biologiques a été réalisée par plusieurs équipes de chercheurs et les données ont été utilisées pour vérifier et caler le modèle. Le premier article, qui correspond au chapitre 2 de la thèse, présente en détail le développement et le calage du modèle avec les données de terrain. Ensuite, l'influence de différents paramètres du modèle a été testée à l'aide de l'analyse de sensibilité. Cela a permis de déterminer les facteurs qui doivent être caractérisés avec précision pour que la réponse du modèle corresponde à la réalité. Les résultats de l'analyse de sensibilité sont présentés dans le deuxième article, correspondant au chapitre 3. Par la suite, le modèle a été utilisé pour le dimensionnement une couche de recouvrement en utilisant la méthode de l'analyse de décision. L'exemple présenté dans le troisième article (chapitre 4) illustre les avantages et les limites de l'analyse de décision. La méthode permet d'intégrer les coûts et les risques associés au projet de réhabilitation dans le but de trouver la solution plus rentable économiquement et la plus efficace d'un point de vue environnemental. Une explication plus détaillée des objectifs de chaque volet ainsi qu'une revue de littérature seront présentées dans l'introduction des articles qui constituent les chapitres 2, 3 et 4.

## **CHAPITRE 1 HISTORIQUE DE LA CONTAMINATION DU FJORD ET PROPRIÉTÉS DES SÉDIMENTS**

## 1.1 Contamination des sédiments du fjord du Saguenay

Plusieurs études ont documenté la distribution de contaminants dans l'eau (Gobeil et Cossa 1984) et dans les sédiments du fjord du Saguenay (Barbeau et al. 1981b, Pelletier et Canuel 1988, Gagnon et al. 1993, Cossa 1990). Cela a permis de reconstruire l'historique de la contamination et de reconnaître son origine anthropique. L'activité industrielle qui a marqué la région du Saguenay depuis les années 1930 jusqu'à la fin des années 1970 a été identifiée comme la principale responsable de la pollution du fjord. Trois types d'industries se sont installées au cours du siècle dans la région: l'usine de chlore et alcali d'Arvida, en activité de 1948 à 1976, les alumineries, présentes à Alma, Jonquière et La Baie, ainsi que quatre usines de pâte et papier, localisées le long de la rivière Saguenay (Alma, Kénogami et Jonquière) et à Port Alfred (Allan 1990). La contamination du fjord a été associée principalement à l'activité de l'usine de chlore et d'alcali d'Arvida ainsi qu'aux alumineries de Jonquière et d'Alma, qui ont déversé des rejets industriels dans la rivière Saguenay pendant plusieurs années. Les déversements ont continué jusqu'au début des années 1970, lorsque le gouvernement fédéral a instauré une réglementation concernant les effluents liquides. Par la suite, une nette diminution de l'apport de contaminants a été rapportée (Gobeil et Cossa 1984, Barbeau et al. 1981b, Pelletier et Canuel 1988, Gagnon et al. 1993, Cossa 1990).

La contamination des sédiments est surtout localisée dans la partie amont du fjord, près de l'embouchure de la rivière Saguenay. Les contaminants présents dans l'eau sont associés aux particules fines apportées par la rivière. Ces particules en suspension sont ensuite déposées dans le bassin profond du Bras Nord ou sont transportées par les courants en direction du bassin central ou de la Baie des Ha! Ha!. Les contaminants présents dans l'atmosphère se déplacent cependant par l'action du vent et peuvent atteindre facilement les régions environnantes. La teneur en métaux trace est maximale dans les sédiments du Bras Nord, et diminue dans les sédiments du bassin central et de la Baie des Ha! Ha! (Barbeau et al. 1981b, Pelletier et Canuel, 1988). Barbeau et al. (1981b)

soutiennent l'hypothèse que le principal vecteur actuel de la contamination du bassin central et de la Baie des Ha! Ha! est l'apport atmosphérique.

Les sédiments du fjord du Saguenay sont contaminés par des métaux lourds (Hg, Pb, Zn, Cu) (Figure 1.1) et des hydrocarbures aromatiques polycycliques (HAP) (Cossa 1990, Gagnon et al. 1993). Le comportement des deux types de contaminants en milieu aquatique est très différent. Les hydrocarbures sont hydrophobes et donc très peu solubles. Les métaux lourds sont cependant solubles et leur solubilité est très sensible aux changements de pH et Eh du milieu. Ils réagissent facilement avec la matrice poreuse et les autres substances dissoutes et peuvent être immobilisés par sorption ou précipitation.

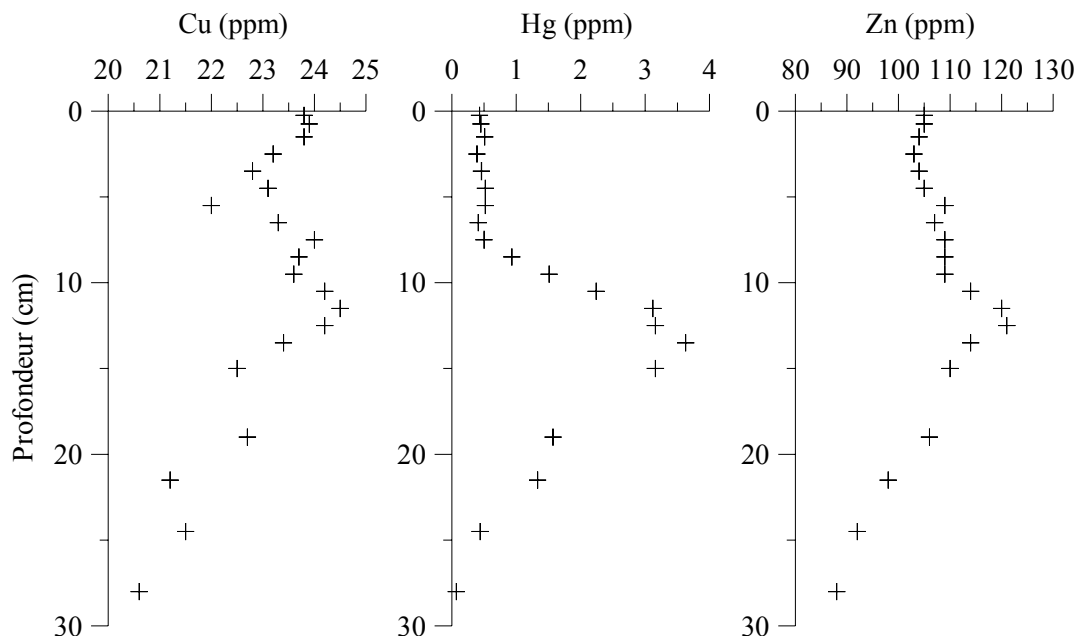


Figure 1.1 : Profil de contamination des sédiments du fjord, à la jonction de la Baie des Ha! Ha! et du Bras Nord, avant le recouvrement de 1996 (d'après Gagnon et al. 1993).

## 1.2 Propriétés des sédiments contaminés

### 1.2.1 Granulométrie et minéralogie

La distribution granulométrique des sédiments déposés dans le fjord avant 1996 varie d'un sable argileux près de l'embouchure de la rivière Saguenay à un mélange argile-limon-sable dans le secteur en aval du Bras Nord et dans la Baie des Ha! Ha!. L'analyse minéralogique montre la présence de quartz et de feldspaths ainsi que de minéraux argileux tels que l'illite et la chlorite (Locat et Leroueil 1987, Perret 1995, Leclerc et al. 1986).

### 1.2.2 Propriétés géotechniques

La résistance au cisaillement ( $C_u$ ) est une propriété qui permet d'estimer l'état de consolidation d'une couche ainsi que la réaction des sédiments lors d'une augmentation de la charge verticale. En effet, grâce aux relations empiriques établies par Perret (1995) nous pouvons estimer la contrainte de préconsolidation  $\sigma'_p$  à partir de la valeur de résistance au cisaillement et du pourcentage de matière organique (MO).

$$\sigma'_p = C_u (0.3 \pm 0.1)^{-1} \text{ pour } MO < 3\% \quad (1.1a)$$

$$\sigma'_p = C_u (0.5 \pm 0.1)^{-1} \text{ pour } MO \geq 3\% \quad (1.1b)$$

Lorsqu'une couche de sédiments est chargée à un niveau qui dépasse la contrainte de préconsolidation, il y a consolidation. Dans le cas des sédiments du Saguenay une consolidation de la couche contaminée suite à la déposition de la couche de turbidite pourrait entraîner une advection de fluides contaminés dans la couche plus propre.

La résistance au cisaillement des sédiments du fjord déposés avant 1996 varie entre 1-3 kPa pour les premiers 0.4 m, avec des valeurs autour de 1.5 kPa pour les

premiers 0.2 m et autour de 2.5 kPa pour les sédiments entre 0.2 et 0.4 m (Locat et Leroueil 1987, Perret 1995). En considérant que les sédiments déposés avant 1996 contiennent environ 5 % de matière organique (MO), et en utilisant l'équation (1.1b) nous obtenons une valeur de  $\sigma'_p$  qui varie de 2.5 kPa à 3.75 kPa pour les premiers 0.2 m et de 4.2 kPa à 6.25 kPa pour les sédiments entre 0.2 m et 0.4 m.

### **1.2.3 Géochimie des sédiments et des contaminants**

L'épaisseur moyenne de la couche contaminée est d'environ 0.2 m (Barbeau et al. 1981b). La matière organique est relativement abondante (Gagnon et al. 1993, Perret 1995) surtout dans le Bras Nord, où elle est composée en grande partie de fragments de bois associés à l'activité de l'industrie de pâte et papier (Schafer et al. 1980). Avant les événements de 1996 la couche oxydante à la surface des sédiments avait une épaisseur de quelques millimètres. Elle était suivie d'une couche réductrice, caractérisée par une fraction de monosulfure de fer (FeS) / pyrite (FeS<sub>2</sub>) particulièrement élevée (Gagnon et al. 1995). Cette caractéristique indique que dans les sédiments du fjord certains métaux traces sont probablement liés au FeS, qui a tendance à s'oxyder plus facilement que la pyrite. Des essais de resuspension ont confirmé cette hypothèse en montrant que dans les sédiments la remobilisation du fer et de l'arsenic en condition oxydante est corrélée à la teneur en FeS des sédiments (Saulnier et Mucci 2000).

## **1.3 Propriétés des sédiments diluviens**

Dans le cadre du Projet Saguenay, plusieurs carottes de sédiments d'une longueur variant entre 0.6 m et plus de 2 m ont été prélevées dans le fjord depuis le déluge de 1996. Ces échantillons montrent la présence d'une couche de turbidite déposée en 1996, d'une épaisseur moyenne d'environ 0.2 m. L'épaisseur de cette couche est très variable et peut atteindre plusieurs mètres à l'embouchure des rivières. Dans le secteur central de la

Baie des Ha! Ha! et du Bras Nord, elle varie entre 0.1 et 0.6 m d'épaisseur (Maurice 2000) .

### **1.3.1 Granulométrie et minéralogie**

La composition granulométrique de la couche varie entre une argile silteuse et un silt argileux. À la base de la turbidite un horizon sablonneux a été observé. La minéralogie des sédiments du déluge est semblable à celle des argiles du fjord et les principales composantes sont le quartz, les feldspaths, l'illite et la chlorite.

### **1.3.2 Géochimie des sédiments**

L'analyse chimique de plusieurs carottes a montré que les nouveaux sédiments sont pauvres en matière organique (1%) et riches en carbonate détritique (Pelletier et al. 1999). En raison de leur provenance, les sédiments de la nouvelle couche montrent une concentration en calcium deux à trois fois supérieure aux sédiments du fjord profond ainsi qu'une absence de contamination. La porosité varie à l'intérieur de la couche entre 0.8 et 0.5, avec une valeur moyenne de 0.7. Le potentiel rédox diminue continuellement avec la profondeur. L'analyse des carottes prélevées en 1996, quelques semaines après le déluge, et en 1997 montre que l'interface entre le milieu oxydant et le milieu réducteur s'est déplacée vers la surface des sédiments (Pelletier et al. 1999) et a atteint un nouvel état d'équilibre. Actuellement la profondeur de pénétration de l'oxygène dans les sédiments est d'environ 5 mm (Pelletier et al. 2003).

La rétention des métaux lourds dans les sédiments dépend des conditions géochimiques du milieu, tel que le pH, le potentiel rédox, la capacité tampon, et la capacité d'échange cationique de la matrice poreuse. Un des principaux mécanismes d'immobilisation est la sorption, qui est causée par des liens physiques (forces de Van der Waals) ou chimiques (échange ionique) avec les sédiments. D'autres mécanismes

d'immobilisation peuvent affecter la mobilité des métaux lourds, tels que la complexation avec des ligands organiques, la précipitation sous forme de sulfures en milieu anoxique et la précipitation avec des carbonates ou des hydroxydes en milieu oxique.

## 1.4 Consolidation et advection suite au déluge

La consolidation des sédiments peut induire le transport de contaminants par advection. Lorsque des sédiments sont chargés avec le poids d'une couche d'une certaine épaisseur, qui se dépose très rapidement, il se crée une surpression dans l'eau interstitielle des sédiments sous-jacents. Cette surpression se dissipe lors de la consolidation, pendant laquelle l'eau interstitielle est drainée et s'écoule vers la surface de la couche. La charge passe de l'eau aux particules des sédiments qui se compactent, causant le tassemement des sédiments par consolidation (Figure 1.2).

Il faut distinguer entre deux types de consolidation: celle qui se produit dans les sédiments sous-jacents sous le poids ajouté de la couche superposée et la consolidation de la nouvelle couche, causé par son propre poids. La première est à considérer avec une attention particulière, car la consolidation de la couche contaminée peut introduire des contaminants dans la couche propre. La consolidation de la couche propre peut par contre accélérer le transport de contaminant éventuellement injecté suite à la consolidation de la couche contaminée.

La consolidation est un phénomène d'une durée limitée. Ainsi, l'advection aura lieu dans une première phase qui peut durer quelques semaines ou quelques mois selon l'épaisseur, la compressibilité et la perméabilité des sédiments.

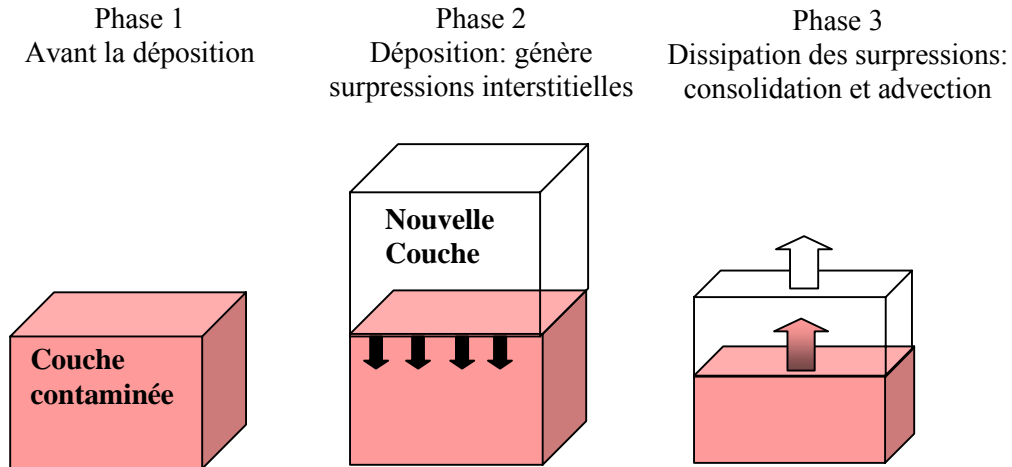


Figure 1.2: *Consolidation suite à la déposition rapide d'une nouvelle couche de sédiments.*

Douze essais de perméabilité ont été réalisés sur des cellules oedométriques afin d'obtenir les paramètres nécessaires à l'évaluation de la consolidation des sédiments de la Baie des Ha! Ha! (Tableau 1.1). Cinq carottes de sédiments, dont trois d'une longueur de 0.6 m, prélevées avec un carottier à boîtes (BX) et deux carottes prélevées avec un carottier lehigh (LE) d'environ 2 m de longueur, ont été sous-échantillonnées à des profondeurs variant entre 0.05 m et 1 m. Six essais ont été réalisés sur la couche de turbidite déposée en 1996 et six sur la couche pre-1996 contaminée. De ces derniers, un essai (10) n'a pas produit de résultats à cause d'un défaut du matériel.

L'essai oedométrique classique consiste à charger une cellule de sédiments avec un poids déterminé et à mesurer le tassement des sédiments après 24 heures (Figure 1.3). Ensuite une nouvelle charge, qui correspond à une fois et demi le poids précédent, est appliquée à la cellule. Les essais de perméabilité se font à des paliers de chargement définis à l'avance, avec une hauteur d'eau variable et pendant 24 heures. La première charge appliquée aux sédiments de surface de la Baie de Ha! Ha! était de 1 kPa. Après quatre paliers de chargement, lorsque la charge appliquée correspondait à 6 kPa, un premier essai de perméabilité a été réalisé. Afin d'éviter un remaniement des sédiments provoqué par une pression d'eau trop élevée, la hauteur d'eau initiale du premier essai était de 0.3 m. Pour le deuxième essai (12 kPa), la hauteur d'eau initiale était de 0.5 m,

pour le troisième (24 kPa) 0.75 m et pour les suivants (48 et 109 kPa) 1 m d'eau a été appliqué.

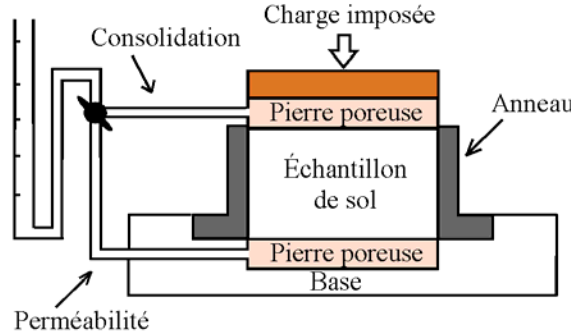


Figure 1.3: Montage de l'essai oedométrique avec mesure de la perméabilité.

Les résultats des essais (voir Annexe 1) ont permis de déterminer des paramètres importants pour évaluer la consolidation, tels l'indice de compression  $C_c$ , l'indice des vides initial  $e_0$  et la conductivité hydraulique initiale  $K_0$ . Les caractéristiques physiques déterminés à l'aide de l'essai sont présentés dans le Tableau 1.1.

Table 1.1: Charactéristiques physiques déterminés en laboratoire.

Essai	Station	Profondeur [m]	Couche	$C_c$	$e_0$	$K_0$ [m/s]
1	B04.2-12-BX	0.05	1996	0.86	2.93	$1.0 \cdot 10^{-8}$
2	B04.2-12-BX	0.11	1996	0.65	2.80	$1.5 \cdot 10^{-8}$
3	B04.04-22-BX	0.05	1996	0.55	2.03	$6.0 \cdot 10^{-9}$
4	B04.04-22-BX	0.12	1996	0.35	1.70	$9.0 \cdot 10^{-9}$
5	B08-16-LE	0.27	pre-1996	1.03	3.35	$7.0 \cdot 10^{-9}$
6	B08.4-17-BX	0.15	1996	0.40	1.88	$1.5 \cdot 10^{-8}$
7	B08.4-17-BX	0.05	1996	0.60	2.23	$7.0 \cdot 10^{-9}$
8	B04.7-19-LE	0.43	pre-1996	0.69	2.41	$4.0 \cdot 10^{-9}$
9	B04.7-19-LE	0.81	pre-1996	-	0.81	$4.0 \cdot 10^{-9}$
10	B08-16-LE	0.67	pre-1996	-	-	-
11	B04.7-19-LE	0.65	pre-1996	0.90	2.92	-
12	B08-16-LE	1.00	pre-1996	0.75	2.36	$5.0 \cdot 10^{-9}$

### 1.4.1 Consolidation de la couche contaminée

La contrainte appliquée à l'ancienne couche par la couche de turbidite est calculée en multipliant l'épaisseur de la turbidite par son poids spécifique déjaugé. Pour une épaisseur moyenne de 0.2 m et un poids spécifique déjaugé  $\gamma'$  de 5.2 kN/m<sup>3</sup> nous calculons une contrainte moyenne de 1 kPa, tandis que pour une épaisseur maximale de 0.6 m nous obtenons une contrainte de 3.1 kPa.

Pour évaluer s'il y a de la consolidation il faut comparer la contrainte ajoutée par la couche de 1996 avec la contrainte de préconsolidation des anciens sédiments. La contrainte de préconsolidation  $\sigma'_p$  a été calculée précédemment à l'aide de la relation empirique établie par Perret (1995) et elle varie entre 2.5 kPa et 3.75 kPa pour les premiers 0.2 m et entre 4.2 kPa et 6.25 kPa pour les sédiments entre 0.2 m et 0.4 m. La contrainte ajoutée ne dépasse pas la contrainte de préconsolidation pour une épaisseur de 0.2 m, tandis que pour une turbidite de 0.6 m la contrainte ajoutée est de l'ordre de grandeur de la contrainte de préconsolidation. Dans les deux cas la consolidation causée par la déposition de la couche de turbidite serait négligeable et il n'y aurait pas d'advection d'eau contaminée dans la couche propre.

### 1.4.2 Consolidation de la couche de turbidite

Le temps de consolidation de la couche de turbidite sous son propre poids peut être évalué à l'aide de l'équation suivante:

$$t = \frac{T \times (H_{dr})^2}{c_v} \quad (1.2)$$

où T représente le temps relatif ( $T = 1$  à la fin de la consolidation),  $H_{dr}$  correspond à la longueur du chemin de drainage [m] et  $c_v$  est le coefficient de consolidation [ $m^2 \text{ an}^{-1}$ ].

Le coefficient de consolidation  $c_v$  peut être estimé à partir de l'équation suivante :

$$c_v = \frac{K \times \sigma'_v \times (1 + e_0)}{0.434 \times \gamma_w \times Cc} \quad (1.3)$$

où  $K$  représente la conductivité hydraulique [ $m s^{-1}$ ],  $\sigma'_v$  est le poids des terres [kPa] et  $e_0$  correspond à l'indice des vides initial et  $\gamma_w$  [ $kN m^3$ ] est le poids spécifique de l'eau.

Les essais oedométriques ont montré que la conductivité hydraulique  $K$  est de l'ordre de  $10^{-8} m s^{-1}$ . L'indice de compression  $Cc$  varie entre 0.35 et 0.86 avec une valeur moyenne de 0.55, tandis que l'indice des vides initial  $e_0$  varie entre 2.9 et 1.7 avec une moyenne de 2.3. On considère que le drainage se fait seulement dans la direction verticale et vers le haut. Le poids des terres  $\sigma'_v$  est alors égal à la contrainte exercée par la charge de la couche de turbidite à la base de la couche même et corresponds à 1 kPa. Le coefficient de consolidation  $c_v$  correspond à  $0.44 m^2 an^{-1}$  et le temps de consolidation est de 33 jours. Par conséquent, la consolidation de la turbidite s'accomplit dans un laps de temps très court par rapport à la durée de vie d'une couche de recouvrement. Ce processus ne sera donc pas incorporé dans le modèle de transport.

**CHAPITRE 2 SIMULATION OF THE MIGRATION  
OF DISSOLVED CONTAMINANTS THROUGH A  
SUBAQUEOUS CAPPING LAYER: MODEL  
DEVELOPEMENT AND APPLICATION FOR  
ARSENIC MIGRATION**

## Résumé

TRANSCAP-1D est un modèle numérique pour la simulation de la migration verticale de contaminants dissous dans une colonne de sédiments. Le modèle a été développé afin d'évaluer l'efficacité à long terme d'une couche de recouvrement sous-marine. Il considère l'advection, la diffusion et l'effet de la bio-irrigation. Le modèle représente un milieu à double porosité, composé de pores et de trous ou tubes de vers. Le modèle numérique a été calé avec les profils de concentration de l'arsenic dissous qui ont été mesurés à deux stations du fjord du Saguenay, au Québec, Canada, après la déposition d'une couche de recouvrement naturelle suite au déluge de 1996. Dans le site à l'étude, l'arsenic n'est pas d'origine anthropique et ne peut donc pas être considéré un contaminant, cependant il a été utilisé pour le calage en raison de la disponibilité des données. Afin d'illustrer l'effet de l'incertitude et de la variabilité des valeurs d'entrée sur la réponse du modèle, nous avons réalisé des simulations numériques avec des valeurs variables de profondeurs de bio-irrigation et d'épaisseurs de la couche. Les simulations indiquent que la profondeur de bio-irrigation est un facteur important pour la distribution de contaminant dissous dans la colonne de sédiments. En outre, pour les contaminants qui coprécipitent avec des monosulfures de fer en milieu anoxique, tel l'As, la réaction de dissolution engendrée par l'oxydation des sulfures, liée à la bio-irrigation, est un facteur à considérer.

## Abstract

TRANSCAP-1D is a numerical model that simulates the vertical migration of dissolved contaminants in a sediment column. The model was developed to evaluate the long-term effectiveness of a subaqueous capping layer. It considers advection, diffusion and the effect of bio-irrigation. The sediments are represented as a dual porosity medium composed of sediment pores and biologically formed tubes. The numerical model was calibrated with the concentration profiles of dissolved arsenic measured in the sediments at two sampling stations in the Saguenay Fjord, in Québec, Canada, where a major flood event caused the natural capping of contaminated sediments. At the studied site arsenic is not of anthropogenic origin and cannot be considered a contaminant. Nevertheless, it has been used for calibration because of the availability of data. Several numerical simulations with variable bio-irrigation depth and variable thickness of the capping layer were performed to evaluate the effect of the uncertainty and variability of the input values on the model response. These simulations indicate that the depth of bio-irrigation is a major factor controlling the distribution of dissolved contaminants in the sediment column. Moreover, for contaminants that coprecipitate with iron monosulfide under anoxic condition, like As, the release from mineral dissolution caused by the exposure to an oxic environment during bio-irrigation, is a factor to be considered.

## 2.1 Introduction

Subaqueous capping consists in covering contaminated sediments to isolate them from the aquatic ecosystem, stabilize the sediments and eliminate, or at least reduce, the contaminant flux towards the water-sediment interface. This method represents an alternative for the containment of contaminated sediments, as opposed to their removal, and can be used for *in situ* remediation as well as for the disposal of dredged contaminated sediments. Any attempt at predicting the long-term effectiveness of a capping layer requires a sound understanding of the physical, chemical and biological factors affecting the migration of contaminants in the sediments.

Boudreau (1999) reviews diagenetic models representing the fate of metals in underwater sediments. The processes that control the migration of metals in these environments include molecular or ionic diffusion, advection caused by the compaction of the sediment particles and chemical reactions. Additionally, the benthic fauna increases the migration through bio-diffusive or non-local mixing and bio-irrigation. The bio-diffusive or non-local mixing is the random displacement of sediments and water particles caused by burrowing and ingestion/excretion of the benthic organisms. Bio-irrigation, on the other hand, results from the same organisms pumping the overlying water into their tubes and burrows to provide oxygen for their respiration and prevent the accumulation of potentially noxious chemical compounds (Jorgensen and Revsbech 1985).

Once a cap is placed over contaminated sediments, two different consolidation processes can occur in the sediments. The underlying contaminated sediments can consolidate because of increased stress caused from the weight of the cap and there can also be consolidation of the clean sediments under their own weight (Mohan et al. 1999, Mohan et al. 2000). Consolidation of the underlying sediments can release contaminated water into the upper clean sediments, whereas the consolidation of the capping layer might induce advection in this same layer. Consolidation is a process of limited duration, thus associated advection may last a few weeks to several months depending on the

sediment properties (Zeman 1994). Thereafter, transport in the sediments will be dominated by diffusion.

Benthic fauna affects the redistribution of the sediment particles as well as the solute transport by burrowing, tube building, ingestion/excretion of sediments and bio-irrigation. The greatest number of organisms is found in the oxygenated zone above the redox boundary, in the top 0.02-0.05 m of the sediment column (Archer and Devol 1992, Forster and Graf 1995). However, some polychaete and oligochaete worms have been observed to penetrate sediments as deep as 0.15 m (Aller and Yingst 1978, Wang and Matisoff 1997, McCaffrey et al. 1980). Tube building worms increase the area of contact between the sediments and water, enhancing diffusive solute exchange across the tube-sediment interface. They pump overlying water into their burrows, modifying the redox and pH conditions, the microbial activity and the fluxes and reactions within and adjacent to the bio-irrigated zone (Marinelli and Boudreau 1996, Aller and Aller 1998). The effect of bio-irrigation on the oxygen concentration in the sediments is limited to the vicinity of the burrow walls (Furukawa et al. 2000, Meyers et al. 1987). Nevertheless several studies have documented an increased solute flux for both organic (Reible et al. 1996) and inorganic (Riedel et al. 1987) compounds in bioturbated sediments compared to sediments without bioturbation.

Under anoxic conditions, some heavy metals are removed from the porewater by coprecipitation or adsorption on iron sulfides and by formation of discrete solid sulfides. The exposure of the anoxic sediments to an oxic environment, which may occur during resuspension, dredging or migration of the redoxcline, may oxidize the iron sulfides resulting in the dissolution and release of the trace metals associated with these phases (Petersen et al. 1997, Morse 1994). Laboratory experiments have shown that metastable Fe monosulfides (FeS) are an important reservoir of reactive trace metals (Huerta-Diaz et al. 1998, O'Day et al. 2000, Simpson et al. 2000). As bio-irrigation modifies the redox conditions near the tubes, it may also induce the oxidation of sulfides and the release of trace metals (Emerson et al. 1984, Aller and Yingst 1978). Under fully oxidizing conditions, there may be precipitation of iron oxides along the burrow walls and the

released metals may be adsorbed. But, as shown by Furukawa et al. (2001), since the burrow walls are not irrigated continuously but rather periodically, the burrow wall interface is subjected to oscillating geochemical parameters, including dissolved O<sub>2</sub> concentration and pH. This geochemical oscillation may affect the stability of mineral phases, especially redox sensitive metals.

Several numerical models that simulate early diagenetic processes occurring in recent sediments, including remineralization of organic matter and the cycling of several elements, have recently been presented (Soetaert et al. 1996, Wang and Van Cappellen 1996, Park and Jaffé 1996). These models incorporate complex biogeochemical reactions and thus require a series of biogeochemical input parameters that can be either obtained by calibration, from the literature or through stoichiometry. Although these models can simulate complex biogeochemical systems and are very valuable for diagenetic studies, they were not designed for specific application to a capping layer and they would need to be adapted to represent the migration of contaminants through a cap. In comparison, the numerical model RECOVERY, developed by the U.S. Army Corps of Engineers (Boyer et al. 1994, Ruiz et al. 2000) was designed for simulating mass transport through capping layers. The model simulates the fluxes of organic contaminants in dissolved and particulate form and represents bioturbation by using a mixing factor but does not consider the effect of bio-irrigation.

Several studies have documented the effect of dwelling organisms on contaminant fluxes from and towards sediments (Petersen et al. 1998, Reible et al. 1996, Riedel et al. 1987, Rivera-Duarte and Flegal 1994). Three different conceptual models have been proposed to describe the effect of bioturbation on solute transport: the enhanced diffusion model (Guinasso and Schink 1975), the cylindrical diffusion model (Aller 1980) and the non-local exchange model (Emerson et al. 1984). The enhanced diffusion model uses an increased effective diffusion coefficient in the surface mixed layer to represent solute exchange. In the cylindrical diffusion model, the geometry of the irrigated burrows is simplified and represented with vertical cylinders (Figure 2.1). The non-local exchange model represents the solute transfer occurring between the sediments and the water by an

exchange coefficient called "non-local". Matisoff and Wang (1998) compared these three models with experimental observations of bio-irrigated sediments and showed that the best fit to the observed concentrations is obtained with the cylindrical diffusion model and the non-local exchange model. As shown by Boudreau (1984), the cylindrical model can be reduced to the non-local exchange model when a linear gradient is assumed between the concentration inside the burrow and the horizontally averaged concentration in the sediment porewater.

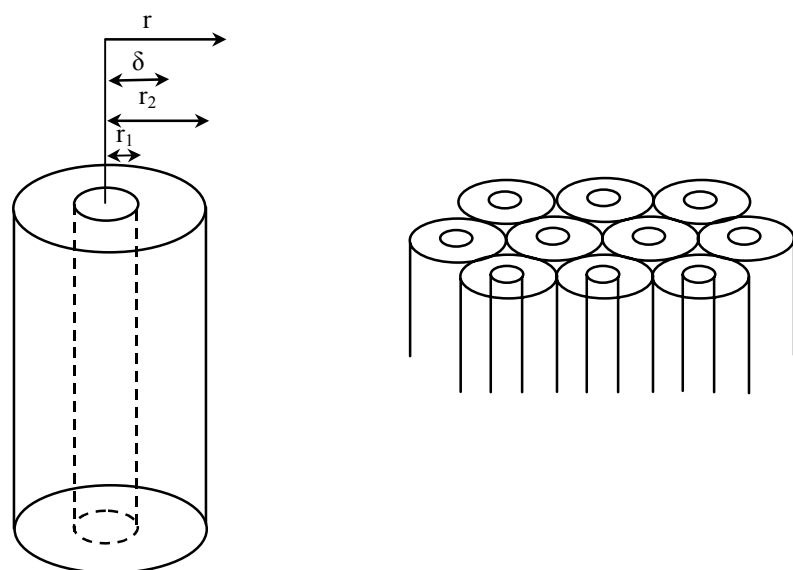


Figure 2.1: *Schematic diagram illustrating the simplified geometry of a tube/burrow and the bio-irrigated layer, approximated by packed cylinders, after Aller (1980). ( $r_1$  = inner radius of cylinders,  $r_2$  = half distance between two cylinders,  $\delta$  = distance to the point where the concentration in the sediments equals the horizontally integrated value)*

The objective of the present study is to develop a numerical model, TRANSCAP-1D, that will simulate the migration of certain dissolved contaminants, through a sediment cap in a marine environment. The model considers the main physical, chemical and biological factors affecting the migration of dissolved contaminants in sediments, including advection, diffusion, bio-irrigation and dissolution. The model was primarily designed to study the migration of contaminants in the sediments of the Saguenay Fjord, where a major flood caused the natural capping of contaminated sediments. Some

simplifying assumptions concerning the governing processes, discussed in the paper, have been used for the application to the Saguenay Fjord. However, the model formulation is general and allows its application to other sites.

## 2.2 Mathematical formulation and numerical solution

The description of dissolved solute transport in sediments containing bio-irrigated tubes, assuming non-local solute exchange between the sediment porewater and the tubes, requires governing equations for both the sediments and the tubes. The following assumptions are made: advection and diffusion are accounted for in both the sediments and the tubes, the effect of temperature and density gradients on solute transport are assumed negligible and we also neglect transient effects of compaction on solute transport. This last assumption is discussed later for the application to the Saguenay Fjord. Because transport processes and concentration gradients in contaminated sediments are predominantly vertical, a one-dimensional representation is used here. However, the model is easily expandable to multi-dimensional systems. Finally, sedimentation and accumulation of contaminants by organisms are not included in this study, but could be incorporated later. The main transport processes are illustrated in Figure 2.2.

The equation describing solute transport in the sediment porewater is given by:

$$n_s \frac{\partial C_s}{\partial t} = n_s \cdot \frac{D_s}{Rt} \left( \frac{\partial^2 C_s}{\partial z^2} \right) - n_s \cdot \frac{v_s}{Rt} \cdot \frac{\partial C_s}{\partial z} - \beta(C_s - C_T) \quad (2.1)$$

where  $C_s$  and  $C_T$  are the solute concentration [ $M L^{-3}$ ] in the sediments and the tubes, respectively,  $n_s$  is the sediment porosity [-],  $v_s$  is the fluid velocity in the sediments [ $L T^{-1}$ ],  $Rt$  is the solute retardation factor [-], and  $\beta$  is a first-order mass transfer coefficient [ $T^{-1}$ ], corresponding to the non-local coefficient discussed in the previous section. The

first term on the right-hand side of equation (2.1) represents diffusion/dispersion in the sediment, the second term represents the advective flux and the last term describes the mass transfer between sediments and tubes. The dispersion coefficient of the solute in the sediments,  $D_s$  [ $L^2 T^{-1}$ ], is given by:

$$D_s = D_d + \alpha_L \cdot v_s \quad (2.2)$$

where  $D_d$  is the effective diffusion coefficient [ $L^2 T^{-1}$ ] and  $\alpha_L$  is the sediment dispersivity [L]. Note that when the fluid velocity is small in the sediments, which is the case for low-permeability material, the dispersion coefficient is approximately equal to the diffusion coefficient.

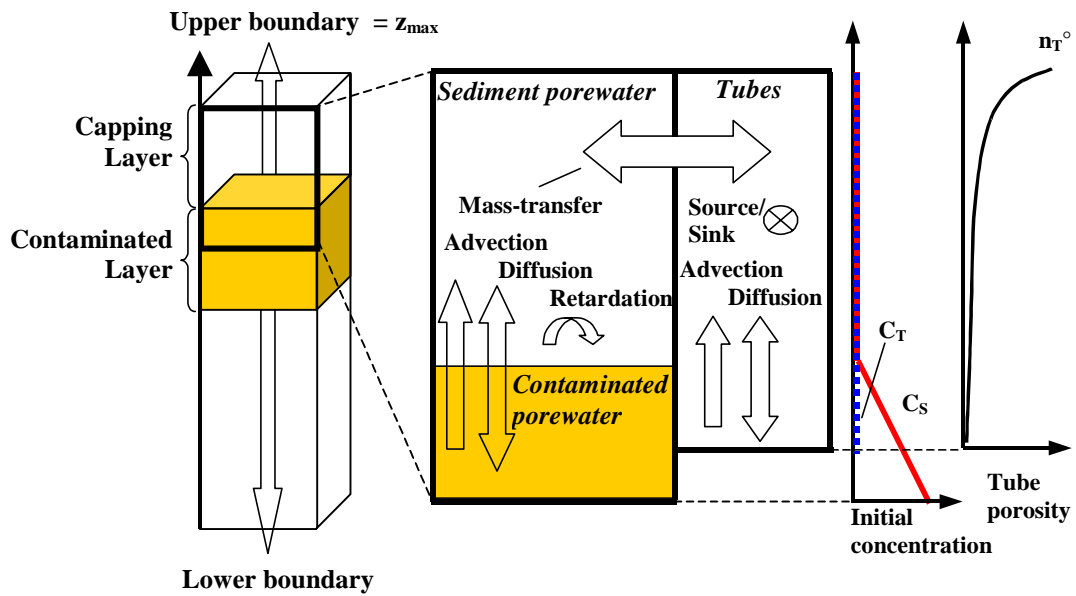


Figure 2.2: Diagram representing the sediment column, the main transport processes in the dual porosity system (sediment pores and tubes), the initial concentration and the variation of tube porosity with depth.

The equation describing solute transport in the tubes is given by:

$$n_T \frac{\partial C_T}{\partial t} = n_T D_m \frac{\partial^2 C_T}{\partial z^2} - n_T v_T \frac{\partial C_T}{\partial z} + \beta(C_s - C_T) + S \quad (2.3)$$

where  $n_T$  is the porosity of the tubes [-],  $D_m$  is the dispersion coefficient for the tubes [ $L^2 T^{-1}$ ], given by an expression similar to equation (2.2), and  $v_T$  is the fluid or irrigation velocity in the tubes [ $L T^{-1}$ ]. The porosity of the tubes represents the volume occupied by the tubes per unit volume of sediments. In equation (2.3),  $S$  is a general source or sink term [ $M L^{-3} T^{-1}$ ] representing the release of contaminant from mineral dissolution associated to bio-irrigation. This term is defined in the application section.

The number of benthic organisms that bio-irrigate their tubes is maximal at the surface of the sediments and decreases exponentially downwards (Martin and Banta 1992). To represent this exponential decrease, the mass transfer coefficient is expressed as:

$$\beta(z) = \beta_1 \cdot \exp[\beta_2(z - z_{max})] \quad (2.4)$$

where  $\beta_1$  [ $T^{-1}$ ] and  $\beta_2$  [ $L^{-1}$ ] are empirical coefficients that are adjusted to reproduce the variation in the number of tubes and  $z_{max}$  [L] is the location of the top of the sediment column. The porosity of the tubes,  $n_T$ , is also modified in a similar manner:

$$n_T(z) = n_T^\circ \cdot \exp[\beta_2(z - z_{max})] \quad (2.5)$$

where  $n_T^\circ$  is the maximum sediment porosity, located at the top of the sediment column (see Figure 2.2).

Initial and boundary conditions are required to solve both equations (2.1) and (2.3). To impose the initial conditions one specifies the initial solute concentration in the

two domains, sediments and tubes. Boundary conditions are required at the top and bottom of the domain and can be either a prescribed concentration or prescribed mass flux for both domains.

The two governing equations (2.1) and (2.3) are discretized with the finite volume method (Versteeg and Malalasekera 1995). The equations are coupled through the mass exchange term and a simultaneous solution for the concentration in the sediments and tube is obtained for each finite volume. The system of equations is thus solved in a fully-coupled fashion, avoiding the use of iteration that is necessary when the equations are decoupled. The block tridiagonal matrix resulting from the discretization and assembly of the terms is solved with the Thomas algorithm adapted to block matrices. Details of the discretization are given in Appendix 2.

## 2.3 Verification

The governing equations (1.1) and (1.3) solved by the TRANSCAP-1D model are mathematically similar to those describing solute transport in a dual-porosity medium in the context of groundwater flow (for example, Zheng and Bennett 2002). The numerical model was verified by comparing the simulation results to the results of the semi-analytical solution of Neville et al. (2000), which has been developed for one-dimensional solute transport in a dual-porosity medium with multiple non-equilibrium processes. The semi-analytical solution solves the equations (1.1) and (1.3) for a uniformly contaminated domain and simple boundary conditions. The tubes and the sediment porosity of the TRANSCAP-1D numerical model correspond to the mobile and the immobile regions of the semi-analytical solution.

The TRANSCAP-1D model was verified against the results of the semi-analytical solution for a specific set of input values and boundary condition. The input parameters used in the semi-analytical solution are presented in Table 2.1. The system is represented by a 0.60-m long column, which was uniformly divided in 60 elements of equal volume.

A constant concentration of 1.0 was specified at the basis of the column and the simulation time was set to 2.5 d. In the TRANSCAP-1D model the tube and sediment porosity were both set to 0.25, which gives a total porosity of 0.5 and respects the mobile fraction of 0.5 stated in the input parameters of the semi-analytical solution. The advection velocity was set to  $0.1 \text{ m d}^{-1}$ , which corresponds to the Darcy velocity of  $2.5 \text{ cm d}^{-1}$  for a porosity of 0.25. The dispersivity of the numerical model was set equal to 0.01 m, which is equivalent to a dispersion coefficient of  $10.0 \text{ cm}^2 \text{ d}^{-1}$  multiplied by the advection velocity. Results of the simulation, shown in Figure 2.3, indicate that the numerical model reproduces almost perfectly the concentrations computed with the semi-analytical solution for the input and boundary conditions considered here.

Table 2.1: *Input parameters for the semi-analytical solution of Neville et al. (2000).*

Parameter	Units	Value
Darcy velocity	[cm d <sup>-1</sup> ]	2.5
Total porosity	[-]	0.5
Mobile fraction	[-]	0.5
Dispersion coefficient	[cm <sup>2</sup> d <sup>-1</sup> ]	10.0
Retardation factor	[-]	1.0
Mass transfer coefficient	[d <sup>-1</sup> ]	0.1

Another test of the numerical model is the calculation of the solute mass balance for the simulations. The verification tests done here produced a relative mass balance error equal to approximately  $10^{-12}$  of the calculated solute fluxes, which indicates almost perfect conservation of mass for the numerical scheme.

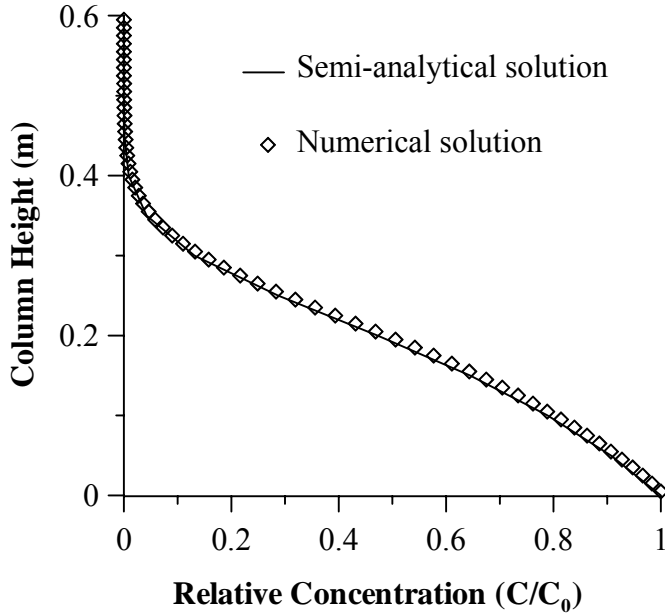


Figure 2.3: *Verification of the model results with the semi-analytical solution of Neville et al. (2000).*

## 2.4 Application of the model to the flood sediments of the Saguenay Fjord

The main motivation for developing the model was its application to the case of the Saguenay Fjord, where a layer of clean sediments was deposited over contaminated sediments during a major flood in 1996. The Saguenay Fjord is 90 km long, with a width varying between 1 and 6 km, and reaches the St. Lawrence estuary in Tadoussac (Figure 2.4). The water column in the fjord is composed of two layers: a thin freshwater layer near the surface overlying a thick layer of saline, well oxygenated water, coming from the estuary. The limit between the two layers is located at a depth of 30 m. From this limit downwards, the salinity is equal to 31 ‰ and the temperature is 1 °C. Two study sites, Stations 1 and 2, are located at the upstream section of the fjord, in the Bras Nord and the Baie des Ha! Ha! (Figure 2.4). The average water depth at the stations is about 150 m.

Several studies have documented the distribution of contaminants in the water (Gobeil and Cossa 1984, Tremblay and Gobeil 1990) and in the sediments (Barbeau and al. 1981, Pelletier and Canuel 1988, Gagnon et al. 1993, Cossa 1990) of the Saguenay Fjord. The pollution originates from the development of the industrial activity in the Saguenay region at the beginning of the 1930s. The introduction of environmental regulations in the 1970s was effective in reducing the industrial discharge of pollutants. Nevertheless, following studies on sediments of the Saguenay Fjord continued to show significant concentrations of heavy metals (Hg, Pb, Zn, Cu) and PAHs (polycyclic aromatic hydrocarbons) (Cossa 1990, Gagnon et al. 1993), related to anthropogenic sources located in the region. On the opposite, the presence of arsenic in the sediments could not be linked to the industrial activity in the Saguenay area. Studies on the distribution of arsenic in the water column suggest that arsenic most likely is introduced to the fjord from the St Lawrence Estuary and accumulates in the sediments by particles settling through the marine waters (Mucci et al. 2000b).

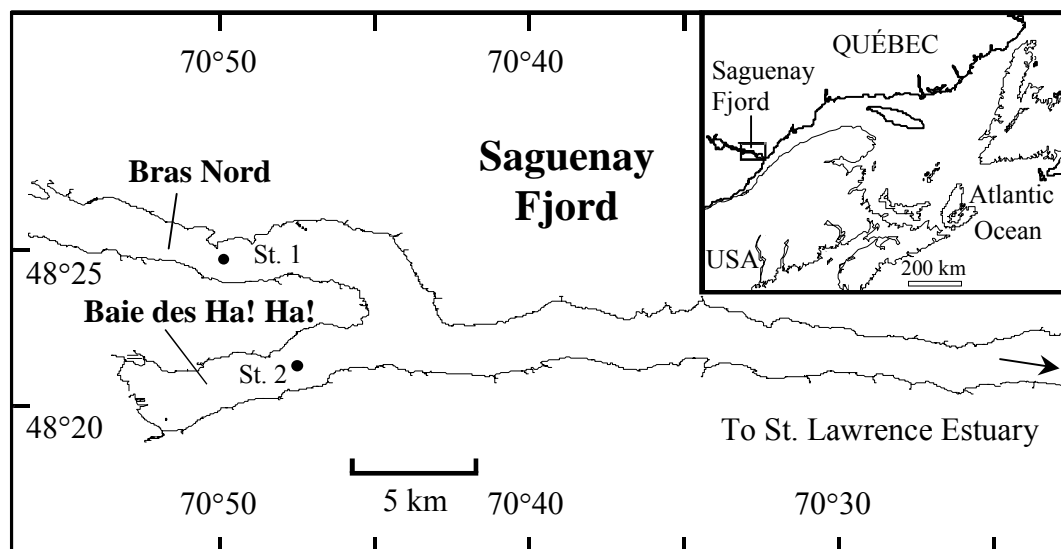


Figure 2.4: *Map of the Saguenay Fjord showing the two stations that were used to test the model.*

In July 1996, two days of intense rainfall caused severe flooding in the Saguenay region and lead to the discharge by rivers of several million cubic meters of clean sediments to the Saguenay Fjord. A turbidite deposit composed mainly of silt and clay and of an average thickness of 0.2 m settled in a few days on the contaminated bottom sediments of the Bras Nord and the Baie des Ha! Ha! (Maurice 2000). The thickness of the turbidite layer varies spatially and reaches a maximum of a few meters at the upstream section of the fjord, near the incoming rivers' mouths. The clean sediments represent a natural barrier, or capping layer, that might isolate the fjord water from the contaminants present in the underlying sediments.

To study the impact of the catastrophic flood event on the fate of the contaminants present in the sediments, a major multidisciplinary project was initiated in 1997. Various research groups collected information on the biological, geochemical and geotechnical characteristics of the sediments, which provided us with valuable input parameters for the numerical simulations (Tremblay et al. 2003, Pelletier et al. 2003). The model was adapted to the simulation of dissolved arsenic, because its chemistry has been extensively studied (Aggett and O'Brien 1985, Belzile and Tessier 1990), especially for the sediments of the Saguenay Fjord (Saulnier and Mucci 2000, Mucci et al. 2000a, Mucci et al. 2000b). Arsenic is not a contaminant in the Saguenay Fjord, but the calibration of the model required profiles of the dissolved concentration in the sediment column, and those data were only available for As. Similar profiles of concentration versus depth were documented for arsenic (As) and iron (Fe), suggesting that in the sedimentary environment the behavior of As is related to that of Fe. The two main mechanisms controlling the distribution of As in the sediment column are the coprecipitation of As with Fe sulfides in the anoxic sediments and the adsorption onto oxihydroxides in the first few millimeters below the sediment-water interface, corresponding to the oxic layer.

In the Saguenay sediments the pyrite concentration is relatively low ( $5\text{-}30 \mu\text{mol g}^{-1}$ , dry weight) whereas the Fe monosulfide concentration is abnormally high and up to seven times more abundant (Mucci and Edenborn 1992). Compared to pyrite, which has slow oxidation kinetics in presence of  $\text{O}_2$ , Fe monosulfide is very reactive and dissolves

rapidly if exposed to an oxic environment. Thus, it is likely that As adsorbed or coprecipitated with the Fe monosulfide in the anoxic layer can be remobilized after exposure to O<sub>2</sub> during bio-irrigation (Figure 2.5). Other trace metals coprecipitate with Fe sulfides (Ni, Cu, Co, Hg, Pb), but compared to As their probability of remobilization is smaller since they prefer the association to less reactive mineral phases (e.g. organic matter). Therefore, the dissolution after exposure to O<sub>2</sub> of the inorganic contaminants present in the sediments of the Fjord (Hg, Pb, Zn, Cu) is expected to be smaller than the one calculated for As.

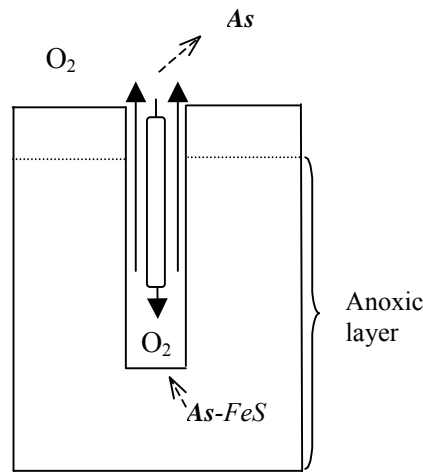


Figure 2.5: *Remobilization of As after oxidation of FeS around the tube walls.*

The present application of the TRANSCAP-1D model includes the remobilization of As in the bio-tubes crossing the anoxic layer, but the coprecipitation of As with oxihydroxides is not explicitly represented. In fact, we assume that the advective transport in the tubes is very fast so that the released As reaches the surface before adsorption onto oxihydroxides. Thus, the simulation rather presents the "worst case scenario", corresponding to the maximal release and mobility of arsenic. Details of the representation of the reaction included in the model will be discussed in the following section.

### 2.4.1 Input parameters for the numerical model

Several input parameters are needed to simulate the migration of contaminants in sediments containing bio-tubes with the TRANSCAP-1D model. These parameters have been either measured in the Saguenay Fjord or they are estimated from other studies. A discussion of the values of all parameters used for the simulations, as well as limitations in some cases, is given below.

As stated in the introduction, the duration of the consolidation and the fluid advection depends on the sediment properties (Zeman 1994). The hydraulic conductivity of the sediments of the Saguenay Fjord is generally so small that fluid velocities are rarely sufficient to induce solute advection and solute transport is primarily carried by diffusion, except if there is consolidation of the sediments. Consolidation of the contaminated sediments can be evaluated knowing that the total vertical stress added with the deposition of the capping layer is about 1 kPa for an average cap thickness of 0.2 m. This stress does not reach the preconsolidation pressure of the underlying sediments, which varies between 1 and 3 kPa (Perret 1995, Locat and Leroueil 1987). Thus, consolidation of the contaminated layer and advection of contaminated water in the clean sediments are assumed to be negligible. To investigate if consolidation can lead to advection of solutes in the new sediment cap, a series of permeability tests in oedometric cells were conducted. These experiments were performed on a few intact sediment samples of the Saguenay Fjord. The test consisted in compressing the sediment sample by imposing a given pressure and measuring the permeability of the sample at different consolidation stages. The test allowed estimating the consolidation that occurred in the sediments of the fjord after the emplacement of the cap in 1996. The laboratory tests showed that the average hydraulic conductivity of the sediments is  $10^{-8}$  m s<sup>-1</sup>. The compression index, Cc, has an average value of 0.55 and the void ratio is 2.3. From these values, we calculate a coefficient of consolidation equal to  $0.44 \text{ m}^2 \text{ a}^{-1}$ . The corresponding consolidation time for a cap thickness of 0.2 m is thus estimated at 33 d. These results suggest that, in the case of the Saguenay Fjord, the consolidation of the

capping layer lasted only a few weeks and that advection related to consolidation is a negligible long-term transport process. Thus, the fluid velocity in the sediments is assumed equal to zero in the numerical simulations.

The release of contaminant associated with the bio-irrigation is represented in the model as a source term  $S$  in the transport equation (2.3) of the tube. The source term can be expanded in the following way:

$$S = \gamma(L - C_T) \quad (2.6)$$

where  $\gamma$  is a kinetic rate [ $T^{-1}$ ]. This term specifically represents the release of trace metals following the exposure of FeS to the oxygenated water circulating in the tubes. It is important to note that, since the source term is located in the tubes-equation, the release only occurs in the tubes. However, the two equation (2.1) and (2.3) are coupled through a mass-transfer term, thus the release will affect the solute concentration in the sediment pores.

As shown by Saulnier and Mucci (2000), the oxidation of FeS is very rapid and the dissolved Fe concentration in water attains its maximum in a few minutes. Thus we assume that the dissolution of trace metals associated to FeS is fast and a large value for  $\gamma$  equal to  $10\,000\,d^{-1}$  is used. Since the model is specifically adapted to simulate the fate of As, the parameter  $L$  represents the maximum dissolved concentration of As for a definite FeS content of the sediments and is given by:

$$L = k_1 C_{FeS} + k_2 \quad (2.7)$$

where  $k_1$  and  $k_2$  are regression parameters that can be viewed as dissolution coefficients and  $C_{FeS}$  [ $M\,L^{-3}$ ] is the concentration of FeS. The resuspension experiments conducted by Saulnier and Mucci (2000) on the sediments of the Saguenay Fjord indicated that the amount of As released is linearly proportional to the content of solid FeS of the

resuspended sediments. These observations suggest that the oxygenated water introduced in the sediments through bio-irrigation may lead to the release of As next to the tubes and burrows. Since the conditions in bio-irrigated sediments are not comparable to resuspension, we do not expect that the coefficients  $k_1$  and  $k_2$  obtained from resuspension experiments can be used for simulating dissolution during bio-irrigation. Thus, we instead derive the coefficients directly from the concentration of dissolved As and solid FeS measured by the group of geochemists of the Saguenay Project, supervised by Prof. Alfonso Mucci, on the sediment cores sampled at the Station 1 and Station 2 of the Saguenay Fjord (see Figure 2.4). The dissolved As concentrations were measured with an atomic absorption spectrophotometer on porewater samples extracted from the sediments with a modified Reeburgh-type squeezer, and successively filtered and refrigerated until analysis. The solid FeS content was determined by measuring the H<sub>2</sub>S generated during acidification of the freeze-dried and homogenized sediment sample. The detailed description of the analytical methods can be found in Mucci et al. (2000a). The values calculated are shown in Table 2.2.

Table 2.2: *Coefficients for the dissolution term, derived from concentrations of dissolved As and solid FeS measured in the Saguenay Fjord.*

Dissolution factors	$k_1$ (g <sup>2</sup> mol <sup>-1</sup> l <sup>-1</sup> )	$k_2$ (μg l <sup>-1</sup> )
Station 1	0.981	1.0993
Station 2	1.7	1.274

The molecular diffusion coefficient  $D_m$  of dissolved As is derived from the values presented in Vanysek (2000) and Domenico and Schwartz (1998) and is assumed equal to  $2.5 \times 10^{-5}$  m<sup>2</sup> d<sup>-1</sup>. The effective diffusion coefficient  $D_d$  is calculated by multiplying the molecular diffusion coefficient  $D_m$  with a mean estimated tortuosity value of 0.64, and corresponds to  $1.6 \times 10^{-5}$  m<sup>2</sup> d<sup>-1</sup>. The retardation factor is fixed to a value of 15, based on the range of the partition coefficient  $K_d$  of As presented in the literature (Fuller 1978).

The bio-irrigation velocity was obtained from values presented in the literature. Riisgard (1989, 1991) carried out laboratory experiments to measure the irrigation velocities of two species of polychaetes, *Chaetopterus Variopedatus* and *Nereis Diversicolor*. They reported velocities of  $130 \text{ m d}^{-1}$  for *Chaetopterus Variopedatus* and  $26 \text{ m d}^{-1}$  for *Nereis Diversicolor*, at a temperature of  $15^\circ\text{C}$ . These velocities represent the pumping activity of two polychaete species that live in a shallow water environment (between 0 and 30 m depth). Because the fauna of the Saguenay Fjord lives at a depth of 150 m under very different conditions, we must adjust the reported velocities to the fjord's settings. Riisgard et al. (1992) observed a linear relationship between the temperature and the pumping efficiency of *Nereis Diversicolor*, at temperature ranges between  $8$  and  $28^\circ\text{C}$ . Moreover, it was observed that lower temperatures correspond to longer pauses between bio-irrigation periods. Since the model cannot represent periodical bio-irrigation, we consider that the irrigation pauses reduce the average bio-irrigation velocity. Accounting for these temperature-effects, we estimate that a velocity value of  $1 \text{ m d}^{-1}$  is more representative for a water temperature of  $1^\circ\text{C}$ , equal to that of the bottom waters of the Saguenay Fjord.

As stated previously, the cylindrical model can be reduced to the non-local exchange model, under specific assumptions. Boudreau (1984) showed that the two models are related with an equation that calculates the non-local exchange coefficient  $\beta_1$  at the surface of the sediments using the parameters of the cylindrical diffusion model (Figure 2.1).

$$\beta_1 = \frac{2D_d r_1}{(r_2^2 - r_1^2)(\delta - r_1)} \quad (2.8)$$

where  $r_1$  is the inner radius of the tubes or burrows [L],  $r_2$  is the half-distance between two tubes/burrows [L] and  $\delta$  is the distance [L] from the burrow axis to a point where the concentration equals the horizontally integrated value. Observations on the sediment cores sampled at the study site suggest that the inner radius of the tubes  $r_1$  is

approximately equal to 0.001 m. The half-distance between two tubes  $r_2$  is related to the quantity of tubes per unit area  $m [L^{-2}]$ :

$$r_2 = \frac{1}{2\sqrt{m}} \quad (2.9)$$

The value of  $m$  was visually determined from photographs of the undisturbed bottom sediments taken during the summer 2001. A total of 1000 structures per square meter represents a good approximation for the study site and we thus assigned to  $r_2$  a value of 0.015 m. The distance  $\delta$  is assumed equal to 0.0026 m (Furukawa et al. 2000). From equation (2.8), using an effective diffusion coefficient for As equal to  $1.6 \times 10^{-5} \text{ m}^2 \text{ d}^{-1}$ , the value of  $\beta_1$  is equal to  $0.0893 \text{ d}^{-1}$ . This value agrees with those published elsewhere for sediments bioturbated by polychaetes and oligochaetes worms (Table 2.3).

Table 2.3: *Bio-irrigation parameters found in the literature for sediments bioturbated by polychaetes and oligochaetes worms.*

Taxonomic group and species	$\beta_1$ (d <sup>-1</sup> )	Density (indiv/m <sup>2</sup> )	$r_1$ (m)	$r_2$ (m)	References
<b>Polychaetes</b>					
<i>Heteromastus and others</i>	0.2	500	0.0005	0.021	Aller (1980)
<i>Cirratulid and others</i>	0.0086-0.0432	-	-	-	Emerson et al (1984)
<i>Heteromastus Filiformis</i>	0.09	360	0.0005	0.0258	Aller and Yingst (1985)
<i>Mediomastus, Nephtys and others</i>	0.03-0.25	-	-	-	Martin and Banta (1992)
<i>Spionide et Capitellide</i>	0.2630016	705±15	0.001	0.0202	Furukawa et al (2000)
<b>Oligochaetes</b>					
<i>Brachiura Sowerbyi</i>	0.013824	2000	0.001	0.025	Wang and Matisoff (1997)
	0.027648	4000	0.001	0.0125	

The sediment porosity is assumed to be equal to 0.7, which is the average of all values measured at the study site, while the porosity of the tubes  $n_T^\circ$  at the surface is calculated by assuming a cylindrical shape:

$$n^o_T = m \cdot r_l^2 \cdot \pi \quad (2.10)$$

where  $m$  represents the quantity of tubes per unit area [ $L^{-2}$ ]. Assuming a radius  $r_l$  of 0.001 m and an average of 1000 tubes per square meter, the tube porosity at the surface of the sediments  $n^o_T$  is equal to 0.003.

The value of  $\beta_2$  in equation (2.4) and (2.5) is directly related to the depth of the burrows. Various sediment cores sampled in the Baie des Ha! Ha! have been analyzed by the axial tomodensitometer of the Regional Hospital Center of Rimouski. This non-destructive method allows to quantify the bioturbation structures (tubes and burrows) (De Montety et al. 2000). The results show that the structures can be observed down to a sediment depth of 0.15 m at two of five sampling stations in the fjord, with a maximum number of structures located in the upper 0.05 m. On the other hand, field and laboratory observations show that the burrows can reach a depth of 0.2 m. Assuming that the burrows reach a maximal depth of 0.2 m, a corresponding value of  $\beta_2$  of  $20 \text{ m}^{-1}$  is used in the model. If the burrows reach only 0.1 m, the value of  $\beta_2$  is increased to  $50 \text{ m}^{-1}$ .

## 2.4.2 Simulations

TRANSCAP-1D is used to simulate the evolution of the dissolved As concentration at two sampling stations located in the Bras Nord (Station 1) and in the Baie des Ha! Ha! (Station 2) (Figure 2.4). The response of the model is compared to the profiles of dissolved As measured at those stations in 1998, 2 years after the flood. The input parameters discussed in the previous section are used to approximate the general conditions at the two stations (Table 2.4).

Table 2.4: *Input parameters of the numerical model.*

Parameter	Name	Units	Value
Sediment porosity	$n_s$	[ $\cdot$ ]	0.7
Tube porosity at surface	$n^o_T$	[ $\cdot$ ]	0.003
Advection velocity	$v_s$	[ $m d^{-1}$ ]	0
Irrigation velocity	$v_T$	[ $m d^{-1}$ ]	1
Retardation factor	$R_t$	[ $\cdot$ ]	15
Dispersivity	$\alpha_L$	[ $m$ ]	0
Effective diffusion coeff.	$D_d$	[ $m^2 d^{-1}$ ]	$1.6 * 10^{-5}$
Molecular diffusion coeff.	$D_m$	[ $m^2 d^{-1}$ ]	$2.5 * 10^{-5}$
Kinetic factor	$\gamma$	[ $\cdot$ ]	10 000
Mass transfer coefficients	$\beta_1$	[ $d^{-1}$ ]	0.0892
	$\beta_2$	[ $m^{-1}$ ]	20
Depth of bioturbation	$b_{\text{iox}}$	[ $m$ ]	0.2

The model simulates the evolution of contamination in a sediment column with a thickness of 0.6 m. The column is equally subdivided in 30 cells, each having a height of 0.02 m. The concentration of dissolved As at the sediment-water interface has been fixed at  $1125 \mu\text{g m}^{-3}$  in accordance to the value measured in 1994 at the water-sediment interface by Mucci et al. (2000b). We assume solutes leaving the sediments from the upper boundary do not accumulate in water but are promptly carried away by the bottom currents. On the other hand the solute mass reaching the lower control volume by diffusion leaves the system at the same rate. Since the sediments underlying the modeled system are assumed to be clean, we define the advective flux entering the sediment column from the lower boundary to be zero. Thus the concentration at the lower limit stays at a constant value of zero. The simulation time is 2 years (730 d) and the time increment is 0.02 d.

The initial concentration of FeS corresponds to the concentration profiles that have been measured at the two sampling stations in 1998, 2 years after the flood. We assume that the distribution of FeS did not significantly change during the 2 years that followed the deposition of the cap, which agrees with the conceptual model proposed by Mucci et al. (2000a) for the migration of the oxidation front through the capping layer

after its deposition. According to Mucci's model, shortly after deposition the depth of penetration of oxygen extended through the flood layer, but within three weeks the oxidation front migrated up towards the new sediment-water interface and attained a new steady state condition. Therefore it can be assumed that the distribution of FeS reached equilibrium a few weeks after deposition and did not change afterwards. The simulations begin immediately after the end of the migration of the oxidation front, when FeS reaches equilibrium, a few weeks after the flood of 1996. Thus the concentration profile of FeS is defined at the beginning of the simulation and is assumed to be constant until the end. At the top cell of the discretized sediment column the concentration of Fe monosulfide was set to zero. This corresponds to the oxic layer, which in the Saguenay sediments has a thickness varying between few millimeters to 0.02 m (Mucci 2000b).

The thickness of the capping layer is 0.2 m at Station 1 and 0.28 m at Station 2. Within this layer, the initial concentration of dissolved As is zero. For the underlying sediments, the initial concentration of dissolved As at the two sampling stations had to be extrapolated by calibrating the model to reproduce the peak concentration measured in 1997 and in 1998. The peak As concentration at Station 1 is located at a depth of 0.29 m and attains  $90\ 000\ \mu\text{g m}^{-3}$  whereas at the Station 2, the maximum concentration is located 0.35 m under the sediment-water interface and reaches  $100\ 000\ \mu\text{g m}^{-3}$ .

The results for the model calibration at the two sampling stations are shown in Figure 2.6, where the simulated profiles of dissolved As are compared to the concentrations measured in 1998, 2 years after the flood. The comparison between the response of the model and the measured profiles shows that the numerical model reproduces the spatial and temporal patterns of As concentrations. The dissolved As profiles at both stations clearly show the effect of bio-irrigation and remobilization, which is represented by the increased concentration of dissolved As in the first 0.2 m beneath the sediment-water interface.

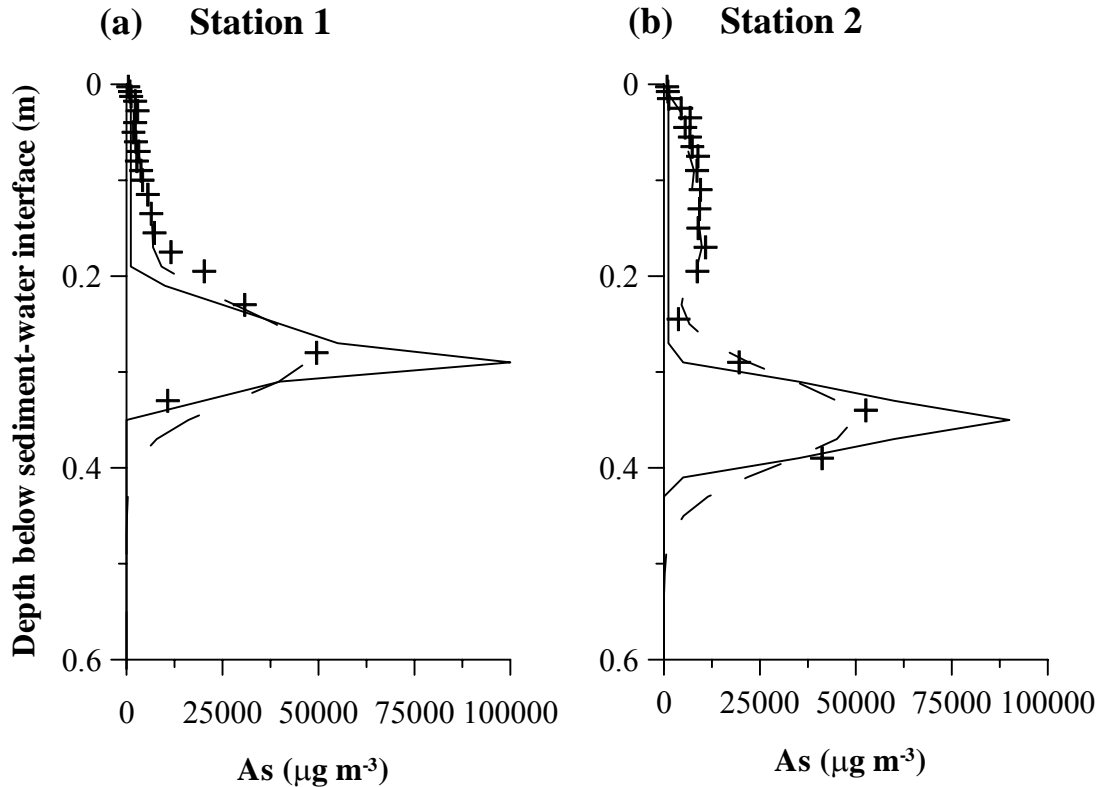


Figure 2.6 (a) and (b): *Response of the numerical model for a simulation time of 2 years (dashed line) compared to the concentrations measured in 1998 (symbols) at Station 1 (a) and at Station 2 (b). The initial concentration of As is represented by the solid line.*

## 2.5 Effect of variable input parameters on the response of the model

Since the flood of 1996, a large amount of data has been collected on the sediments of the Saguenay Fjord. More than 300 stations were sampled to define the geotechnical, geochemical and biological characteristics of the sediments. The collected data show a very strong spatial variability. For example, the thickness of the capping layer varies from 0 m to 2 m, the number of benthic structures (tubes and burrows) can fluctuate from less than  $500 \text{ m}^{-2}$  to more than  $1500 \text{ m}^{-2}$  and the depth of bio-irrigation varies from 0.1 m to more than 0.2 m. These characteristics not only change from station to station, but also show a degree of variability within a single station. Moreover, it is

very difficult to correlate data from samples collected at a given station, but at different times, because the exact positioning of the sampling instruments with respect to the ship location could not be determined most of the time. Also, since the sampling stations were often located at depths greater than 100 m, the tool collecting the sample drifted under the influence of the strong bottom currents.

Although the calibration of the model to the dissolved As profiles at Stations 1 and 2 is satisfactory, those stations do not necessarily reflect the conditions everywhere in the fjord. A series of simulation is presented here to illustrate the variability of the model response for six different cases (Table 2.5). The first four simulations represent the possible evolution of As depending on the cap thickness and the bio-irrigation depth. The last two simulations show the response of the model for a general contaminant, without reactions. All simulations are performed over a period of 5 years and show the evolution of the contamination at a simulated time of 1 day, 2 years and 5 years. The initial concentration of contaminant in the capping layer is zero.

Table 2.5: *Specific characteristics of the simulations and total mass of contaminant released from the upper boundary of the system 5 years after the capping event.*

Simulation	Cap thickness (m)	Depth of bio-irrigation (m)	Dissolution	Contaminant flux entering the Fjord ( $\mu\text{g m}^{-2}$ )
1	0.2	0.2	Y	5791
2	0.2	0.1	Y	2421
3	0.1	0.2	Y	5791
4	0.1	0.1	Y	2422
5	0.14	0.2	N	1729
6	0.14	0.1	N	101

The evolution of contamination using the same input parameters as those used for Station 1 (Table 2.2 and 2.4) is shown in Figure 2.7a. In that case, the cap is 0.2 m thick and the bio-irrigation reaches a depth of 0.2 m, which means that the worm tubes completely penetrate the clean sediments and create a direct connection between the contaminated sediments and the well oxygenated water of the fjord. The contact between the bio-irrigated oxygenated water and the As associated to FeS in the sediments leads to

the release of As next to the tubes and burrows. This process is clearly shown by the rapid increase of the concentration in the first 0.2 m below the sediment-water interface. A similar simulation, with a depth of bio-irrigation reduced to 0.1 m, is shown in Figure 2.7b. In this case, the worm tubes do not completely penetrate the clean sediment cap. The upper part of the graphic shows a different trend compared to the previous simulation with concentrations of dissolved As decreasing above the contaminated sediments, with a minimum value at about 0.14 m, and then increasing again to a second maximum. The asymmetry observed in the upper part of the sediments after a simulation time of 2 years becomes smoother and finally disappears after 5 years. The lower section of the sediments follows the normal evolution of a diffusing contaminant peak, showing a symmetric trend. The bio-irrigation causes the subdivision of the concentrations in two regions: an upper region controlled by the pumping activity of the benthic fauna and a lower region dominated by diffusive processes.

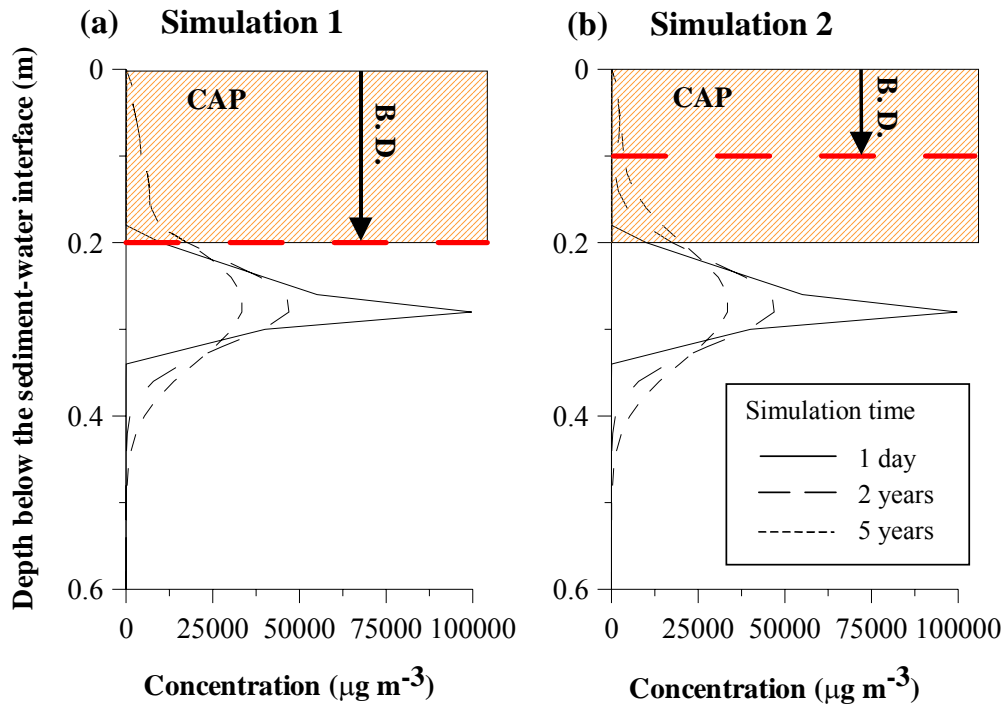


Figure 2.7 (a) and (b): *Evolution of contamination after the deposition of a capping layer of 0.2 m. The bio-irrigation depth (B. D.) attains 0.2 m in Simulation 1 (a) and 0.1 m in Simulation 2 (b).*

The next simulation (simulation 3) shows the evolution of the contamination for sediments with a bio-irrigation depth of 0.2 m and a capping layer of only 0.1 m in thickness (Figure 2.8a). The effect of bio-irrigation is clearly illustrated by the decrease of the concentration peak from  $100\ 000\ \mu\text{g m}^{-3}$  to  $25\ 000\ \mu\text{g m}^{-3}$  within 2 years. This decrease results from the exchange of dissolved As between the sediments and the tubes. Once the contaminant is transferred from the sediment pores to the tubes, it is pumped very rapidly towards the upper boundary. On the other hand, bio-irrigation brings oxygenated water into the sediments, inducing the dissolution of As associated to FeS, and thus maintaining the dissolved As concentration in the upper 0.2 m of the sediments at a relatively high concentration. For simulation 4, the depth of bio-irrigation is reduced to 0.1 m, which modifies the simulated concentration profile as shown in Figure 2.8b. In this case, the effect of bio-irrigation is weaker but can still be recognized in the asymmetrical contaminant distribution, which shows a slightly higher concentration in the upper few centimeters. Because the bio-irrigation depth does not reach the contaminated layer, the peak decreases more slowly.

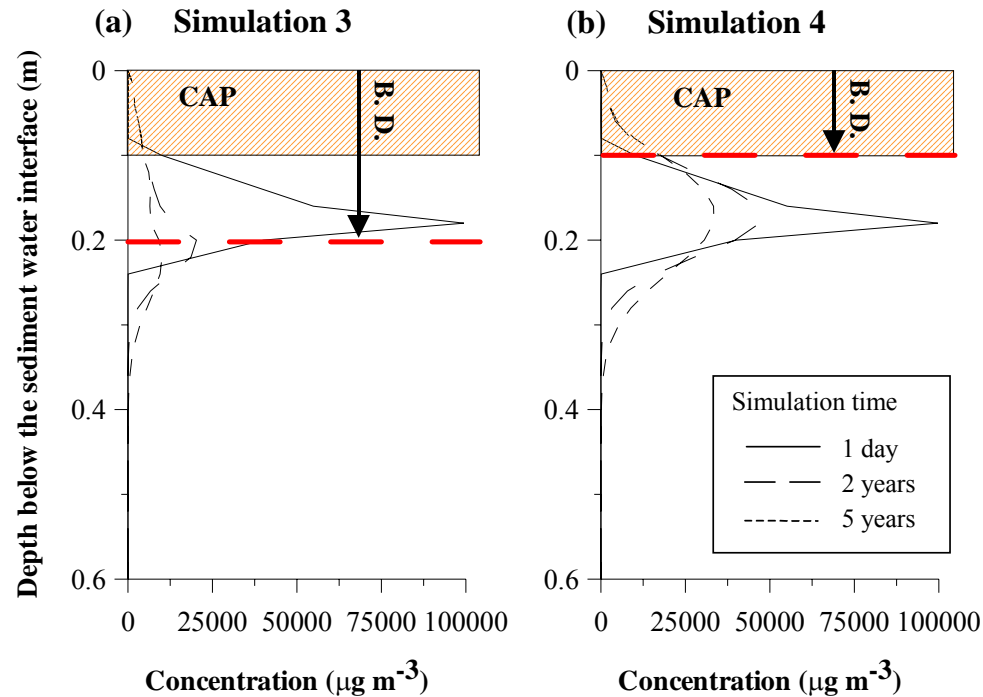


Figure 2.8 (a) and (b): *Evolution of contamination after the deposition of a capping layer of 0.1 m. The bio-irrigation depth attains 0.2 m in Sim. 3 (a) and 0.1 m in Sim. 4 (b).*

The last two simulations investigate the case of a non-reactive contaminant, where "non-reactive" means a compound that does not undergo dissolution following the exposure to oxygen. In fact dissolution may not affect the fate of other inorganic compounds. Figures 2.9a and 2.9b illustrate the response of the model for a non-reactive contaminant for a capping layer of 0.14 m and two different values of bio-irrigation depth, equal to 0.1 m and 0.2 m. The concentrations in the first 0.2 m below the sediment-water interface (Figure 2.9a) are smaller than those for the reactive case (Figures 2.7a and 2.8a). This difference comes from the exclusion of the dissolution term, thus the lack of a contaminant source in the bio-irrigated layer. A similar trend exists for the case where the bio-irrigation depth is equal to 0.2 m (Figure 2.9b). The absence of dissolution produces smaller concentrations in the bio-irrigated layer compared to reactive cases of Figures 2.7b and 2.8b. The profile in Figure 2.9b is also more symmetrical than those presented in Figures 2.7b and 2.8b.

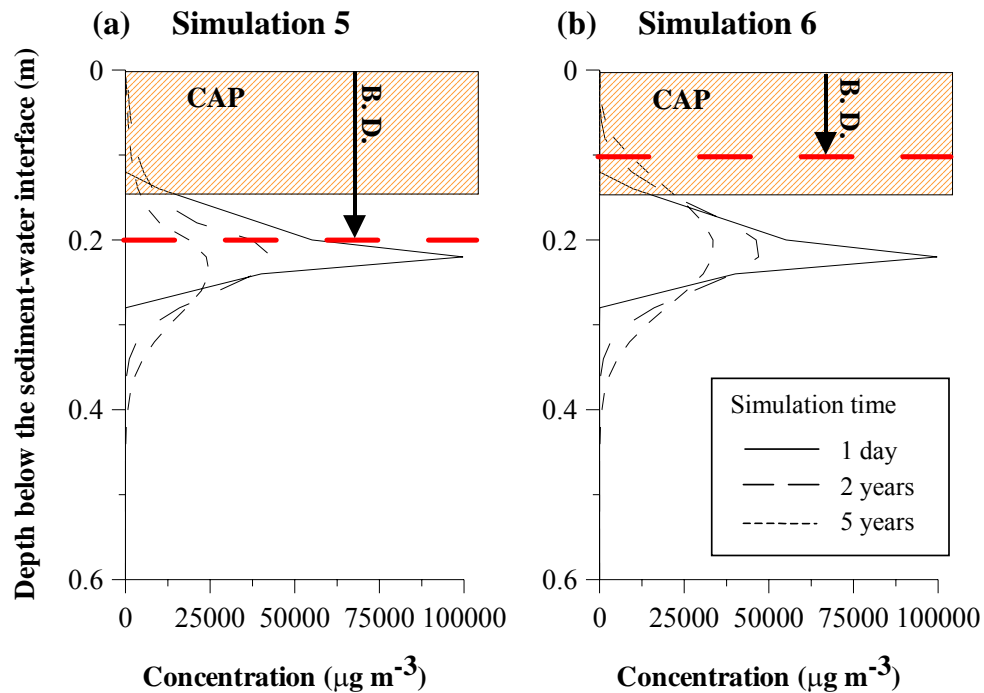


Figure 2.9 (a) and (b): *Evolution of contamination for a non-reactive contaminant after the deposition of a capping layer of 0.14 m. The bio-irrigation depth attains 0.2 m in Sim. 5 (a) and 0.1 m in Sim. 6 (b).*

The total mass of contaminant released from the upper boundary of the model, 5 years after capping, is presented in Table 2.5 for the six simulations. After 5 years, the total mass of contaminant that reaches the water column in simulation 1 is  $5791 \mu\text{g m}^{-2}$  for a bio-irrigation depth of 20 and it is equal to  $2421 \mu\text{g m}^{-2}$  for simulation 2 with a reduced bio-irrigation depth of 0.1 m. These results indicate that the depth of bio-irrigation has an important effect on the contaminant mass leaving the sediments from the upper boundary. On the other hand, simulations 3 and 4 show similar results to the ones obtained for the first two simulations. Since simulations 3 and 4 only differ from simulations 1 and 2 by the thickness of the capping layer, this thickness does not seem to influence the total contaminant flux at the upper boundary. For simulations 5 and 6, the simulated mass released is much smaller than for the simulations with dissolution. This result is not surprising, because dissolution increases the amount of dissolved contaminant in the bio-irrigated layer, enhancing the mass leaving from the upper boundary of the sediments. Thus, the lack of dissolution leads to smaller concentrations in the bio-irrigated layer and to a smaller release of contaminant. Comparing simulation 5 and 6, we observe that in simulation 6, where the bio-irrigation depth is only 0.1 m, the release of contaminant is much smaller. This result indicates that if the burrows do not reach the contaminated layer the release of contaminant will be minimal. Thus for the case without dissolution, the bio-irrigation depth as well as the thickness of the capping layer are the more significant factors in preventing the contaminant release.

The cumulative contaminant mass released by the sediments for the 5-year period, shown in Figure 2.10, reveals the effect of the depth of bio-irrigation and dissolution on mass release. For the case with dissolution (simulations 1 and 2), the total mass release follows a linear trend with a gradient depending on the depth of bio-irrigation. Conversely, for a non-dissolving contaminant (simulation 5 and 6), the release decreases with time and the cumulated mass seems to be heading towards a plateau.

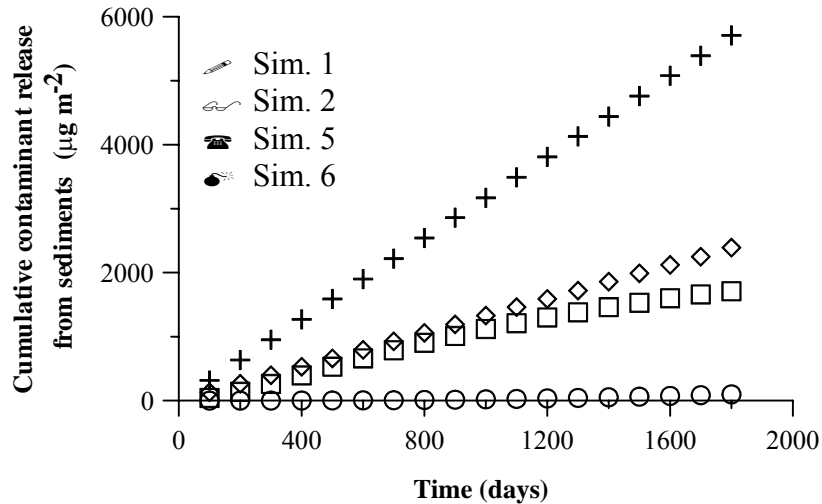


Figure 2.10: *Predicted contaminant release from the sediments to the water column, over period of 5 years, for a contaminant undergoing dissolution (Sim. 1 and 2) and for a non-reactive contaminant (Sim. 5 and 6).*

## 2.6 Summary and conclusion

A numerical model that simulates one-dimensional vertical migration of dissolved compounds through a sediment cap is presented. The model has been calibrated with the dissolved As concentrations in the sediments, measured at two sampling stations in the Saguenay Fjord. A good match of the simulated and measured values indicates that the model can represent the evolution of As through a sediment cap. The calibrated simulations represent a "worst case scenario" and for the inorganic contaminants present in the sediments of the Fjord (Hg, Pb, Zn, Cu) a smaller release is expected.

Detailed data collection for the fjord's sediments indicates that physical and chemical parameters are quite variable and change according to the location of the sampling station. To illustrate how the variability of the input parameters might affect the response of the model, we present the results of hypothetical simulations where the bio-irrigation depth and the thickness of the capping layer are varied. Also, in an attempt to

represent the possible evolution of the contamination for other dissolved compounds, some simulations that exclude the dissolution term from the transport equation are presented. The model was also used to calculate the total mass of contaminant that left the sediments from the upper boundary at the end of the simulation. If we compare these values for the first series of simulations, we notice that the bio-irrigation depth has a more significant influence on the release of contaminant than the thickness of the capping layer. In fact, for a contaminant having properties similar to those of As, which undergoes dissolution if exposed to oxygenated water, the contaminant concentration in the bio-irrigated layer is dominated by the dissolution reaction and this process controls the release of contaminant. On the other hand, for a non-reactive contaminant (simulations 5 and 6) the release of contaminant is highly reduced and depends very much on the penetration depth of the tubes compared to the cap thickness. The release will be increased only if the tubes reach the contaminated layer. Whether or not there is dissolution, the depth of bio-irrigation is a very important factor.

A comparison of the dissolved concentrations calculated by the model for the upper boundary of the sediments with the water quality criteria recommended by the USEPA (USEPA 1999) shows that the As concentration does not exceed the Criterion Continuous Concentration for saltwater, which is equal to  $36\,000 \mu\text{g m}^{-3}$ . This criterion is an estimate of the highest concentration to which an aquatic community can be exposed indefinitely without resulting in an unacceptable effect. Moreover the As released through oxidation of FeS will migrate to the new sediment-water interface where As(III) will be oxidized to As(V) and adsorbed to oxihydroxides. Thus a significant fraction of the released As will precipitate again at the surface of the sediments with the iron oxides and only a small part will be transferred to the overlying water. In addition As leaving the sediments from the upper boundary will not accumulate in the water layer over the sediments, but will be transported by the bottom currents, thus mixing and diluting with the bottom water. Therefore we do not expect the released As to become an environmental problem in the case of the Saguenay Fjord.

Even if the Saguenay Fjord does not present real concern regarding the concentration of dissolved As in the water column, it is very instructive to study the evolution of this compound through the capping layer. In fact the data collected after the flood event could be used to calibrate the model and assess the importance of bio-irrigation in the transport of As. To better understand the system and its interactions, additional simulations are needed to incorporate in more details the variability and the uncertainty of the input parameters. A detailed sensitivity analysis, based on factorial design, has been undertaken to identify the parameters with the most significant effect on the response of the model.

## 2.7 References

- Aggett, J. and O'Brien, G. A. 1985. Detailed model for the mobility of arsenic in lacustrine sediments based on measurements in Lake Ohakuri. *Environ. Sci. Technol.* **19**: 231-238.
- Aller, R. C. 1980. Quantifying solute distributions in the biotubated zone of marine sediments by defining an average microenvironment. *Geochim. Cosmochim. Acta* **44**: 1955-1965.
- Aller, R. C. and Aller, J. Y. 1998. The effect of biogenic irrigation intensity and solute exchange on diagenetic reaction rates in marine sediments. *J. Mar. Res.* **56**: 905-936.
- Aller, R. C. and Yingst, J. Y. 1978. Biogeochemistry of tube-dwellings: A study of the sedentary polychaete *Amphitrite ornata* (Leidy). *J. Mar. Res.* **36**(2): 201-254.
- Aller, R. C. and Yingst, J. Y. 1985. Effects of the marine deposit-feeders *Heteromastus filiformis* (Polychaeta), *Macoma balthica* (Bivalvia), and *Tellina texana* (Bivalvia) on averaged sedimentary solute transport, reaction rates, and microbial distributions. *J. Mar. Res.* **43**: 615-645.
- Archer, D. and Devol, A. 1992. Benthic oxygen fluxes on the Washington shelf and slope: A comparison of in situ microelectrode and chamber flux measurements. *Limn. Oceanogr.* **37**(3): 614-629.
- Barbeau, C., Bougie, R. and Côté, J.-E. 1981. Temporal and spatial variations of mercury, lead, zinc and copper in sediments of the Saguenay fjord. *Can. J. Earth Sci.* **18**: 1065-1074.

- Belzile, N. and Tessier, A. 1990. Interactions between arsenic and iron oxyhydroxides in lacustrine sediments. *Geochim. Cosmochim. Acta* **54**: 103-109.
- Boudreau, B. P. 1984. On the equivalence of nonlocal and radial diffusion models for porewater irrigation. *J. Mar. Res.* **42**: 731-735.
- Boudreau, B. P. 1999. Metals and models: Diagenetic modelling in freshwater lacustrine sediments. *J. Paleolimn.* **22**: 227-251.
- Boyer, J. M., Chapra, S. C., Ruiz, C. E. and Dortch, M. S. 1994. RECOVERY, a mathematical model to predict the temporal response of surface water to contaminated sediments. Technical report W-94-4, U.S. Army Engineer Waterways Experiment Station, Vicksburg, MS.
- Cossa, D. 1990. Chemical contaminants in the St. Lawrence Estuary and Saguenay Fjord. In : El-Sabh, M. I., Silverberg, N. (Eds.), *Oceanography of a large scale estuarine system, The St. Lawrence. Coastal and Estuarine Studies* **39**: 239-268, Springer Verlag.
- De Montety, L., Long, B., Desrosiers, G., Crémer, J.-F. and Locat, J. 2000. Quantification des structures biogènes en fonction d'un gradient de perturbation dans la baie des Ha! Ha! à l'aide de la tomodensitométrie axiale. Proceedings of the 53th Canadian Geotechnical Conference, Montréal, 15-18 Oct. 2000, Vol. 1, pp. 131-135.
- Domenico, P. A. and Schwartz, F. W. 1998. *Physical and chemical hydrogeology*. Wiley, New York.
- Emerson, S., Jahnke, R. and Heggie, D. 1984. Sediment-water exchange in shallow water estuarine sediments. *J. Mar. Res.* **42**: 709-730.
- Forster, S. and Graf, G. 1995. Impact of irrigation on oxygen flux into the sediment: intermittent pumping by Callianassa subterranea and "piston-pumping" by Lanice conchilega. *Mar. Biol.* **123**: 335-346.
- Fuller, W. H. 1978. Investigation of landfill leachate pollutant attenuation by soils. US EPA, Municipal Environmental Research Laboratory, Cincinnati, OH
- Furukawa, Y., Bentley, S. J., Shiller, A. M., Lavoie, D. L. and Van Cappellen, P. 2000. The role of biologically-enhanced pore water transport in early diagenesis: an example from carbonate sediments in the vicinity of North Key Harbor, Dry Tortugas National Park, Florida. *J. Mar. Res.* **58**: 493-522.
- Furukawa, Y., Bentley, S. J. and Lavoie, D. L. (2001). Bioirrigation modeling in experimental benthic mesocosms. *J. Mar. Res.* **59**: 417-452.

- Gagnon, C., Pelletier, É. and Maheu, S. 1993. Distribution of trace metals and some major constituents in sediments of the Saguenay Fjord, Canada. *Mar. Pollut. Bull.* **26** (2): 107-110.
- Gobeil C. and Cossa D. 1984. Profils des teneurs en mercure dans les sédiments et les eaux interstitielles du fjord du Saguenay (Québec): données acquises au cours de la période 1978-83. *Rapport Technique Canadien Hydrographie et Sciences Océaniques* : **53**.
- Guinasso, N. L. and Schink, D. R. 1975. Quantitative estimates of biological mixing rates in abyssal sediments. *J. Geoph. Res.* **80**: 3032-3043.
- Huerta-Diaz, M. A., Tessier, A. and Carignan, R. 1998. Geochemistry of trace metals associated with reduced sulfur in freshwater sediments. *Appl. Geochem.* **13**: 213-233.
- Jorgensen, B. B. and Revsbech, N. P. 1985. Diffusive boundary layers and the oxygen uptake of sediments and detritus. *Limn. Oceanogr.* **30**(1): 111-122.
- Locat, J. and Leroueil, S. 1987. Physicochemical and geotechnical characteristics of recent Saguenay Fjord sediments. *Can. Geotech. J.* **25**: 382-388
- Marinelli, R. L. and Boudreau, B. P. 1996. An experimental and modeling study of pH and related solutes in an irrigated anoxic coastal sediment. *J. Mar. Res.* **54**: 939-966.
- Martin, W. R. and Banta, G. T. 1992. The measurement of sediment irrigation rates: A comparison of the  $\text{BR}^-$  tracer and  $^{222}\text{RN}/^{226}\text{RA}$  disequilibrium techniques. *J. Mar. Res.* **50**: 125-154.
- Matisoff, G., Wang, X. 1998. Solute transport in sediment by freshwater infaunal bioirrigators. *Limn. Oceanogr.* **43**(7): 1487-1499.
- Maurice, F. 2000. Caractéristiques géotechniques et évolution de la couche de sédiment déposée lors du déuge de 1996 dans la Baie des Ha! Ha! (Fjord du Saguenay, Québec). M.Sc. Thesis, Université Laval.
- McCaffrey, R. J., Myers, A. C., Davey, E., Morrison, G., Bender, M., Luedtke, N., Cullen, D., Froelich, P. and Klinkhammer, G. 1980. The relation between pore water chemistry and benthic fluxes of nutrients and manganese in Narragansett Bay, Rhode Island. *Limn. Oceanogr.* **25**(1): 31-44.
- Meyers, M. B., Fossing, H. and Powell, E. N. 1987. Microdistribution of interstitial meiofauna, oxygen and sulfide gradients, and the tubes of macro-infauna. *Mar. Ecol. Progr. Ser.* **35**: 223-241.

- Mohan, R. K., Mageau, D. W. and Brown, M. P. 1999. Modeling the geophysical impacts of underwater in-situ cap construction. *Mar. Tech. Soc. J.* **33**(3): 80-87.
- Mohan, R. K., Brown, M. P. and Barnes, C. R. 2000. Design criteria and theoretical basis for capping contaminated marine sediments. *Appl. Ocean Res.* **22**: 85-93.
- Morse, J. W. 1994 . Interactions of trace metals with authigenic sulfide minerals: implications for their bioavailability. *Mar. Chem.* **46**: 1-6.
- Mucci, A. and Edenborn, H. M. 1992. Influence of an organic-poor landslide deposit on the early diagenesis of iron and manganese in coastal marine sediment. *Geochim. Cosmochim. Acta* **56**: 3909-3921.
- Mucci, A., Guignard, C. and Olejczuk, P. 2000a. Mobility of metals and As in sediments following a large scale episodic sedimentation event. Proceedings of the 53th Canadian Geotechnical Conference, Montréal, 15-18 Oct. 2000, Vol. 1, pp. 169-175.
- Mucci, A., Richard, L.-F., Lucotte, M. and Guignard, C. 2000b. The differential geochemical behaviour of arsenic and phosphorous in the water column and sediments of the Saguenay fjord estuary, Canada. *Aquatic Geochem.* **6**: 293-324.
- Neville C. J., Ibaraki, M. and Sudicky, E. A. 2000. Solute transport with multiprocess nonequilibrium: a semi-analytical solution approach. *J. Cont. Hydr.* **44**: 141-159.
- O'Day, P. A., Carroll, S. A., Randall, S., Martinelli, R. E., Anderson, S. L., Jelinski, J. and Knezovich, J. P. 2000. Metal speciation and bioavailability in contaminated estuary sediments, Alameda Naval Air Station, California. *Environ. Sci. Technol.* **34**: 3665-3673.
- Park, S. S. and Jaffé P. R. 1996. Development of a sediment redox potential model for the assessment of postdepositional metal mobility. *Ecol. Model.* **91**: 169-181.
- Pelletier, E. Desrosiers, G., Locat, J., Mucci, A. and Tremblay, H. 2003. The origin and behavior of a flood capping layer deposited on contaminated sediments of the Saguenay Fjord (Quebec). In: *Contaminated sediments: Characterization, Evaluation, Mitigation/Restoration and Management strategy Performance*, ASTM STP1442, J. Locat, R. Galvez-Cloutier, R.C. Chaney, and K.R. Demars, Eds. ASTM International, West Conshohocken, PA, pp. 3-18.
- Pelletier , E. and Canuel G. 1988. Trace metals in surface sediment of the Saguenay fjord, Canada. *Mar. Pollut. Bull.* **19**: 336-338
- Perret, D. 1995. Diagenèse mécanique précoce des sédiments fins du fjord du Saguenay. Ph.D Thesis, Université Laval

- Petersen, W., Willer, E. and Willamowski, C. 1997. Remobilization of trace elements from polluted anoxic sediments after resuspension in oxic water. *Wat. Air Soil Poll.* **99**: 515-522.
- Petersen, K., Kristensen, E. and Bjerregaard, P. 1998. Influence of bioturbating animals on flux of cadmium into estuarine sediment. *Mar. Environ. Res.* **45**(4/5): 403-415.
- Reible, D. D., Popov, V., Valsaraj, K. T., Thibodeaux, L. J., Lin, F., Dikshit, M., Todaro, M. A. and Fleeger, J. W. 1996. Contaminant fluxes from sediment due to tubificid oligochaete bioturbation. *Wat. Res.* **30** (3): 704-714.
- Riedel, G. F., Sanders, J. G. and Osman, R. W. 1987. The effect of biological and physical disturbances on the transport of arsenic from contaminated estuarine sediments. *Estuarine, Coast. Shelf Sci.* **25**: 693-706.
- Riisgard, H. U. 1989. Properties and energy cost of the muscular piston pump in the suspension feeding polychaete *Chaetopterus varioipedatus*. *Mar. Ecol. Progr. Ser.* **56**: 157-168.
- Riisgard, H. U. 1991. Suspension feeding in the polychaete *Nereis diversicolor*. *Mar. Ecol. Progr. Ser.* **70**: 29-37.
- Riisgard, H. U., Vedel, A., Boye, H. and Larsen, P. S. 1992. Filter-net structure and pumping activity in the polychaete *Nereis diversicolor* : effects of temperature and pump-modelling. *Mar. Ecol. Progr. Ser.* **83**: 79-89.
- Rivera-Duarte, I. and Flegal, A. R. 1994. Benthic lead fluxes in San Francisco Bay, California, USA. *Geochim. Cosmochim. Acta* **58**: 3307-3313.
- Ruiz, C. E., Schroeder, P. R. and Aziz, N. M. 2000. RECOVERY: A contaminant sediment-water interaction model. ERDC/EL SR-D-00-1, U.S. Army Engineer Research and Development Center, Waterways Experiment Station, Vicksburg, MS.
- Saulnier, I. and Mucci, A. 2000. Trace metal remobilization following the resuspension of estuarine sediments: Saguenay Fjord, Canada. *Appl. Geochem.* **15**: 191-210
- Simpson, S. L., Rosner, J. and Ellis, J. 2000. Competitive displacement reactions of cadmium, copper, and zinc added to a polluted, sulfidic estuarine sediment. *Environ. Toxicol. Chem.* **19**: 1992-1999.
- Soetaert, K., Herman, P. M. J. and Middelburg J. J. 1996. A model of early diagenetic processes from the shelf to abyssal depths. *Geochim. Cosmochim. Acta* **60**(6): 1019-1040.

- Tremblay, G.-H. and Gobeil, C. 1990. Dissolved arsenic in the St Lawrence Estuary and the Saguenay Fjord, Canada. *Mar. Pollut. Bull.* **21**(10): 465-469.
- Tremblay, H., Desrosiers, G., Locat, J., Mucci, A. and Pelletier, É. 2003. Characterization of a catastrophic flood sediment layer: geological, geotechnical, biological, and geochemical signatures. In: *Contaminated sediments: Characterization, Evaluation, Mitigation/Restoration and Management strategy Performance*, ASTM STP1442, J. Locat, R. Galvez-Cloutier, R.C. Chaney, and K.R. Demars, Eds. ASTM International, West Conshohocken, PA, pp. 87-101.
- USEPA 1999. National recommended water quality criteria - Correction. United States Environmental Protection Agency, Office of Water 4304. EPA 822-Z-99-001.
- Vanysek P. 2000. Ionic Conductivity and diffusion at infinite dilution. In CRC handbook of chemistry and physics, 81st edition, Cleveland, Ohio.
- Versteeg, H.K. and Malalasekera, W. 1995. An introduction to computational fluid dynamics : the finite volume method. Longman Scientific & Technical, Burnt Mill, Harlow, Essex.
- Wang, X. and Matisoff, G. 1997. Solute transport in sediments by a large freshwater oligochaete, *Brachiura sowerbyi*. *Environ. Sci. Technol.* **31**: 1926-1933.
- Wang, Y. and Van Cappellen, P. 1996. A multicomponent reactive transport model of early diagenesis: application to redox cycling in coastal marine sediments. *Geochim. Cosmochim. Acta* **60**(16): 2993-3014.
- Zeman, A. J. 1994. Subaqueous capping of very soft contaminated sediments. *Can. Geotech. J.* **31**: 570-577.
- Zheng, C. and Bennett, G. D. 2002. *Applied Contaminant Transport Modeling*. 2<sup>nd</sup> edition, John Wiley, New York.

**CHAPITRE 3 FACTORS CONTROLLING  
CONTAMINANT TRANSPORT THROUGH THE  
FLOOD SEDIMENTS OF THE SAGUENAY FJORD:  
NUMERICAL SENSITIVITY ANALYSIS**

## Résumé

En juillet 1996 la région du Saguenay fut marquée par un déluge exceptionnel qui causa la crue des rivières et entraîna la déposition de plusieurs millions de mètres cubes de sédiments propres dans le fjord du Saguenay. Cette couche de turbidite, composée de sédiments propres représente une barrière contre la migration de métaux lourds et de HAP de la couche contaminée sous-jacente vers la nouvelle interface sédiments-eau. Un modèle numérique a été développé pour simuler la migration verticale et la remobilisation de contaminants dissous dans la couche de recouvrement naturelle. Le modèle représente les principaux processus physiques, chimiques et biologiques qui influencent le transport de soluté dans une colonne de sédiment. Le calage du modèle a été réalisée avec les profils de concentration de l'arsenic dissous dans les sédiments qui ont été mesurés à deux stations du fjord du Saguenay. Une analyse de sensibilité détaillée, basée sur la méthode du design factoriel, montre que les paramètres du modèle associés à la bio-irrigation ont un impact important sur la réponse du modèle et donc sur l'efficacité d'une couche de recouvrement.

## Abstract

In July 1996, two days of intense rainfall caused severe flooding in the Saguenay region and led to the discharge by rivers of several million cubic meters of clean sediments to the Saguenay Fjord. This turbidite layer, composed of clean sediments, represents a potential barrier for the migration of heavy metals and PAHs from the underlying contaminated sediments towards the new sediment-water interface. A numerical model has been developed to simulate the vertical migration and remobilization of dissolved contaminants in the capping layer. The model includes the main physical, chemical and biological factors affecting the transport of a dissolved compound in a sediment column. Calibration of the model has been achieved through comparison with the profiles of dissolved arsenic in the sediments, measured at two sampling stations of the Saguenay Fjord. A detailed sensitivity analysis, based on factorial design, shows that the model parameters associated with bio-irrigation have the greatest impact on the model output and by extension on the effectiveness of a capping layer.

### 3.1 Introduction

The capping of contaminated sediments with clean material is considered as a promising alternative for the isolation of contaminants from the water column and the prevention of the diffusion of pollution through the ecosystem. This approach has the advantage of being applicable to large contaminated surfaces. A capping layer is designed to physically isolate the contaminants from the benthic fauna, stabilize the sediments, and prevent or at least reduce the contaminant flux towards the new water-sediment interface. Any attempt to predict the long-term effectiveness of the cap requires an understanding of the physical, chemical and biological factors affecting the migration of contaminants in the sediments.

The TRANSCAP-1D numerical model was developed to simulate the migration of dissolved contaminants through a subaqueous capping layer. The model considers the physical, chemical and biological processes affecting the fate of a dissolved contaminant in a sedimentary environment and can be used to predict the effectiveness of a sediment cap in isolating the contaminant from the water column. The transport equation includes advection, diffusion and the effect of bio-irrigating worms.

The model has been applied to the Saguenay Fjord, where a major flood led to the deposition of a natural capping layer over contaminated sediments. Since the catastrophic flood, which occurred in 1996, the geotechnical and geochemical characteristics of the capping layer, as well as the recolonisation of the benthic fauna, have been extensively studied in the context of a multidisciplinary research project. The ultimate objective of this research project is to assess if the new capping layer effectively isolates the contaminants from the water column. A large database was available for the model calibration and the response of the numerical model was successfully matched to concentrations of dissolved arsenic measured in the Saguenay Fjord. Arsenic is not a contaminant in the Saguenay Fjord, but the calibration of the model required profiles of the dissolved concentration in the sediment column, and those data were only available for this compound.

Sensitivity analysis is commonly used in engineering to assess the influence of a model input on the output. The simplest form of sensitivity analysis consists in increasing or decreasing the value of one input parameter at a time by some fraction, or perturbation, and then to evaluate the corresponding variation in the model output. This procedure is repeated for each parameter tested and the parameter causing the greatest modification in the model output is deemed the most important. Although this approach is simple and commonly used, there is no guideline for the selection of parameters to evaluate and for the magnitude of the perturbation to impose. In addition, since parameters are evaluated one by one, any significant combined effect of two or more parameters cannot be detected.

Kabala (2001) presents an overview of sensitivity analysis, with an application to pumping tests in aquifers. The definition of sensitivity of model output to input parameters given by Kabala (2001) is more precise than the general definition given above, because it is expressed in a mathematical form as the differential in the model output with respect to selected input parameters. By using this definition, sensitivities can be calculated with more precise mathematical techniques, such as the direct method that requires differentiating the governing equations or the adjoint method that requires solving the governing equation and its mathematical adjoint.

Other approaches have been developed in chemical engineering to determine the combined effect of several parameters on model output. An example is a two-level factorial design, which is used to determine the influence of  $n$  parameters on some observed value with a minimum number of experiments (Box et al. 1978). Two levels, or values, are selected for each parameter and a total of  $2^n$  experiments are sufficient to test the impact of each parameter, as well as every possible combination of parameters, on the experimental output. By limiting the number of trials and still considering all combined effects, the method is well suited for the rapid identification of the main parameters for the model, which could then be studied or characterized in more detail. The application of this method to the sensitivity analysis of numerical models has been very limited, especially in the environmental domain, although it is well suited for that purpose. A

good example of the application of the factorial design to simulation results is presented by Elliott et al. (2000), where the method was used to determine the kinetic parameters with a significant effect on the efficiency of an anaerobic treatment process.

A large variability and uncertainty associated to several physical, chemical and biological parameters was observed for the Saguenay Fjord. This situation requires a systematic approach in order to identify the dominant parameters affecting the fate of contaminants in sediments. To investigate the sensitivities of the model parameters that are either variable or uncertain, a factorial design approach is presented here for the model simulating the migration of contaminants in sediments of the Saguenay Fjord. The purpose of the sensitivity analysis presented here is to deepen our understanding of the effect of variable input values on the model output and to identify the factors that have the greatest influence on the contaminant migration towards the new sediment-water interface.

### **3.2 Model equations and parameters**

The TRANSCAP-1D model simulates advection, diffusion, chemical reactions and the effect of bio-irrigation. The consolidation of the sediments and associated fluid advection are not included. The sediments are represented as a dual porosity medium composed of sediment pores and bio-irrigated tubes. The mathematical formulation consists of two partial differential equations, corresponding to the contaminant transport in the two media. These equations are coupled via a non-local exchange term that represents the mass transfer of contaminant between the sediments and the tubes. The formulation is mathematically similar to the one describing solute transport in a dual-porosity medium, in the context of groundwater flow (for example, Zheng and Bennett 2002).

The equation describing solute transport in the sediment porewater is given by:

$$n_s \frac{\partial C_s}{\partial t} = n_s \cdot \frac{D_s}{Rt} \left( \frac{\partial^2 C_s}{\partial z^2} \right) - n_s \cdot \frac{v_s}{Rt} \cdot \frac{\partial C_s}{\partial z} - \beta(C_s - C_T) \quad (3.1)$$

where  $C_s$  and  $C_T$  are the solute concentration [ $M L^{-3}$ ] in the sediments and the tubes, respectively,  $n_s$  is the sediment porosity [-],  $v_s$  is the fluid velocity in the sediments [ $L T^{-1}$ ],  $Rt$  is the solute retardation factor [-], and  $\beta$  is a first-order mass transfer coefficient [ $T^{-1}$ ]. The dispersion coefficient of the solute in the sediments,  $D_s$  [ $L^2 T^{-1}$ ], is given by:

$$D_s = D_d + \alpha_L \cdot v_s \quad (3.2)$$

where  $D_d$  is the effective diffusion coefficient [ $L^2 T^{-1}$ ] and  $\alpha_L$  is the sediment dispersivity [L]. Note that when the fluid velocity is small in the sediments the dispersion coefficient is approximately equal to the diffusion coefficient.

The equation describing solute transport in the tubes is given by:

$$n_T \frac{\partial C_T}{\partial t} = n_T D_m \frac{\partial^2 C_T}{\partial z^2} - n_T v_T \frac{\partial C_T}{\partial z} + \beta(C_s - C_T) + S \quad (3.3)$$

where  $n_T$  is the porosity of the tubes [-],  $D_m$  is the dispersion coefficient for the tubes [ $L^2 T^{-1}$ ], given by an expression similar to equation (3.2), and  $v_T$  is the fluid or irrigation velocity in the tubes [ $L T^{-1}$ ]. In equation (3.3),  $S$  is a general source or sink term [ $M L^{-3} T^{-1}$ ] representing the release of contaminant from mineral dissolution associated to bio-irrigation. This term is defined later in this section.

The mass transfer coefficient  $\beta$  and the porosity of the tubes  $n_T$  decrease exponentially with depth, following the distribution of bio-irrigated tubes (Martin and Banta 1992). The mass transfer coefficient  $\beta$  can be split in two coefficients  $\beta_1$  [ $T^{-1}$ ] and  $\beta_2$  [ $L^{-1}$ ], representing the maximal value of the mass transfer coefficient at the surface of the sediments and the coefficient of exponential decrease respectively:

$$\beta(z) = \beta_1 \cdot \exp[\beta_2(z - z_{\max})] \quad (3.4)$$

As illustrated by Boudreau (1997), the value of the non-local term  $\beta_1 [T^{-1}]$  at the surface of the sediments can be estimated using the parameters of Aller's cylindrical diffusion model (Aller 1980):

$$\beta_1 = \frac{2 \cdot D_d \cdot r_i}{(r_2^2 - r_i^2)(\delta - r_i)} \quad (3.5)$$

where  $r_i$  is the inner radius of the tubes/burrows [L],  $r_2$  is the half-distance between two tubes/burrows [L] and  $\delta$  is the distance [L] from the burrow axis to a point where the concentration equals the horizontally integrated value.

The porosity of the tubes  $n^\circ_T$  at the surface is calculated using cylinders to approximate their geometry:

$$n^\circ_T = m \cdot r_i^2 \cdot \pi \quad (3.6)$$

where  $m$  represents the quantity of tubes per unit area [ $L^{-2}$ ]. The exponential decrease with depth of the tube porosity can be represented with the same coefficient  $\beta_2 [L^{-1}]$ :

$$n_T(z) = n_T^\circ \cdot \exp[\beta_2(z - z_{\max})] \quad (3.7)$$

The source term  $S$  of the equation for the tubes (3.3) represents a chemical reaction responsible for the remobilization of contaminants. The representation of the chemistry is simplified and the model only considers the dissolution of trace metals, originally adsorbed or coprecipitated with iron-monosulfides (FeS). The model was calibrated with profiles of dissolved arsenic (As), a compound that was extensively

studied in the Saguenay Fjord (Mucci et al. 2000a, 2000b, Salunier and Mucci 2000). In the anoxic zone, As is associated to FeS, but the oxidation of the Fe-sulfides in the bio-irrigated tubes, can lead to the remobilization of this compound. Other trace metals coprecipitate with Fe-sulfides (Ni, Cu, Co, Hg, Pb) and could possibly be affected by the rapid exposure to an oxic environment. However, compared to As, the trace metals that contaminate the Fjord sediments (Hg, Pb, Zn, Cu) are probably less mobile, as they are more likely associated to less reactive mineral phases (e.g. organic matter).

The dissolution mechanism represented in the model is a consequence of the exposure of the anoxic sediments, containing sulfides, to oxygenated water advected in the tubes by bio-irrigation. As observed by Furukawa (2001) the irrigated burrow walls are the interface between oxic-anoxic media and are characterized by steep geochemical gradients and rapid chemical mass transfer. In the model, the dissolution term is composed of a kinetic factor  $\gamma$  [ $L^{-1}$ ] and a coefficient  $L$  [ $ML^{-3}$ ], representing the maximal dissolved contaminant concentration for a given FeS concentration in the sediments. The coefficient  $L$  is derived from the linear correlation between the released As and initial solid FeS that was observed during resuspension tests of Saguenay sediments (Saulnier and Mucci 2000). The source term can be expanded in the following way:

$$S = \gamma(L - C_T) \quad (3.8)$$

$$L = k_1 C_{FeS} + k_2 \quad (3.9)$$

where  $k_1$  and  $k_2$  are regression parameters that can be viewed as dissolution coefficients and  $C_{FeS}$  [ $ML^{-3}$ ] is the concentration of FeS.

Initial and boundary conditions are required to solve both equations (3.1) and (3.3). To impose the initial conditions one specifies the initial solute concentration in the two domains, sediments and tubes. Boundary conditions are required at the top and

bottom of the domain and can be either a prescribed concentration or prescribed mass flux for both domains.

The two governing equations (3.1) and (3.3) are discretized with the finite volume method (Versteeg and Malalasekera 1995). The equations are coupled through the mass exchange term and a simultaneous solution for the concentration in the sediments and tube is obtained for each finite volume. The system of equations is thus solved in a fully-coupled fashion, avoiding the use of iteration that is necessary when the equations are decoupled. The block tridiagonal matrix resulting from the discretization and assembly of the terms is solved using Thomas algorithm adapted to block matrices. The numerical solution was tested by comparing to the semi-analytical solution of Neville et al. (2000), which has been developed for one-dimensional solute transport in a dual porosity medium with multiple non-equilibrium processes. The numerical model reproduced almost perfectly the concentrations computed with the analytical solution (results not presented).

### **3.3 Design of the Sensitivity Analysis**

The first step of the two-level factorial design is to determine the number of factors, or parameters, that have to be tested and define the two levels, which are the minimum and maximum value for each input parameter. Each factor is assumed independent of the other factors, but a factor can be composed of a set of dependent input values. For  $n$  factors at two levels each, a total of  $2^n$  simulations are necessary for a full factorial design.

The choice of the parameters to be tested is based on the available information about the processes affecting the migration of contaminants in the sediments of the Saguenay Fjord. At the study site the sediments show a low permeability but are intensively bio-irrigated. Thus bio-irrigation, dissolution and retardation are supposed to influence the migration of contaminant. Consequently, a factorial design with five factors

was selected: three factors related to bio-irrigation (number of tubes per square meter, depth of the tubes and bio-irrigation velocity) one factor related to the reactions (dissolution coefficients) and the retardation factor. The fluid velocity in the sediments  $v_s$  was not considered for the sensitivity analysis because in the sediments of the Saguenay Fjord there is no evidence for such advection. This parameter was therefore set equal to zero for all simulations.

The minimum and maximum values of each tested parameter were determined from the available information, which includes data measured at the Saguenay Fjord and data derived from the literature. The values of the parameters are discussed in the following paragraphs and are presented in Table 3.1.

Table 3.1: *Minimum and maximum values for the tested factors*

Factor	Parameters	Name (Units)	Minimum	Maximum
Bio-Irrigation Depth $B_1$	Depth of Tubes	$b_{\text{iox}}$ (m)	0.06	0.26
	Mass Transfer Coefficient	$\beta_2$ ( $\text{m}^{-1}$ )	70	16
Number and Dimension of Tubes $B_2$	Porosity of Tubes at Surface	$n_{T0}$ (-)	0.00039	0.00471
	Mass Transfer Coefficient	$\beta_1$ ( $\text{d}^{-1}$ )	0.0157	0.119
Retardation Factor $R_t$		$R_t$ (-)	5	45
Bio-Irrigation Velocity $V$		$v_T$ ( $\text{m d}^{-1}$ )	0.2	5
Dissolution Coefficients $D$		$k_1$ ( $\text{g}^2 \text{ mol}^{-1} \text{ L}^{-1}$ )	1	1.7
		$k_2$ ( $\mu\text{g L}^{-1}$ )	1	1.3

The depth of bio-irrigation is represented in the model by two parameters: the maximum depth attained by the tubes,  $b_{\text{iox}}$ , and the corresponding coefficient  $\beta_2$ , where  $\beta_2$  describes the exponential decrease of both the mass transfer between tubes and sediments  $\beta$  and the tube porosity  $n_T$ . The two parameters,  $b_{\text{iox}}$  and  $\beta_2$ , are related since the maximum depth corresponds to the location where the mass transfer  $\beta$  and the tube porosity  $n_T$  exponentially tend to zero. According to field observations and to measured bioturbation intensities (De Montety et al. 2000), the minimal value of the bio-irrigation

depth biox was set to 0.06 m and the maximal value to 0.26 m. This corresponds to values of  $\beta_2$  equal to  $70 \text{ m}^{-1}$  and  $16 \text{ m}^{-1}$ , respectively.

The number and the dimension of the tubes in the upper sediment layer are an indicator of the intensity of bio-irrigation in this zone. This factor affects two input values of the model: the tube porosity at the surface  $n^o_T$  and the mass transfer coefficient  $\beta_1$ . To calculate these parameters, one must first set the minimum and maximum values of the inner radius of the tubes  $r_1$ , as well as the number of tubes per square meter,  $m$ . The value of  $m$  also defines the half-distance between two tubes  $r_2$  according to:

$$r_2 = \frac{1}{2\sqrt{m}} \quad (3.10)$$

The value of  $r_1$  results from observation on sediments sampled with a box-corer in the Saguenay Fjord during summer 1999 and 2000 and varies between 0.0005 m and 0.001 m. The minimum and maximum values of the number of tubes  $m$  were visually determined from photographs of the undisturbed bottom sediments, taken during the summer of 2001, and are equal to 500 and 1500 tubes per square meter, respectively. Thus, the mass transfer coefficient  $\beta_1$  may vary between  $0.0157 \text{ d}^{-1}$  and  $0.119 \text{ d}^{-1}$ , whereas the tube porosity  $n^o_T$  varies between 0.00039 and 0.00471.

The value for the retardation factor,  $R_t$ , has been estimated from the model calibration on two measured arsenic concentration profiles and taking into account the average of the range of values presented by Fuller (1978) for arsenic. The minimum and maximum values of  $R$  have thus been set to 5 and 45, respectively.

The values for the bio-irrigation velocity  $v_T$  were derived from data measured during laboratory tests carried out on polychaete families living in shallow water (Riisgard 1989, Riisgard 1991). In the calibrated model, the irrigation velocity is equal to  $1 \text{ m d}^{-1}$ . The minimum and maximum values for the factorial design were determined by

modifying this value by a factor of five. Thus, we obtain a minimum bio-irrigation velocity of  $0.2 \text{ m d}^{-1}$  and a maximum value of  $5 \text{ m d}^{-1}$ .

The minimum and maximum values of the dissolution coefficients  $k_1$  and  $k_2$  were derived from the linear correlation between the dissolved As and solid FeS measured at two sampling stations of the Saguenay Fjord in 1998 (Saulnier and Mucci 2000). To define the levels of these parameters, it has been assumed that the regression coefficients, determined by means of the measured data, correspond to the minimum and maximum values of the dissolution coefficients. Thus, we assume that  $k_1$  varies between 1 and 1.7 and that  $k_2$  varies between 1 and 1.3.

The input parameters that were not tested in the present sensitivity analysis were set to constant values according to the calibrated model (Dueri et al. in press). Thus, the sediment porosity  $n_s$  was set to 0.7, whereas the effective diffusion coefficient  $D_d$  and the molecular diffusion coefficient  $D_m$  were set to  $1.6 \times 10^{-5} \text{ m}^2 \text{ d}^{-1}$  and  $2.5 \times 10^{-5} \text{ m}^2 \text{ d}^{-1}$ , respectively. Moreover, the initial concentration profile of contaminant corresponds to the one used for calibration, which was extrapolated from the arsenic concentration measured in the sediments of the Saguenay Fjord in 1998.

Four series of simulations were carried out for the sensitivity analysis (Table 3.2). The first two series of simulations considered five variable factors, including a variable dissolution coefficient, and were thus composed of  $2^5 = 32$  simulations. These simulations use dissolution coefficients determined for arsenic in the Saguenay sediments and thus represent a compound with a higher remobilization potential compared to the inorganic contaminants of the Fjord. Series 3 and 4 simulated the response of the model for a non-reactive contaminant and the dissolution coefficient was therefore equal to zero. This means that there were only four factors to test and the factorial design was composed of  $2^4 = 16$  simulations. To evaluate the influence of the thickness of the capping layer, two of the series were performed with a cap thickness of 0.2 m (series 1 and 3) and the other two with a cap thickness of 0.1 m (series 2 and 4).

Table 3.2: *Description of the series of simulations for the sensitivity analysis*

Series of Simulations	Thickness of Cap	Number of Reactions	Number of Simulations
1	0.2 m	Yes	32
2	0.1 m	Yes	32
3	0.2 m	No	16
4	0.1 m	No	16

Each series was composed of simulations representing every possible combination of the minimal and maximal values of each factor (Table 3.3). The results of the simulation of each series were sorted in a standard order and thereafter the Yates algorithm was applied in order to calculate the effect of each factor and of the combination of factors (Box et al. 1978). Although these effects are calculated from the results of simulations, which are values with a physical meaning, like fluxes or concentrations, after the application of the algorithm they represent the significance of the tested factors and are no longer directly linked to physical parameters. The effects can also be described as the change in the response as we move from the maximum value to the minimum value of a factor, and thus the significance of a factor or a combination of factors for the simulation results.

### 3.4 Results

The sensitivity analysis was performed over a simulation time of 10 years after the capping event and considers two types of model output:

1. The total cumulative mass that leaves the sediment column from the upper boundary and reaches the water column during the simulation.
2. The final concentration at the top of the sediment column, to which the benthic fauna may be exposed.

Table 3.3: *Simulation protocol for the factorial design of four tested factors: variable input values used for a set of 16 simulations.*

Simulation	Factors					
	Depth of Bio-Irrigation B <sub>1</sub>		Quantity and Dimensions of Tubes B <sub>2</sub>		Retardation Factor Rt	Bio-Irrigation Velocity V
	biox	$\beta_2$	n <sub>T0</sub>	$\beta_1$	Rt	v <sub>T</sub>
1	0.06	70	0.00039	0.0157	5	0.2
2	0.26	16	0.00039	0.0157	5	0.2
3	0.06	70	0.00471	0.119	5	0.2
4	0.26	16	0.00471	0.119	5	0.2
5	0.06	70	0.00039	0.0157	45	0.2
6	0.26	16	0.00039	0.0157	45	0.2
7	0.06	70	0.00471	0.119	45	0.2
8	0.26	16	0.00471	0.119	45	0.2
9	0.06	70	0.00039	0.0157	5	5
10	0.26	16	0.00039	0.0157	5	5
11	0.06	70	0.00471	0.119	5	5
12	0.26	16	0.00471	0.119	5	5
13	0.06	70	0.00039	0.0157	45	5
14	0.26	16	0.00039	0.0157	45	5
15	0.06	70	0.00471	0.119	45	5
16	0.26	16	0.00471	0.119	45	5

The results of the sensitivity analysis were represented in a normal probability plot. This type of plot is generally used to test the normality of a distribution, but in our case it allows a straightforward identification of the factors with a significant influence on the output of the model. Each point on the graph corresponds to the effect of one or a combination of factors. The effects do not have units since they represent the average variation of the response for a changing factor over all conditions of the other factors (Box et al. 1978). The points that fall on or near the straight line are normally distributed and thus these effects cannot be distinguished from the normally distributed error. On the opposite, the effects that deviate from the straight line and therefore from the normal error distribution point out significant factors. The sum of squares indicates the deviation of the effect from the normal distribution and thus this value can be used to quantify the importance of a factor for the response.

### 3.4.1 Total mass released from the sediment to the water column after 10 years

The result of the first set of simulations, representing a reactive compound migrating through a cap of 0.2 m, is displayed in Figure 3.1. The graph illustrates that the factors with the greatest influence on the released mass are those associated to bio-irrigation (irrigation velocity V, number and dimension of tubes  $B_2$  and depth of the tubes  $B_1$ ). There is also a second group of factors affecting the output of the model. This group is composed of the combination of bio-irrigation factors with the factor of dissolution D. As the second group of effects shows a smaller deviation from the normal distribution, represented by the straight line, the influence on the model response is less significant.

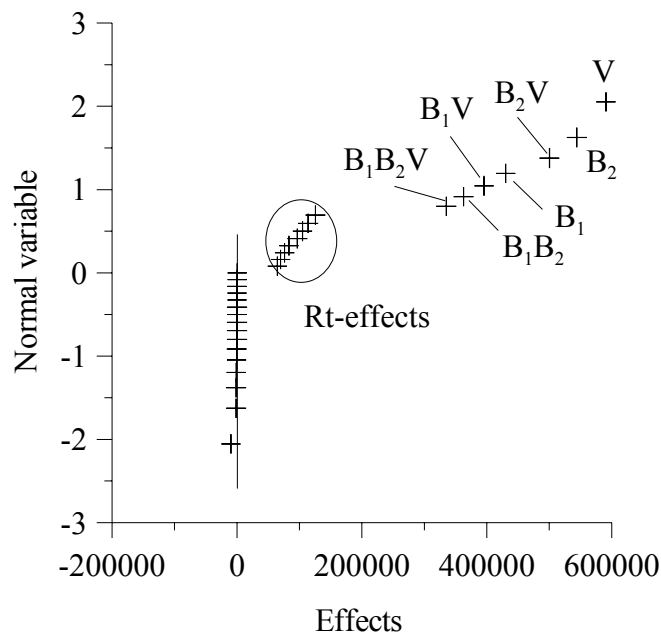


Figure 3.1: Effect of tested factors on the mass release of a reactive compound. Cap thickness of 0.2 m. Significant effects are identified by the variable name.

The result of the second series of simulations, representing a reactive compound migrating through a cap of 0.1 m, shows a very similar trend to the previous series. The similarity is best illustrated by comparing the sums of squares, presented in Table 3.4.

Table 3.4: *Sums of squares for a reactive compound migrating through a cap of 0.2 m (Series 1, illustrated in Figure 3.1) and a cap of 0.1 m (Series 2, not illustrated).*

	Sum of Squares %	
	Series 1	Series 2
V	22.47	22.53
B <sub>2</sub>	19.10	19.01
B <sub>2</sub> V	16.13	16.17
B <sub>1</sub>	11.96	11.79
B <sub>1</sub> V	10.08	10.10
B <sub>1</sub> B <sub>2</sub>	8.46	8.57
B <sub>1</sub> B <sub>2</sub> V	7.23	7.25
<b>SOFS Total</b>	<b>95.43</b>	<b>95.41</b>

Figure 3.2 shows the results of the third series of simulations, representing a non-reactive compound migrating through sediments covered by a cap of 0.2 m. In this case the release is strongly affected by the bio-irrigation depth B<sub>1</sub>, followed by the combination of bio-irrigation factors B<sub>1</sub>, B<sub>2</sub> and V. The retardation factor R<sub>t</sub> also exhibits a significant deviation from the normally distributed values. Figure 3.3 illustrates the results of series 4, representing the effects for a non-reactive compound migrating through a cap of 0.1 m. In this case, the depth of the tubes B<sub>1</sub> is the only important factor identified on the graph.

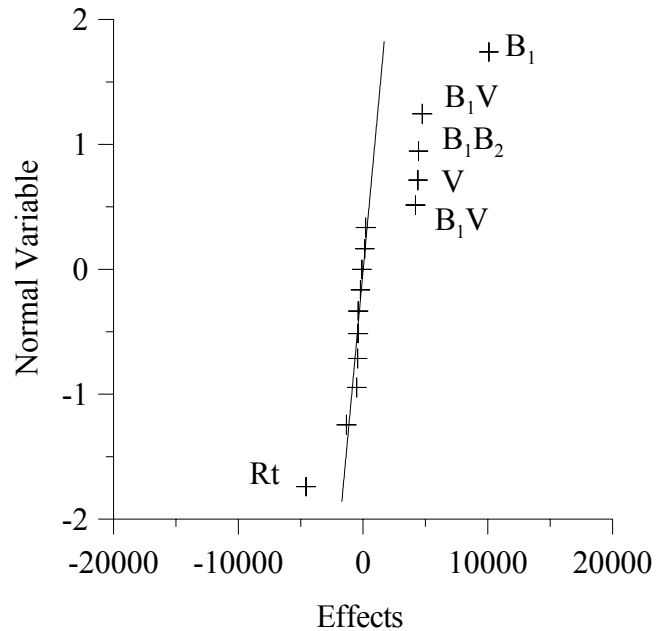


Figure 3.2: Effect of tested factors on the mass release of a non-reactive compound. Cap thickness of 0.2 m. Significant effects are identified by the variable name.

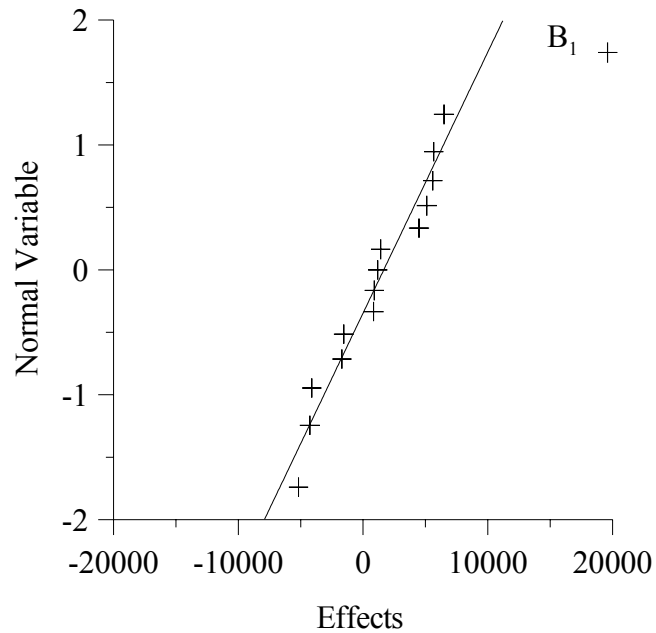


Figure 3.3: Effect of tested factors on the mass release of a non-reactive compound. Cap thickness of 0.1 m. Significant effect is identified by the variable name.

### 3.4.2 Final concentration at the top of the sediment column after 10 years

In this section, the sensitivity analysis was used to determine the significant factors affecting the concentration at the top of the sediment column from the four series of simulations described previously. Figure 3.4 shows the result of the first series of simulations, considering a reactive compound and a cap thickness of 0.2 m. The graph shows the significant influence of the dissolution coefficients D, the bio-irrigation depth  $B_1$ , the number and dimensions of the tubes  $B_2$  as well as the retardation factor Rt.

Shown in Figure 3.5 are the results of the factorial design for a reactive compound migrating through a cap of 0.1 m. In this set of simulations the most significant factor is the bio-irrigation depth  $B_1$ , followed by the dissolution coefficients D. The combination of the depth and the number and dimensions of the tubes  $B_1B_2$  is also an important factor, whereas the retardation factor Rt does not play a significant role.

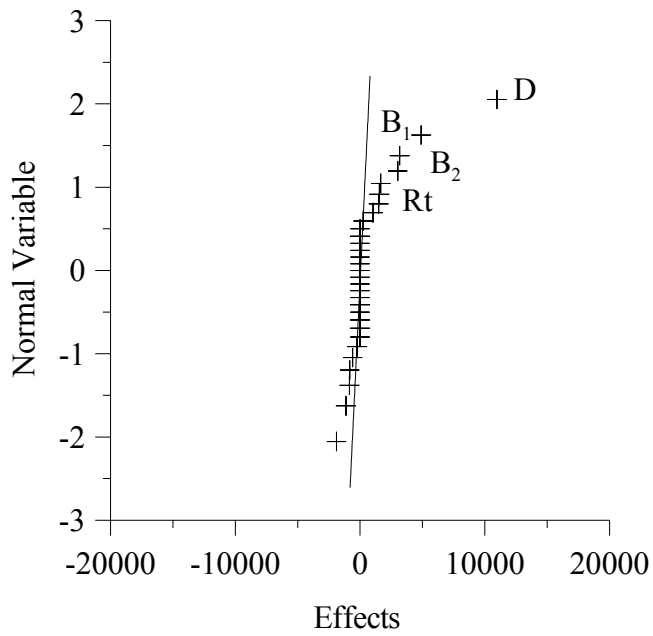


Figure 3.4: Effect of tested factors on the surface concentration of a reactive contaminant. Cap thickness of 0.2 m. Significant effects are listed.

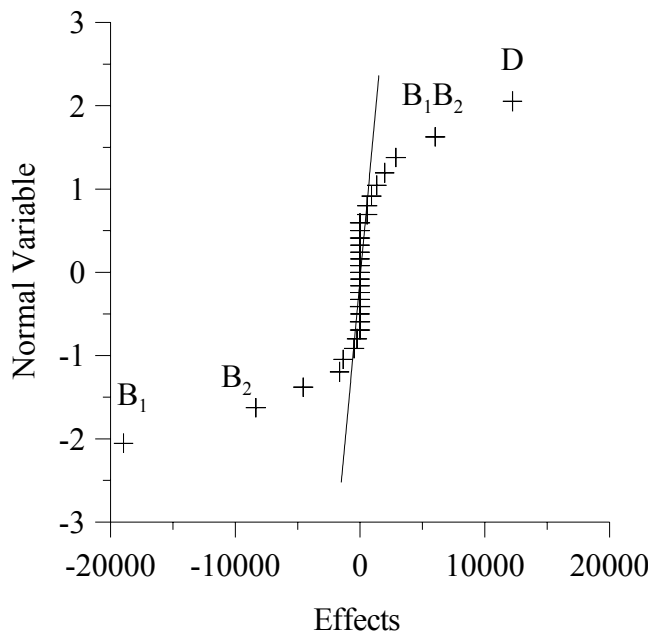


Figure 3.5: *Effect of tested factors on the surface concentration of a reactive contaminant. Cap thickness of 0.1 m. Significant effects are listed.*

The series representing a non-reactive compound are illustrated in Figures 3.6 and 3.7. The graphs do not display any outliers and none of the factors shows a significant deviation from the normally distributed population, represented by the straight line. Thus, they do not reveal any significant factor affecting the concentration in the surface layer.

Table 3.5 summarizes the significant factors highlighted by the sensitivity analysis. The second and third columns define the variable characteristics of the physical system (cap thickness) and of the contaminant (possibility of dissolution). The fourth and the fifth columns review the significant factors determined by the factorial design, depending on the considered output variable, i.e., the released mass or the surface concentration.

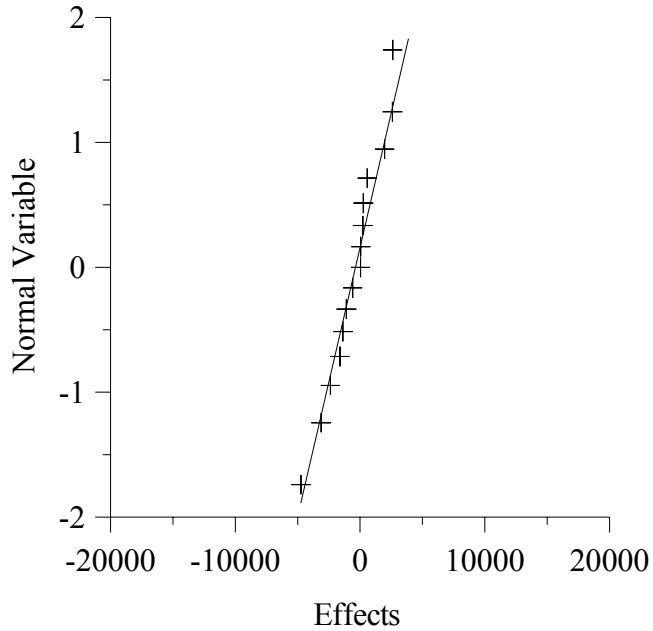


Figure 3.6: Effect of tested factors on the surface concentration of a non-reactive contaminant. Cap thickness of 0.2 m.

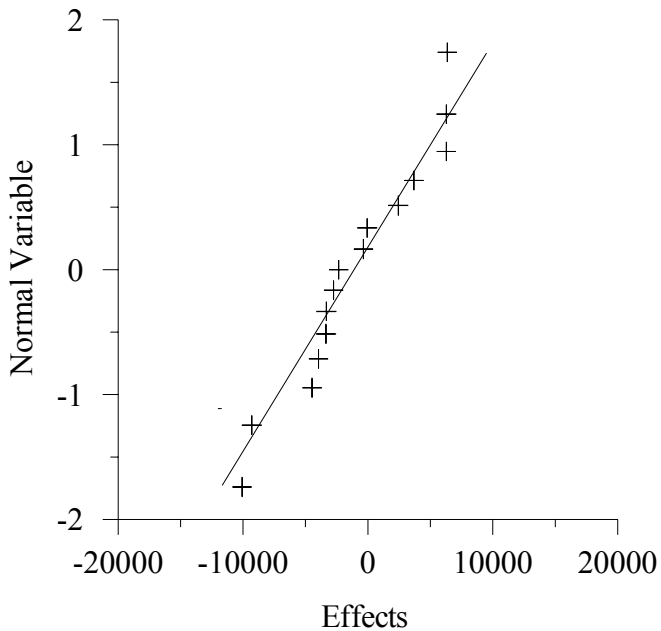


Figure 3.7: Effects of tested factors on the surface concentration of a non-reactive contaminant. Cap thickness of 0.1 m.

Table 3.5: *Review of the factors having a significant effect on the output of the model*

Series	Parameters		Response	
	Cap Thickness	Dissolution	Released Mass	Surface Concentration
1	0.2 m	Yes	V, B <sub>2</sub> , B <sub>1</sub>	D, B <sub>2</sub> , B <sub>1</sub> , Rt
2	0.1 m	Yes	V, B <sub>2</sub> , B <sub>1</sub>	B <sub>1</sub> , D, B <sub>2</sub>
3	0.2 m	No	B <sub>1</sub> , V, Rt	-
4	0.1 m	No	B <sub>1</sub>	-

For a reactive compound (Series 1 and 2), the mass released over a period of 10 years is mainly affected by bio-irrigation factors (B<sub>1</sub>, B<sub>2</sub>, V). The cap thickness variation does not lead to relevant differences in the results of these two series. The dissolution factor D is not listed between the significant factors, thus the variations of the dissolution coefficients tested in this study do not have a significant effect on this type of response. However, if we consider a non-reactive contaminant (Series 3 and 4) and set the dissolution coefficients to zero, the result of the factorial design are different from those of the first and second series. In this case the influence of the cap thickness is evident and for a different thickness we obtain different significant factors.

The results for the surface concentration 10 years after capping show that in the case of a reactive compound, the cap thickness slightly influences the results of the factorial design. For a cap thickness of 0.2 m, the most important factor is the dissolution coefficient D, whereas if the cap is only 0.1 m thick, the depth of bio-irrigation B<sub>1</sub> becomes the most important factor. In both cases, the bio-irrigation velocity V does not affect the results. Comparing the results of both output variables, one observes that for a reactive contaminant the bio-irrigation velocity V dominates the mass release, whereas the surface concentration is regulated by the dissolution coefficients D. The model is generally very sensitive to bio-irrigation parameters, except for the surface concentration of a non-reactive contaminant.

### 3.5 Conclusions

Factorial design has been used to determine the most significant parameters for the theoretical transport of reactive or non-reactive inorganic contaminants (trace metals) through the natural capping layer of the Saguenay Fjord. Two types of responses were considered for the sensitivity analysis: the total mass released from the system to the water column in the first 10 years after capping and the final concentration at the top of the sediment column. Both responses represent a potential harm for the aquatic fauna, since they indicate an exposure pathway for the organisms living in the marine environment. The results of the study pointed out that for the simulated conditions the significant parameters are a function of the response variable, the contaminant type (reactive or non-reactive) and to a lesser extent the cap thickness. The sensitivity analysis showed that the bio-irrigation parameters are generally very important for the prediction of the released mass, especially for reactive compounds that are associated to sulfides under anoxic condition and can be released if exposed to bio-irrigated water. It also demonstrated that the concentration of reactive compounds in the upper sediment layer depends on the bio-irrigation parameters as well as the dissolution coefficient.

The present study identifies the input values with a significant effect on the result, thus highlighting the parameters that should be studied carefully in order to reduce the uncertainty and get a better estimate of the performance of the capping layer. However, the most accurate characterization will not be able to eliminate the variability of the input values. Therefore, an uncertainty analysis will be performed to determine the distribution of the response considering the variability of the input parameters.

### 3.6 References

- Aller, R. C. 1980. Quantifying Solute Distributions in the Biotubated Zone of Marine Sediments by Defining an Average Microenvironment. *Geochim. Cosmochim. Acta.* **44** : 1955-1965.

- Box, G. E. P., Hunter, W. G., Hunter, J. S. 1978. Statistics for Experimenters: an Introduction to Design, Data Analysis, and Model Building. John Wiley, New York.
- Boudreau, B. P. 1997. Diagenetic Models and Their Implementation: Modelling Transport and Reactions in Aquatic Sediments. Springer-Verlag, Berlin Heidelberg.
- De Montety, L., Long, B., Desrosiers, G., Crémer, J.-F. and Locat, J. 2000. Quantification des structures biogènes en fonction d'un gradient de perturbation dans la baie des Ha! Ha! à l'aide de la tomodensitométrie axiale. Proceedings of the 53th Canadian Geotechnical Conference, Montréal, 15-18 Oct. 2000, Vol. 1, pp. 131-135.
- Dueri, S., Therrien, R. and Locat, J. (In press). Numerical modeling of the migration of dissolved contaminants through a subaqueous capping layer. *J. Environ. Eng. Sci.*
- Elliott, M., Zheng, Y. and Bagley, D. M. 2000. Determining Significant Anaerobic Kinetic Parameters Using Simulation. *Environ. Technol.* **21** : 1181-1191.
- Fuller, W. H. 1978. Investigation of Landfill Leachate Pollutant Attenuation by Soils, US EPA, Municipal Environmental Research Laboratory, Cincinnati, OH.
- Furukawa, Y., Bentley, S. J. and Lavoie, D. L. 2001. Bioirrigation Modeling in Experimental Benthic Mesocosms. *J. Mar. Res.* **59** : 417-452.
- Kabala, Z. J. 2001. Sensitivity Analysis of a Pumping Test on a Well with Wellbore Storage and Skin. *Adv. Wat. Res.* **24** : 483-504.
- Martin, W. R. and Banta, G. T. 1992. The Measurement of Sediment Irrigation Rates :A Comparison of the  $\text{Br}^-$  Tracer and  $^{222}\text{RN}/^{226}\text{RA}$  Disequilibrium Techniques. *J. Mar. Res.* **50** : 125-154.
- Mucci, A., Guignard, C. and Olejczuk, P. 2000a. Mobility of metals and As in sediments following a large scale episodic sedimentation event. Proceedings of the 53th Canadian Geotechnical Conference, Montréal, 15-18 Oct. 2000, Vol. 1, pp. 169-175.
- Mucci, A., Richard, L.-F., Lucotte, M. and Guignard, C. 2000b. The differential geochemical behaviour of arsenic and phosphorous in the water column and sediments of the Saguenay fjord estuary, Canada. *Aquatic Geochem.* **6**: 293-324.
- Neville C. J., Ibaraki, M. and Sudicky, E. A. 2000. Solute Transport with Multiprocess Nonequilibrium: a Semi-Analytical Solution Approach. *J. Cont. Hydrol.* **44** : 141-159.

- Riisgard, H. U. 1989. Properties and Energy Cost of the Muscular Piston Pump in the Suspension Feeding Polychaete *Chaetopterus Variopedatus*. Mar. Ecol. Progr. Ser., **56** : 157-168.
- Riisgard, H. U. 1991. Suspension Feeding in the Polychaete *Nereis Diversicolor*. Mar. Ecol. Progr. Ser. **70** : 29-37.
- Saulnier, I. and Mucci, A. 2000. Trace Metal Remobilization Following the Resuspension of Estuarine Sediments : Saguenay Fjord, Canada. Appl. Geochem. **15** : 191-210.
- Versteeg, H.K. and Malalasekera, W. 1995. An introduction to computational fluid dynamics: the finite volume method. Longman Scientific & Technical, Burnt Mill, Harlow, Essex.
- Zheng, C. and Bennett, G. D. 2002. Applied Contaminant Transport Modeling. 2<sup>nd</sup> Edition, John Wiley, New York.

**CHAPITRE 4 DECISION ANALYSIS:  
APPLICATION TO THE DESIGN OF A  
SUBAQUEOUS CAPPING LAYER**

## Résumé

Les sédiments contaminés peuvent constituer une source de contaminants pour la colonne d'eau ainsi que pour la faune benthique qui vit et se nourrit des sédiments de surface. Ces organismes représentent un vecteur de contamination pour l'environnement puisqu'ils peuvent accumuler les composants toxiques contenus dans les sédiments et les transmettre aux organismes supérieurs à travers la chaîne alimentaire. La mise en place d'une couche de recouvrement composée de matériaux propres réduit et dans le meilleur des cas élimine le risque associé à la présence de contaminants dans les sédiments. Une couche de recouvrement constitue une barrière physique qui isole les contaminants de la colonne d'eau et de la faune. Le design d'une telle couche doit tenir compte des facteurs physiques, chimiques et biologiques qui affectent la migration de contaminant et qui déterminent son efficacité à long terme. Lorsque ces facteurs sont caractérisés par une variabilité ou une incertitude importante, la conception de la couche peut être faite à l'aide de l'analyse de décision. Cette méthode considère l'incertitude et compare les différentes alternatives de recouvrement sur la base des coûts et des risques ainsi que par rapport à l'objectif technique du projet. L'approche a été appliquée ici à un projet de réhabilitation hypothétique, afin de trouver l'épaisseur idéale pour une couche qui recouvrerait un secteur contaminé qui est fréquenté régulièrement par la population de bélugas de l'estuaire du Saint Laurent. Afin de déterminer la probabilité de succès des différentes options, nous avons réalisé des simulations Monte Carlo avec un modèle numérique représentant la migration de contaminants dissous à travers une couche de recouvrement et par la suite nous avons intégré l'aspect économique. Les résultats montrent que le coût total du projet dépend du coût d'échec, un paramètre difficile à évaluer. Néanmoins, l'analyse de décision s'est avérée une méthode efficace et utile pour identifier le design optimal.

## Abstract

Contaminated sediments represent a potential source of contaminants for the water column and for the benthic fauna. These sediment-feeding organisms act as a contamination vector for the environment, because they accumulate toxic compounds and transmit them to higher level organisms through the food chain. Capping contaminated sediments with a clean layer can reduce or eliminate the risks of contaminant release to the environment. The cap represents a physical barrier that isolates the contaminants from the water column and from the fauna and its effectiveness depends upon its physical, chemical and biological characteristics, which are spatially variable and imperfectly known. Decision analysis is a method that accounts for uncertainty in engineering design to compare different alternatives considering the costs and risks associated to each management option. In this paper, we illustrate the application of the decision analysis approach for the design of a capping layer in a hypothetical remediation project, loosely based on a real situation. The decision analysis includes the risks related to the exposition of the St. Lawrence beluga population to contaminated sediments. In order to determine

the probability of success of each management option, we performed Monte Carlo simulations using a numerical model that represents the migration of dissolved contaminants through a capping layer and thereafter we included the economical aspect. The result of the decision analysis shows that the total cost of the project depends on the cost of failure, a parameter that is difficult to estimate. Nevertheless, decision analysis has proven to be an effective and useful method to identify the optimal design.

## 4.1 Introduction

Environmental engineers have to face uncertainty arising from the incomplete knowledge of natural environments when designing operational systems to prevent or reduce contamination. For example, the planning of waste-containment facilities, remediation of contaminated soil or ground water and dewatering systems requires choosing the best option among a series of possible management alternatives. In this paper, we examine the design of a protective capping layer to isolate contaminated sediments from the water column. Given the complex geometry and interactions of natural systems, engineers have to rely on the results of numerical models to predict the effectiveness of management options. Unfortunately, due to the elevated costs associated with field investigation, the information concerning the input parameters and their spatial distribution is usually incomplete. The input values have therefore to be estimated and simulations are performed under conditions of uncertainty, implying that there is a probability, or risk, that the predicted value will not correspond to the true response of the system. If uncertainty is neglected and the management option is chosen uniquely from deterministic simulations, the reliability of the prediction remains unknown.

Decision analysis takes into account uncertainty when establishing the risk that a management option will fail to achieve the technical objective imposed by the project. The method calculates the total costs and benefits of each management option and transforms the results of the numerical model into an economic value. Thus, the decision-maker can compare the design alternatives on an economical basis, and choose the design that meets the technical target, maximizing benefits and minimizing the costs of the project.

Freeze et al. (1990) clearly illustrated the advantages of the application of decision analysis to engineering design concerned with uncertainty in hydrogeological parameters. The authors developed a general framework that combines three types of models: a decision model, a numerical model and an uncertainty model (Figure 4.1). The decision model compares the costs, benefits and risks associated to each design

alternative. The numerical model, for example a groundwater model, is utilized in a stochastic mode to calculate the expected performance of the system and particularly the probability of failure, which is a component of the risk factor used in the decision model. The uncertainty model describes the distribution of the system parameters, used as input values for the stochastic simulations, and is based on the data collected during field investigation. Freeze et al. (1990) illustrated the decision analysis framework by means of a hypothetical project involving the design of a containment facility at a new landfill. The usefulness and versatility of the methodology was further illustrated by applications to groundwater contamination (Massmann et al. 1991), open pit mine design (Sperling et al. 1992) and hydraulic leachate containment design (Lepage et al. 1999). The methodology was also applied to sediment remediation, for the design of the optimal sediment volume to be dredged in a contaminated area (Dakins et al. 1994).

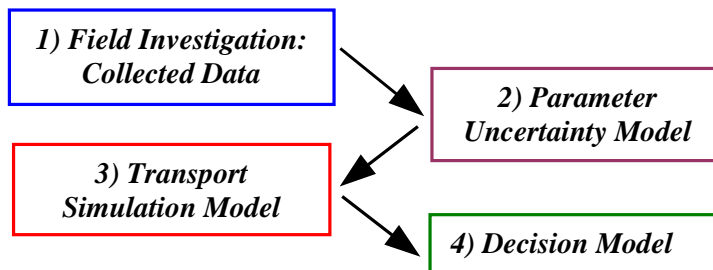


Figure 4.1: *Decision analysis framework (adapted, after Freeze et al. 1990)*.

Decision analysis is usually preceded by sensitivity and uncertainty analyses (Figure 4.2). The sensitivity analysis compares the output of a numerical model for minimum and maximum values of input parameters. A limited number of simulations is performed to identify the input parameters that show the most important effect on the response of the model. The parameters are further investigated in the uncertainty analysis, which computes the effect of the global parameter uncertainty on the response of the model. The input values are represented by their *probability density function* PDF. A Monte Carlo analysis is then performed, where a large number of simulations are conducted with randomly sampled PDFs, to get a representative probability distribution

of the response (an example of the output PDF for mass flux is shown in Figure 4.2). The resulting distribution is used for the decision analysis, which provides a link between uncertainty analysis and the economic framework of a management decision.

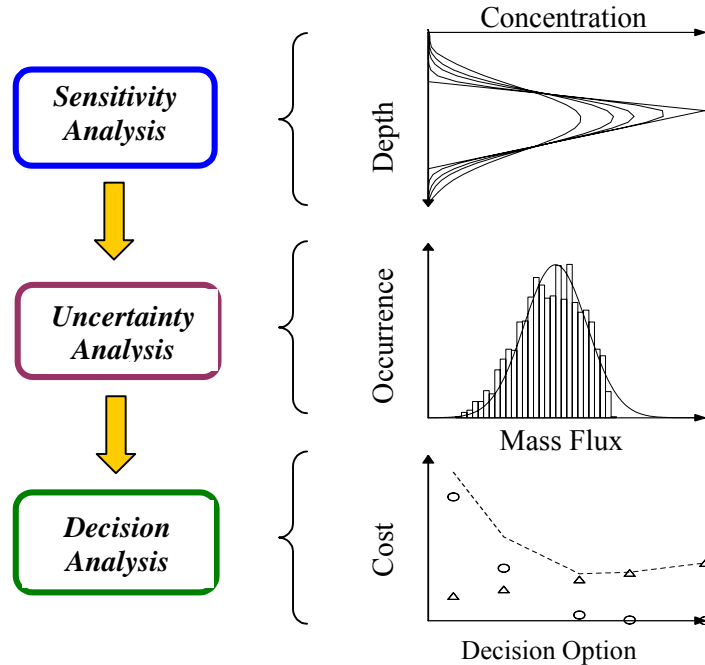


Figure 4.2: *Progressive investigation of uncertainty. The graph on the right illustrates the typical output for each analysis.*

In this paper, we present the application of the decision analysis method to choose the optimal design of a hypothetical capping layer. The capping of contaminated sediments with clean material is a promising alternative for the isolation of contaminants from the water column and the prevention of the transfer of pollution through the ecosystem. This approach has the advantage of being effective and low-cost compared to other management options that require removal and ex-situ treatment of sediments and it is applicable to large contaminated surfaces. A capping layer is designed to physically isolate the contaminants from the benthic fauna, stabilize the sediments and prevent or at least reduce the contaminant flux towards the new water-sediment interface.

The objective of the study is to illustrate the advantages of combining the numerical model TRANSCAP-1D with the decision analysis method. The numerical model simulates the migration of dissolved contaminants through a subaqueous capping layer, accounting for advection, diffusion and bio-irrigation (Dueri et al. in press). The model was calibrated with concentration profiles of arsenic measured in the sediments of the Baie des Ha! Ha! and the Bras Nord, located in the upstream area of the Saguenay Fjord, where a major flood led to the deposition of a natural capping layer over contaminated sediments (Figure 4.3). Since the catastrophic flood, which occurred in 1996, the geotechnical and geochemical characteristics of the capping layer, as well as the recolonisation of the benthic fauna, have been extensively studied in the context of a multidisciplinary research project (Pelletier et al. 1999, Mucci et al. 2000a, Pelletier et al. 2003, Mucci et al. 2003). The collected information was used for a detailed sensitivity analysis, to assess the effect of variable input parameters on the mobility of dissolved contaminants that migrate through the capping layer (Dueri and Therrien 2003). The sensitivity analysis was performed for both non-reactive and reactive contaminants, where "reactive" means that in the anoxic sediment the compound is associated to sulfides and that it can be remobilized if exposed to oxygenated water. This mechanism was observed for arsenic, but it could affect other trace metals associated with sulfides, like Ni, Cu, Co, Hg, Pb. However, compared to As, these trace metals are probably less mobile than As, since they are more likely associated to less reactive phases (e.g. organic matter). The sensitivity analysis tested five factors: the depth of bio-irrigated tubes, the quantity and dimensions of bio-irrigated tubes per square meters, the bio-irrigation velocity, the retardation factor and the dissolution coefficient. The results showed that the effect of each factor on the response of the model depends on the reactivity of the contaminant and on the considered response.

In the present study, we want to exploit the knowledge gained using the data collected at the Baie des Ha! Ha! and Bras Nord area, by applying it to another area of the Saguenay Fjord, near Baie Ste-Catherine (Figure 4.3), where similar grain size distribution and benthic fauna are found (Héroux 2000). The previous studies on the capping layer deposited in the Baie des Ha! Ha! and Bras Nord showed that the fine-

grained cap with an average thickness of 0.2 m is effective in isolating inorganic contaminants from the water column (Mucci et al. 2003). The deposition of that cap was the result of a natural event, therefore free of charge. Conversely, the design of a new capping layer for the remediation of a contaminated area requires consideration of costs and risks associated with the different options. Thus, it is useful to apply the decision analysis approach for the design.

The present decision analysis considers two capping materials: a fine-grained cap (similar to the natural cap) and a more sandy cap. The analysis evaluates the total costs for different values of cap thickness. The hypothetical capping layer should cover an area that hosts the southernmost population of belugas. Since whale watching is an important tourist attraction of the region, the contamination of the beluga population could cause significant economical losses. The analysis presented here aims at illustrating the decision analysis with its advantages and limitations and should be considered with care for any actual decision on the remediation of contaminated sediments of the Saguenay Fjord or their impact on the beluga population.

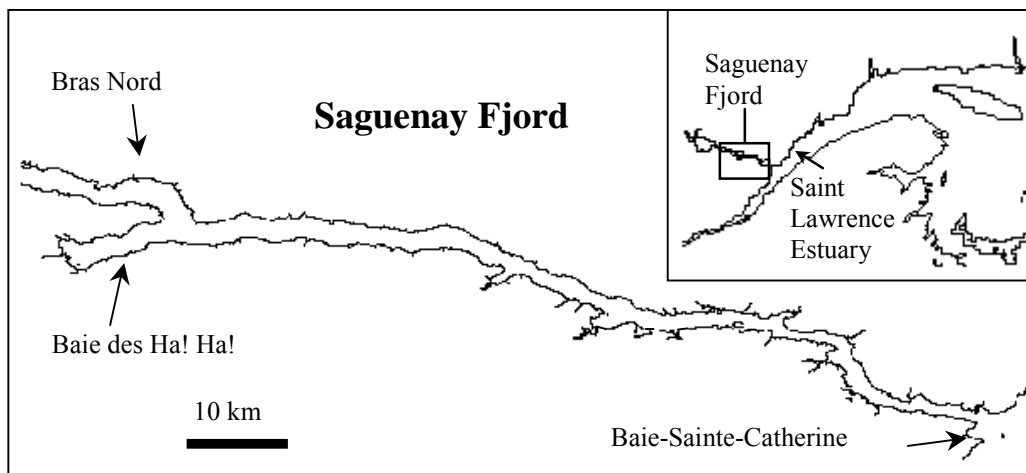


Figure 4.3: Localization map of the study site.

## 4.2 Decision analysis method

Because decision analysis compares a finite number of different design alternatives defined by the project managers, it does not apply to cases where a possibly infinite number of designs are to be evaluated. The different options are compared using a risk-cost-benefit objective function (Freeze et al. 1990), which is expressed in monetary value and incorporates the technical and the economical objective of the project. The technical objective of a remediation project is to meet the regulatory standard imposed by environmental laws, whereas the economical objective is to minimize the costs and maximize the benefits of the project. The objective function includes the costs, benefits and risk of failure for a given management option  $j$ , over a specified time horizon and accounting for the interest rate. The objective function is represented by the equation:

$$\Phi_j = \sum_{t=0}^T \frac{1}{(1+i)^t} [B_j(t) - C_j(t) - R_j(t)] \quad (4.1)$$

where  $\Phi_j$  is the objective function for management option  $j$  [\$],  $T$  is the time horizon [a],  $i$  is the discount rate [decimal fraction],  $B_j(t)$  is the benefit of option  $j$  in year  $t$  [\$],  $C_j(t)$  is the cost of option  $j$  in year  $t$  [\$] and  $R_j(t)$  is the risk of option  $j$  in year  $t$  [\$].

The costs associated to the risk factor are calculated by multiplying the cost of failure with the probability that the management option does not meet the technical objective and are described by the following equation:

$$R(t) = P_f(t)C_f(t) \quad (4.2)$$

where  $P_f(t)$  is the probability of failure in year  $t$  [decimal fraction] and  $C_f(t)$  is the cost associated with failure in year  $t$  [\$].

In the case studied here, the probability of failure associated with different values of capping thickness can be calculated from the output distributions of stochastic simulations, provided by the uncertainty analysis. Given a normal distribution, the probability of failure can be graphically represented as the part of the distribution exceeding a specific limit, defined as the non-attainment of the technical objective of the project (Figure 4.4).

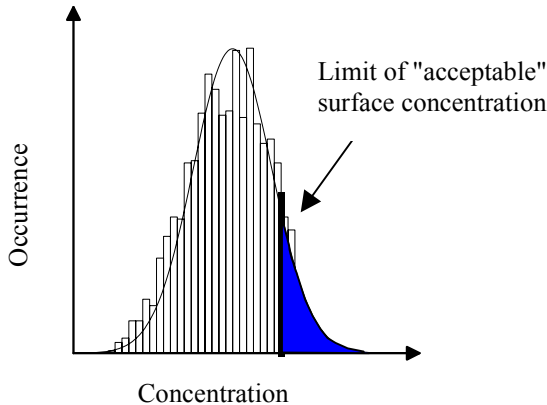


Figure 4.4: *Definition of the probability of failure (shadowed area) for a normal distribution.*

In our example, we simulate the contaminant migration over a time limited to 10 years and the time dependencies of the equation (4.2) are therefore assumed to be negligible. Moreover, we assume that there are no direct benefits associated with the remediation of the contaminated sediments of the study site. The example assumes that the government would accept to meet the cost for remediation to preserve this very sensitive and particular ecosystem and to prevent economical losses associated to the persistence of diseases in the beluga population. Combining equation (4.1) and (4.2), the objective function becomes:

$$\Phi = -[C + P_f C_f] \quad (4.3)$$

## 4.3 Site Description

Several studies have documented the distribution of contaminants in water (Gobeil and Cossa 1984, Tremblay et Gobeil 1990) and in sediments (Barbeau and al. 1981, Pelletier and Canuel 1988, Gagnon and al. 1993, Cossa 1990, Coakley and Poulton 1993, Muris 2001) of the Saguenay Fjord and the St. Lawrence Estuary. The presence of trace metals (Hg, Pb, Zn, Cd) and organic compounds (PAH, DDT, PCB) are related to the industrial and agricultural activities located in the region. At the beginning of the 20<sup>th</sup> century, the tributaries of the Saguenay Fjord and the St. Lawrence Estuary started to carry the effluents from a highly industrialized area. However, after the introduction of environmental regulations in the 1970s, the industrial discharge of pollutants was markedly reduced. Although regulations lead to an improvement of water quality, the sediments of the Saguenay fjord and the St Lawrence estuary still store large amounts of contaminants and represent a risk for the environment.

The Saguenay Fjord and the St. Lawrence Estuary represent a very sensitive ecosystem, because they are inhabited by the world's southernmost population of belugas. This population is isolated from other beluga populations, located in the Arctic, and is exceptional for its accessibility for public viewing and research. Unfortunately, due to the past hunting activity, the beluga population is now only 500-600 individuals and is classified as an endangered species by the Committee on the Status of Endangered Wildlife in Canada. Despite hunting prohibition since the end of the 1970's, the population has not recovered. The main causes of this failure are the deterioration of their habitat caused by contamination, the disturbance by recreational and commercial traffic and the low genetic variability (Lesage and Kingsley 1998). A large whale watching industry has developed at the confluence of the Saguenay fjord and the St. Lawrence estuary. Thus, contamination not only represents a risk for the preservation of this particular ecosystem, but could eventually compromise the income related to the whale watching business.

A comparative study of Wagemann et al. (1990) reports that belugas of the St. Lawrence Estuary have significantly higher levels of lead, mercury and selenium, than most Arctic whales. Moreover, the St. Lawrence population has higher levels of PCB, DDT and mirex (Muir et al. 1990) compared to Arctic populations. The presence of toxic compounds in their environment surely affects these mammals, but the exact long-term consequences of the exposure to contaminants are difficult to evaluate. Nevertheless, the results of Martineau et al. (2002) indicate that the population living in the Saguenay Fjord and the St. Lawrence Estuary has an annual rate of cancer much higher than that reported for any other population of cetaceans.

Belugas are exposed to contaminants through their consumption of contaminated fish and benthic organisms as well as through accidentally ingestion of polluted sediments (Vladykov 1946). Since the benthic fauna lives inside the sediments and is at the lower level of the food chain, these organisms are an important vector for the diffusion of contaminants from the sediments towards higher level organisms (e.g. fishes and marine mammals). The bioaccumulation of toxic compounds in the benthic fauna occurs either by direct ingestion of sediment particles containing insoluble contaminants, like PAH, PCB or DDT, or by adsorption of soluble compounds from the solute phase (Otero et al. 2000, Yan and Wang 2002).

Belugas move in groups and exhibit a tendency to fidelity to some areas. The distribution of the population depends on the season, but specific zones are preferred for feeding, calving or resting (Pippard and Malcolm 1978). A list of sites representing a risk of contamination for the belugas has been published, considering the seasonal distribution of belugas and the concentration of toxic compounds (Comité multipartite sur les sites contaminés pouvant affecter le béluga du Saint-Laurent 1998).

Even if our example is based on a real situation, we have to make a few assumptions and approximations in order to perform the decision analysis. The proposed strategy usually assumes that in a previous stage remediation has been judged necessary. In the case of the Saguenay Fjord, even if the observations suggest that the contaminated sediments contribute to the deterioration of the beluga population (Martineau et al. 2002),

no environmental agency assessed the necessity to cover the contaminated sediments with a capping layer. In fact, the problem has complex interactions and other sources of contamination have been identified for the beluga population, like the American eels migrating from Lake Ontario (Hickie et al. 2000). Moreover the beluga population is mobile, lives and feeds on a large surface extending over the Saguenay Fjord and the St Lawrence Estuary and several sectors present contaminated sediments. Nevertheless, the dock of Baie-Sainte-Catherine has been identified as a site at risk, where further characterization is highly requested, since it is highly contaminated and intensively frequented by belugas (Comité multipartite sur les sites contaminés pouvant affecter le béluga du Saint-Laurent, 1998).

## 4.4 Cost estimates

The cost for in situ capping of contaminated sediments are derived from the cost estimates of the Palos Verdes Shelf capping project, off the coast of Los Angeles, California (Palermo et al. 1999). The cap placement costs are divided in three components: the costs for the mobilization/demobilization of the dredging equipment  $C_M$ , the costs to dredge, transport and dispose the material  $C_{DTD}$  and the engineering and design costs  $C_E$ . Thus, the construction cost of the project is described by the following equation:

$$C = C_M + C_{DTD} + C_E \quad (4.4)$$

The cost for the mobilization  $C_M$  and the engineering costs  $C_E$  are fixed and do not depend on the cap thickness, whereas the dredging/transportation/disposal cost  $C_{DTD}$  are a function of the volume of sediments required for the capping project. The value of the construction cost components are based on values reported for the Palos Verdes Project and are described in Table 4.1.

Table 4.1: *Costs of components used for the capping management options (in \$ CAD).*

Components	Symbol	Cost
Mobilization/Demobilization	$C_M$	\$750 000
Engineering	$C_E$	\$250 000
Dredging/Transportation/Disposal	$C_{DTD}$	\$5 m <sup>-3</sup>
Cost of failure	$C_f$	\$3 000 000 year <sup>-1</sup>

Estimating the cost of failure of the capping layer is associated here with the impact of belugas on the economy. Whale watching is a worldwide fast growing industry that stimulates tourism, contributes to the economic development of coastal communities and encourages regional business. Recent studies report that throughout the St. Lawrence Estuary there are 75 operators offering whale-watching tours. About 300 000 people participated in 1995 to these tours spending \$7 million CAD on tickets, \$44 million CAD on travel, meals and accommodation and \$17 million CAD on additional direct economic spin-offs for a total of \$68 million CAD (Hoyt 2000, Le Groupe Type 1996).

Local and international newspapers reported the results presented by Martineau et al. (2002) relating the cancer rates of belugas with the degradation and contamination of their habitat. The economical consequences of the diffusion of this information on the whale watching industry are difficult to evaluate. Belugas represent a patrimony with a high recreational, commercial and scientific value. In order to quantify the cost of failure  $C_f$ , we have to estimate the regional economic loss associated to the bad publicity due to the persistence of the health problems of the beluga population. We considered that bad publicity could slightly reduce the attractiveness of the whale watching tours and affect the incomes associated with tourism. Thus we approximate the cost of failure to the conservative value of \$3 million CAD per year, which represents less than 5% of the total economic spin-off of the whale watching industry (Table 4.1).

In our example, we consider six capping options with different values of cap thickness, varying between 0.1 and 0.34 m (Table 4.2). The cost of a capping layer

depends upon the area to be covered and thus upon the extension of the contamination. At the dock of Baie-Sainte-Catherine the contaminant distribution is poorly documented, but in order to perform the decision analysis we had to estimate this parameter and based on the morphology of the dock we assumed a contaminated area of about  $4 \text{ km}^2$ . Thus the sediment volume necessary for the capping options varies between 0.4 million  $\text{m}^3$  and 1.36 million  $\text{m}^3$  and construction costs fluctuate between \$3 million CAD and \$7.8 million CAD (Table 4.2).

Table 4.2: *Capping options and construction cost to cap an area of  $4 \text{ km}^2$ .*

Capping option	Thickness [m]	Volume [ $10^6 \text{ m}^3$ ]	Total Cost [ $10^6 \$$ ]
1	0.10	0.40	3.0
2	0.14	0.56	3.8
3	0.20	0.80	5.0
4	0.24	0.96	5.8
5	0.30	1.20	7.0
6	0.34	1.36	7.8

## 4.5 Numerical Model

The numerical model used for contaminant transport in capped sediments (TRANSCAP-1D) simulates advection, diffusion and bio-irrigation. The sediments are represented as a dual porosity medium composed of microscopic sediment pores and macroscopic tubes and burrows (Dueri et al. in press). The benthic fauna, and particularly polychaete worms, dig and live in these mainly vertical tubes and burrows. Bio-irrigation results from the pumping of overlying water into the tubes and burrows to provide oxygen for respiration and prevents the accumulation of potentially noxious chemical compounds.

The mathematical formulation in the model consists of two partial differential equations, corresponding to the contaminant transport in the bio-irrigated tubes and in the sediment pores. These equations are coupled via a non-local exchange term that

represents the mass transfer of contaminant between the sediments and the tubes. The formulation is mathematically similar to the one describing solute transport in a dual-porosity medium, in the context of groundwater flow (for example, Zheng and Bennett 2002). The consolidation of the sediments and associated fluid advection are not included in the model, because for the studied cap thickness the full consolidation is usually achieved relatively rapidly compared to the lifetime of a capping layer.

The model was calibrated with profiles of dissolved arsenic because its chemistry has been extensively studied in the sediments of the Saguenay Fjord (Saulnier and Mucci 2000, Mucci et al. 2000a, 2000b). For the simulation presented here, the sediment column represented in the model has a constant thickness of 0.6 m. The column is equally subdivided in 30 cells, each having a height of 0.02 m (Figure 4.5). The contaminated layer has a total thickness of 0.14 m and its position in the column varies with the thickness of the cap. The simulation time varies between 2.5 years (912 d) and 10 years (3650 d) and the time increment is set at 0.02 d.

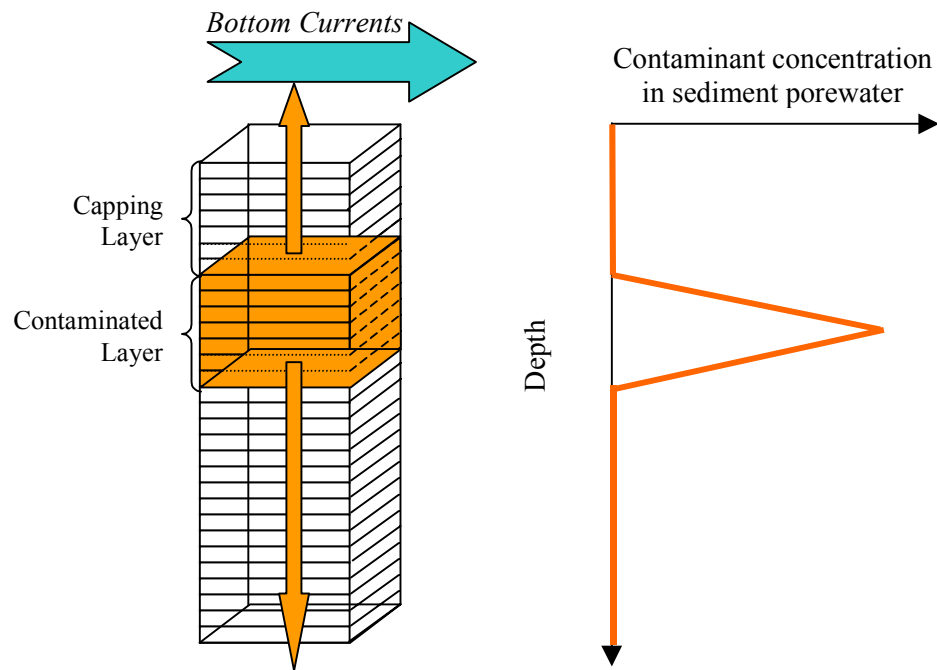


Figure 4.5: *Conceptual model: discretization of the sediment column and initial contaminant concentration.*

The input parameters of the model are presented in Table 4.3. The values of the sediment porosity  $n_s$  and of the inner radius of the tubes  $r_1$  reflect the values observed in the sediments of the Bras Nord and the Baie des Ha! Ha! (Dueri et al. in press). Two values were used to represent the porosity of the capping layer  $n_{scap}$ , one corresponding to a fine-grained cap composed of silt and clay ( $n_{scap} = 0.7$ ) and the other representing a sandy cap ( $n_{scap} = 0.4$ ). Advection velocity in the sediments and dispersivity are set to zero, because we assume that there is no advection in the sediments of the Saguenay Fjord. The molecular diffusion coefficient  $D_m$  corresponds to the range of values presented in Vanysek (2000) and Domenico and Schwartz (1998) for cations having a charge of 3+. This value was chosen because it represents the  $\text{As}^{3+}$  cation, which was used for model calibration (Dueri et al. in press). The effective diffusion coefficient  $D_d$  is calculated by multiplication of the molecular diffusion coefficient  $D_m$  with a mean tortuosity value of 0.64.

Table 4.3: *Input parameters of the numerical model.*

Parameter	Name	Units	Value
Sediment porosity	$n_s$	[-]	0.7
Cap porosity	$n_{scap}$	[-]	0.4 and 0.7
Advection velocity	$v_s$	[m d <sup>-1</sup> ]	0
Dispersivity	$\alpha_L$	[m]	0
Effective diffusion coeff.	$D_d$	[m <sup>2</sup> d <sup>-1</sup> ]	1.6 * 10 <sup>-5</sup>
Molecular diffusion coeff.	$D_m$	[m <sup>2</sup> d <sup>-1</sup> ]	2.5 * 10 <sup>-5</sup>
Inner radius of tubes	$r_1$	[m]	0.001

Initial and boundary conditions are required to solve the coupled system of equations. To impose the initial conditions one specifies the initial solute concentration in the two domains, sediments and tubes. Boundary conditions are required at the top and bottom of the domain and can be either a prescribed concentration or prescribed mass flux for both domains. We assume that solutes leaving the sediments from the upper boundary do not accumulate in water but are promptly carried away by the bottom currents. On the other hand, the solute mass reaching the lower control volume by

diffusion leaves the system by the same rate. Since sediments underlying the modeled system are assumed to be clean, we set the advective flux entering the sediment column from the lower boundary to zero. Thus, the concentration at the lower limit stays at a constant value of zero.

The governing equations are discretized with the finite volume method (Versteeg and Malalasekera 1995). The equations are coupled through a mass exchange term and a simultaneous solution for the concentration in the sediments and tubes is obtained for each finite volume. The system of equations is thus solved in a fully-coupled fashion, avoiding the use of iteration that is necessary when the equations are decoupled. The block tridiagonal matrix resulting from the discretization and assembly of the terms is solved with the Thomas algorithm adapted to block matrices. The numerical solution was tested by comparing to the semi-analytical solution of Neville et al. (2000), which has been developed for one-dimensional solute transport in a dual-porosity medium with multiple non-equilibrium processes (Dueri et al. in press).

## 4.6 Uncertainty analysis

The objective of the uncertainty analysis presented in this section is to define the distribution of the model response for conditions similar to those observed in the Saguenay Fjord. The uncertainty analysis considers the results of the previously performed sensitivity analysis (Dueri and Therrien 2003), which tested five factors: the depth of bio-irrigated tubes, the number of bio-irrigated tubes per square meters and their dimension, the bio-irrigation velocity, the retardation factor and the dissolution coefficient. In the Saguenay Fjord, the depth and number of tubes are characterized by spatial variability, whereas the value of the bio-irrigation velocity, the retardation factor and the dissolution coefficient are poorly documented and have to be estimated. Only the first four of those factors are varied in the uncertainty analysis. The dissolution coefficient is kept constant, because we do not have enough information to justify upper and lower limits for this parameter.

The uncertainty analysis is performed using the TRANSCAP-1D numerical model and applying the Monte Carlo method (Morgan and Herion 1990). A Monte Carlo realization is a simulation with input values, which are randomly sampled within their specific PDFs and for which the numerical model calculates the corresponding output. A series of Monte Carlo realizations forms a Monte Carlo simulation and produces a finite range of independent output values that corresponds to the probability distribution of the inputs (see graph illustrating the output of uncertainty analysis presented in Figure 4.2). The Monte Carlo method allows estimating the output distribution from the sample of calculated output values, but the accuracy and stability of the distribution depends on the number of performed realizations. For a larger number of realizations we expect a better accuracy and stability of the Monte Carlo simulation.

The present uncertainty analysis is used to design the optimal Monte Carlo simulation for the decision analysis, minimizing the number of realizations and thus the time required for each simulation, and maximizing the accuracy and stability of the output distribution. Moreover, we use this analysis to verify whether the output distribution is normal or lognormal and to test the effect of the shape of the input distribution.

#### **4.6.1 Input distributions**

Two types of PDFs are used for the input of the uncertainty analysis: uniform distribution and normal distribution. The number of tubes per square meter and the irrigation depth are defined by both distribution types, in order to investigate the impact of the distribution type on the response. The normal distribution is defined so that the upper and lower limits of the uniform distribution correspond to the 5% and 95% limit of the normal distribution. The minimum and maximum values of each tested parameter were determined from the available information, which includes data measured at the Saguenay Fjord and data derived from the literature. The values of the parameters are discussed in the following paragraphs and are presented in Table 4.4.

The values for the bio-irrigation velocity were derived from data measured during laboratory tests carried out on polychaete families living in shallow water (Riisgard 1989, Riisgard 1991). In the calibrated model, the irrigation velocity is equal to  $1 \text{ m d}^{-1}$ . The minimum and maximum values of this parameter were estimated by modifying the calibrated value by a factor of five. Thus, we obtain a range of values going from a minimum bio-irrigation velocity of  $0.2 \text{ m d}^{-1}$  to a maximum value of  $5 \text{ m d}^{-1}$ , which represents a reasonable approximation of the variation of this parameter for the studied site.

Table 4.4: *Definition of uniform and normal PDFs describing the variable parameters.*

Parameter	Uniform Distribution		Normal Distribution	
	Minimum	Maximum	Mean	Variance
Irrigation Velocity [ $\text{m d}^{-1}$ ]	0.2	5		
Retardation Factor	5	45		
Number of Tubes [ $\text{m}^{-2}$ ]	500	1500	1000	62,500
Irrigation Depth [m]	0.06	0.26	0.16	0.0025

The minimum and maximum values for the retardation factor have been estimated from the calibration of the model on two measured arsenic concentration profiles (Dueri et al. in press), from the values presented by Fuller (1978) for different metals, as well as from the values determined by Bourg (2002) for the transport of Zn and Cu in the Saguenay sediments. The range of retardation factors is very wide and depends on the element and on the sediment composition. For our uncertainty analysis we chose the range of values with the smallest retardation, therefore assuming that the contaminant has a good mobility and taking the “worst case” for contaminant migration. The minimum and maximum values of Rt have thus been set to 5 and 45, respectively.

The values of the number of tubes per square meter were visually determined from photographs of the undisturbed bottom sediments taken in the Saguenay Fjord during the summer 2001. The minimum and maximum values of this parameter are 500 and 1500 tubes per square meter, respectively. The number and the dimension of the

tubes in the upper sediment layer are an indicator of the intensity of bio-irrigation in this zone. Two input values of the model are directly calculated from the number of tubes: the tube porosity at the surface and the mass transfer coefficient.

The depth of bio-irrigation is represented in the model by the maximum depth attained by the tubes. The value of this parameter has direct consequences on the mass transfer coefficient between tubes and sediments as well as the value of the tube porosity. The three parameters are related since the maximum bio-irrigation depth corresponds to the location where mass transfer and tube porosity exponentially tend to zero. According to field observations and measured bioturbation intensities (De Montety et al. 2000), the minimum value of the bio-irrigation depth was set to 0.06 m and the maximum value to 0.26 m.

In order to test the stability and accuracy of the output distributions for a wide range of possible scenarios, we performed several Monte Carlo simulations considering different values of maximal simulation times, cap thickness and maximal concentration of contaminant. For the maximal simulation time, values of 2.5, 5, 7.5 and 10 years were chosen, whereas the ranges of cap thickness varied between 0.04, 0.10, 0.14, 0.20, 0.24 and 0.30 m. Two values were chosen for the maximal concentration of contaminant, which was set at  $25\ 000\ \mu\text{g m}^{-3}$  and at  $100\ 000\ \mu\text{g m}^{-3}$ . The distribution of contaminant is represented by a symmetrical peak (Figure 4.5) with a limited thickness of 0.14 m. This representation was chosen for practical reason and is not based on observation since, to the authors' knowledge, the contaminant distribution in the sediment column of Baie Ste Catherine has not been reported so far. The response that was considered for the uncertainty analysis is the released mass and the concentration at the surface of the sediment. The maximal number of realizations was determined considering the time required to perform the Monte Carlo simulation. For a prediction of contaminant migration over 5 years and 4000 realizations, the Monte Carlo simulations required 28 hours on a Pentium III computer, 450 MHz.

#### 4.6.2 Shape, stability and accuracy of the output distribution

The output distribution resulting from the uncertainty analysis was tested for normality with the Kolmogorov-Smirnov test. The test was used to assess if the distribution is normal or lognormal and to investigate the effect of increasing the number of simulations. A distribution is considered normal if the calculated Kolmogorov-Smirnov-coefficient is smaller than the critical value of the test, for a given confidence level. The results of the test are presented in Figure 4.6. Both responses, concentration at the top of the sediment column and mass flux, diverge from normality for almost every Monte Carlo simulation. On the opposite, the Kolmogorov-Smirnov-coefficients calculated from the natural logarithm of the output values (filled symbols) fall near the critical value for a confidence level of 95%. Therefore, the lognormal distribution seems to better represent the distribution of the output values.

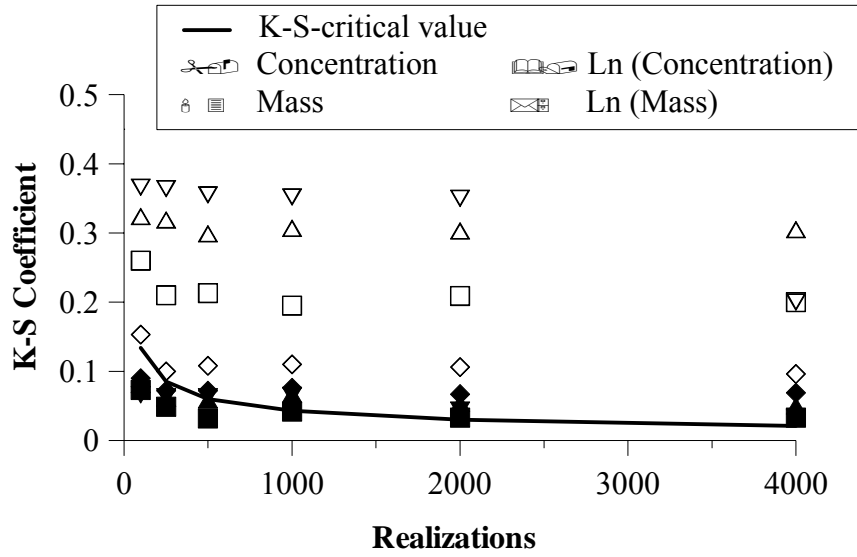


Figure 4.6: Results of the Kolmogorov-Smirnov test for normality, for different model responses and different Monte Carlo series. squares correspond to a 0.1 m cap, triangles a 0.2 m cap and the straight line represents the critical value of the test.

The coefficient of skewness, which determines the asymmetry of the distribution, and the coefficient of kurtosis, a measure of the sharpness of the data peak, were calculated for the model output and for its logarithm. The coefficients calculated with the

logarithm of the response were generally nearer zero, which corresponds to the value for a normal distribution (results not presented). Therefore, we validate the assumption that the lognormal distribution better approximates the output than the normal distribution.

Several series of Monte Carlo simulations were performed in order to evaluate the stability of the response as a function of the number of realizations. The simulations consider two types of responses: the cumulative sum of the released mass and the concentration in the top layer of the sediments. Since the lognormal PDF describes reasonably well the distribution of the model response, the logarithm of the output values can be represented by a normal distribution, characterized by a mean and a standard deviation. As the number of realizations increases, these parameters should converge towards a stable value. In order to verify this hypothesis and to determine the number of realizations that is required to get a stable response we performed a series of 48 Monte Carlo simulations, gradually increasing the number of realizations, from 100 to 4000. The simulation time was set to 5 years and the series include Monte Carlo simulations with a cap thickness of 0.1 m or 0.2 m and normal or uniform distribution of the input variables. The mean and the standard deviation of the result of each Monte Carlo simulation were calculated and thereafter compared to the mean and standard deviation of the Monte Carlo simulation composed of 4000 realization, which is supposed to present the best convergence towards the true distribution of the model response. The mean deviation of the mean  $MD\mu$  [%] and the mean deviation of the standard deviation  $MD\sigma$  [%] and are obtained with equation (4.5) and (4.6) and presented in Figure 4.7. A mean deviation of 0% means that the result perfectly overlaps the 4000-realizations output.

$$MD\mu = \left( \frac{\mu_x - \mu_{4000}}{\mu_{4000}} \right) \cdot 100 \quad (4.5)$$

$$MD\sigma = \left( \frac{\sigma_x - \sigma_{4000}}{\sigma_{4000}} \right) \cdot 100 \quad (4.6)$$

The results show that for a number of realizations greater than 1000 both responses present a good stability and that the mean and the standard deviation fluctuate around the 4000-realizations value with a deviation of  $\pm 2\%$ . The response was similar for uniform or normal distribution of the input value.

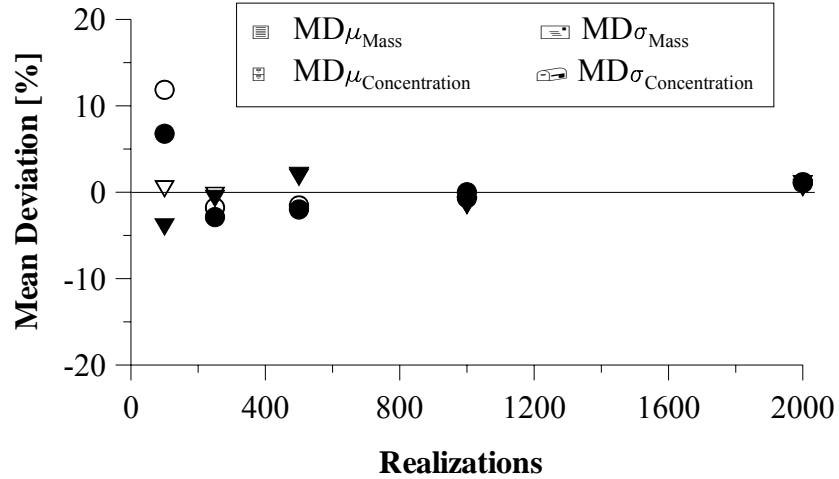


Figure 4.7: Mean deviation of the mean ( $MD\mu$ ) and of the standard deviation ( $MD\sigma$ ) for different Monte Carlo series.

## 4.7 Mobility of low solubility contaminant

Sediment contamination at the dock of Baie-Sainte-Catherine is poorly documented, but since the municipal effluents represent the main source of pollution, the sediments are expected to contain both metals and organic contaminants (Gagnon 1995). TRANSCAP-1D represents only the migration of dissolved compounds, thus the model is well suited to simulate the fate of inorganic contaminants (metals). The organic compounds commonly found in the Saguenay sediments (PAH, PCB, DDT) have a very low solubility and are associated with sediment particles. Therefore they cannot be represented by the numerical model. In order to include these contaminants in the

decision and calculate the probability that they reach the surface of the capping layer another method has to be used.

Since the organic compounds are bound to the solid particles, their migration is related to the mixing of sediments caused by the activity of the benthic organisms. This process is called bioturbation. The representation of the bioturbation depth is based on the observation of sediments collected with a box-corer in the Bras Nord and Baie des Ha!Ha! during summer 2000 and 2001 and we assume that the bioturbation profile is similar in Baie-Sainte-Catherine. Since the bioturbation depth shows a very strong spatial variability, this parameter is represented with a normal distribution, having a mean value of 0.1 m and a standard deviation of 0.05 m. The probability that a sediment particle located under the cap reaches the top of the sediment layer is set equivalent to the probability that the bioturbation depth reaches the contaminated layer. This simple method gives an approximation of the probability that the cap thickness is effective in isolating organic contaminants from the sediment-water interface.

## 4.8 Results of the decision analysis

The decision analysis is performed for both, soluble and low solubility contaminants, in order to account for trace metals and organic compounds. The probability that trace metals migrate as a solute through the capping layer is obtained from Monte Carlo simulations using the TRANSCAP-1D model with uniform input distributions. The mobility of the organic compounds is evaluated by accounting for the bioturbating activity of the benthic fauna.

The decision analysis strategy requires the definition of a criterion for the failure of the cap. Since we do not dispose of exact information about the concentration of contaminants in the sediments of the studied site, we cannot define the criterion for failure from toxicological thresholds. Thus, we have to define the limit between success and failure from the improvement comparatively to the situation before capping. The objective of a capping layer is to reduce significantly the contaminant concentration in

the upper layer of the sediments. Therefore, we assess that the cap fails if 10 years after capping, the contaminant concentration at the surface of the sediments exceeds 10% of the concentration before capping.

#### 4.8.1 Trace metals

In order to obtain stable and accurate output distributions for the decision analysis, we performed Monte Carlo simulations composed of 1000 realizations and the simulation time was set to 10 years. Since the contamination level at the studied site is poorly documented, two values were chosen for the maximal concentration of contaminant in the sediment column:  $25\ 000\ \mu\text{g m}^{-3}$  and  $100\ 000\ \mu\text{g m}^{-3}$ . Both simulations gave very similar output distributions, thus we only present the results obtained with the peak value of  $100\ 000\ \mu\text{g m}^{-3}$ .

Figure 4.8 shows the graphical result of decision analysis presenting the trend of the objective function for the six capping options and a cap porosity of 0.7. The analysis uses the values of the construction cost  $C$  presented in Table 4.1. The cost associated with the risk of failure  $R$  is calculated multiplying the probability of failure  $P_f$  (schematically represented in Figure 4.4) with the cost of failure  $C_f$  that is conservatively assumed to attain \$3 million CAD per year (Table 4.1). As presented in equation (4.3), the objective function is the total cost of the project corresponding to the sum of the cost of construction and the cost associated with the risk of failure. Figure 4.8 shows that, due to the reduction of the cost associated with the risk of failure, the total cost of restoration decreases rapidly from 32 million CAD to 7 million CAD corresponding to increasing thickness from 0.1 m to 0.2 m and seems to attain a minimum between 0.2 m and 0.24 m. The true least-cost option is the 0.24 m option, because this alternative has a total cost of \$6.98 million CAD whereas the 0.2 m options has a total cost of \$7.02 million CAD. The two options are considered equivalent.

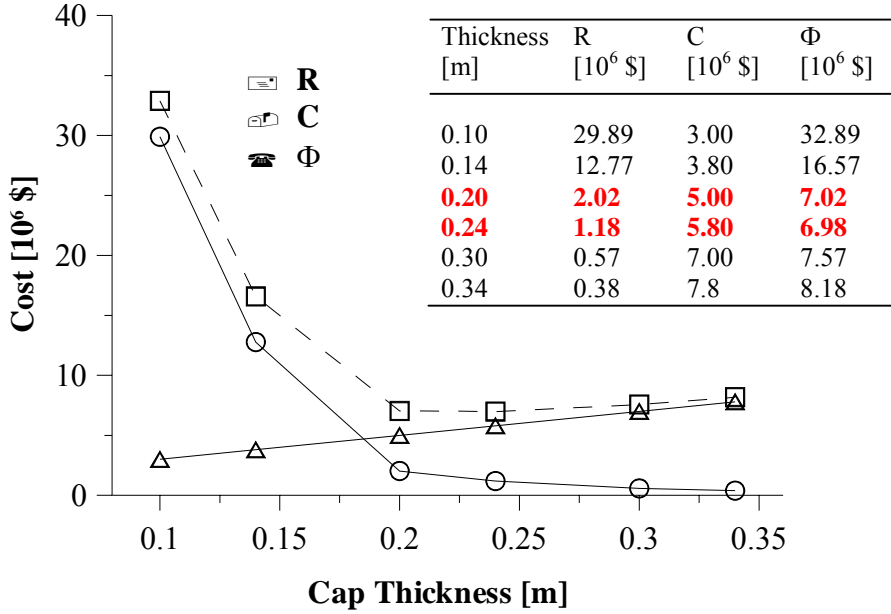


Figure 4.8: Costs of different management options, considering a dissolved contaminant and a fine-grained cap ( $R$ : Cost associated to the risk of failure;  $C$ : Cost of construction;  $\Phi$ : Total cost).

Figure 4.9 shows the graphical result of decision analysis for the same values of capping thickness, but with a cap porosity of 0.4, thus representing a more sandy cap. This time the least-cost option is the 0.3 m option with a total cost of \$7.84 million CAD, but we note that this option is almost equivalent to the 0.24 m option, which has a total cost of \$7.92 million CAD. Once more we observe the very rapid decrease of the objective function from 33 million CAD to 9.4 million CAD between 0.1 m and 0.2 m.

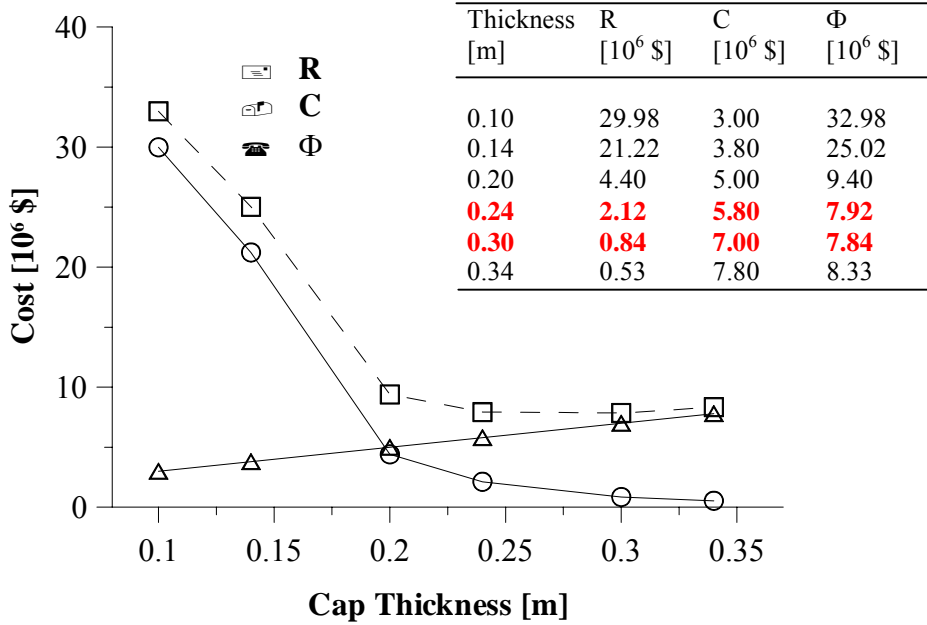


Figure 4.9: Costs of different management options, considering a dissolved contaminant and a sandy cap (R: Cost associated to the risk of failure; C: Cost of construction;  $\Phi$ : Total cost).

#### 4.8.2 Organic contaminants

The strategy used in this example to represent the migration of the organic contaminants is very simplified. Low solubility contaminants are transported with sediment particles by bioturbation and the probability that the contaminant reaches the surface of the cap is equivalent to the probability that the bioturbation depth reaches the contaminated layer under the cap. The results illustrated in Figure 4.10 show that for an organic contaminant the objective function decreases rapidly from 0.1 m to 0.2 m and thereafter increases again. The cap thickness of 0.2 m represents the least cost option with a total cost of \$5.68 million CAD and a probability of failure of 2%.

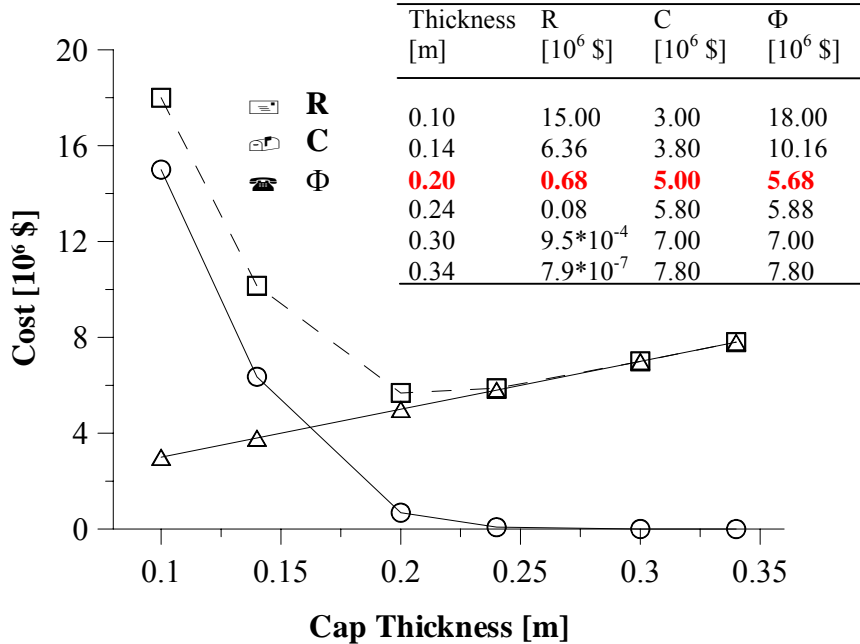


Figure 4.10: Costs of different management options, for a low solubility contaminant ( $R$ : Cost associated to the risk of failure;  $C$ : Cost of construction;  $\Phi$ : Total cost).

#### 4.8.3 Evaluation of the influence of the cost of failure

The representation of the results of the decision analysis is straightforward and shows clearly that if the capping layer is too thin, the risk of failure is high, affecting the total cost of the project. Since the cost associated to the risk of failure depends on the cost of failure  $C_f$ , which is difficult to estimate, we investigated the influence of different costs of failure on the result of the decision analysis. Figure 4.11 represents the variation of the objective function for different costs of failure considering a soluble contaminant. For  $C_f$  values of \$ 0.75 and \$ 1.5 million CAD, the least cost option is the 0.2 m cap thickness, while for a  $C_f$  of \$ 3 million CAD, the optimal alternative is the 0.24 m option. Finally for a  $C_f$  of \$ 6 million CAD the least cost alternative is the 0.3 m cap thickness. We observe that between 0.1 m and 0.2 m cap thickness, for increasing values of cost of failure we obtain steeper decreases in the total cost of the capping project. On the other hand, between 0.2 m and 0.34 m cap thickness, the total cost function seems to attain a

plateau. Thus, even if the optimal option is affected by the variation of the cost of failure, the general trend of the total cost function does not change.

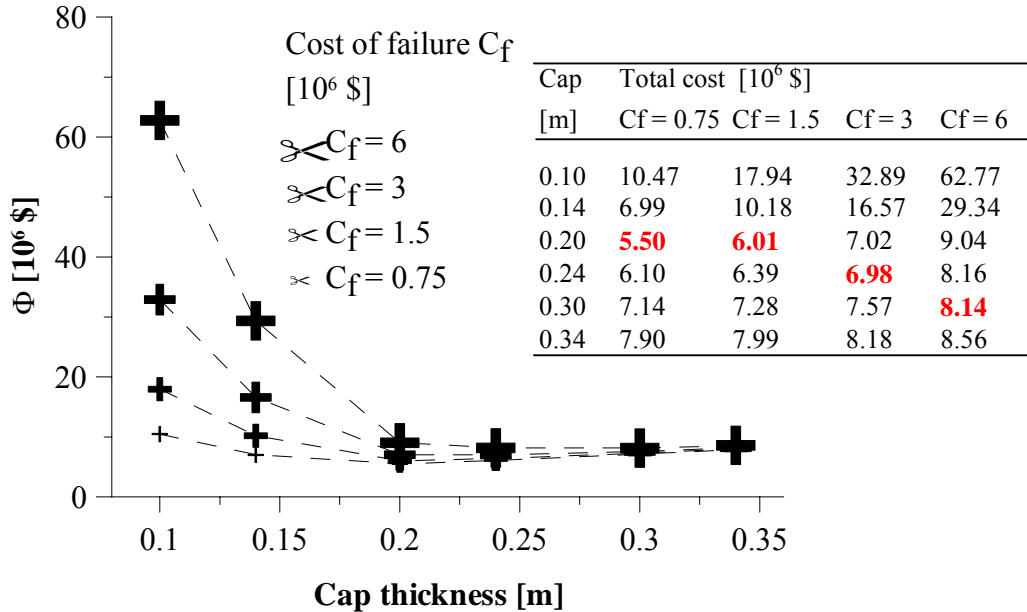


Figure 4.11: *Total cost for different capping options, considering various costs of failure.*

## 4.9 Discussion and Conclusion

The decision analysis method was applied to the design of a hypothetical capping project, loosely based on a real situation (concern for belugas health in the St. Lawrence Estuary). The main advantage of this strategy is that it allows for systematic comparison of different capping alternatives, accounting for uncertainty and for the costs associated with the construction and the risks of failure of the project. The design alternatives are evaluated by comparing the total cost associated to construction and risk of failure of the project. The representation of the results is straightforward and suitable for communication with decision-makers.

The presented decision analysis is based on several hypotheses. The PDFs of the input parameters are estimated from the limited available data. Since we disposed of very few informations on the Baie Ste-Catherine area, we had to extrapolate the necessary parameters from the studied sites located in the Bras Nord and the Baie des Ha! Ha! and we used the numerical model that was calibrated at those sites. These hypotheses were necessary to carry out the decision analysis but they limit the reliability of the results. A better characterization of the study site is recommended in order to confirm the results of the decision analysis.

The current knowledge about the ecosystem does not allow linking the contamination of the study site with the health problems observed in belugas. Nevertheless, environmental reports already assessed the need to collect more information at the site in order to produce a more accurate description of the contamination and its extension. Furthermore, a better knowledge of the site characteristics would also reduce the uncertainty in the decision analysis. If the link between the contamination of this area and the health problems of belugas was provided, the decision analysis method could be used under the condition that more accurate information on the contaminant types and the characteristics of the area be included.

The cost of failure is often difficult to evaluate. However, the evaluation of the cost of failure is required not only for the presented decision analysis method, but also for decision techniques, which do not include variability. In our example, we approximated the cost of failure with a value equivalent to about 5% of the total economic benefits of whale watching industry. This estimation does not consider the uniqueness of the beluga population of the St. Lawrence Estuary. A more detailed analysis of the economic value of belugas could be performed to better estimate the cost of failure.

## 4.10 References

- Barbeau, C., Bougie, R. and Côté, J.-E. 1981. Temporal and spatial variations of mercury, lead, zinc and copper in sediments of the Saguenay fjord. Can. J. Earth Sci. **18**: 1065-1074.

- Bourg, C. 2002. Étude du transport de métaux lourds par advection et diffusion dans des sédiments de la couche de 1996 au Saguenay (Québec). MSc Thesis, Département de génie civil, Faculté des Sciences et Génie, Université Laval.
- Coakley, J. P. and Poulton, D. J. 1993. Source-related classification of St. Lawrence estuary sediments based on spatial distribution of adsorbed contaminants. *Estuaries* **16**(4): 873-886.
- Comité multipartite sur les sites contaminés pouvant affecter le béluga du Saint-Laurent 1998. Sites contaminés du Saint-Laurent susceptibles d'avoir un impact sur le béluga. Rapport présenté au comité de gestion de l'entente du Plan d'action Saint-Laurent Vision 2000. Environnement Canada, Pêches et Océans Canada, Patrimoine canadien et Ministère de l'Environnement et de la Faune du Québec.
- Cossa, D. 1990. Chemical contaminants in the St. Lawrence Estuary and Saguenay Fjord. In : El-Sabh, M. I., Silverberg, N. (Eds.), Oceanography of a large scale estuarine system, The St. Lawrence. Coastal and Estuarine Studies **39**: 239-268, Springer Verlag.
- Dakins, M. E., Toll, J. E. and Small, M. J. (1994). Risk-based environmental remediation: decision framework and role of uncertainty. *Environ. Toxicol. Chem.* **13**(12): 1907-1915.
- De Montety, L., Long, B., Desrosiers, G., Crémer, J.-F. and Locat, J. 2000. Quantification des structures biogènes en fonction d'un gradient de perturbation dans la baie des Ha! Ha! à l'aide de la tomodensitométrie axiale. Proceedings of the 53th Canadian Geotechnical Conference, Montréal, 15-18 Oct. 2000, Vol. 1, pp. 131-135.
- Domenico, P.A. and Schwartz, F.W. 1998. Physical and chemical hydrogeology. Wiley, New York.
- Dueri, S. and Therrien, R. 2003. Factors controlling contaminant transport through the flood sediments of the Saguenay Fjord: Numerical sensitivity analysis. In: Contaminated sediments: Characterization, Evaluation, Mitigation/Restoration and Management strategy Performance, ASTM STP1442, J. Locat, R. Galvez-Cloutier, R.C. Chaney, and K.R. Demars, Eds. ASTM International, West Conshohocken, PA, 167-182.
- Dueri, S., Therrien, R. et Locat, J. (In press). Numerical modeling of the migration of dissolved contaminants through a subaqueous capping layer. *J. Environ. Eng. Sci.*
- Freeze, R. A., Massmann, J., Smith, L., Sperling, T. and James, B. 1990. Hydrogeological decision analysis: 1. A framework. *Ground Water* **28**(5): 738-766.

- Fuller, W. H. 1978. Investigation of landfill leachate pollutant attenuation by soils. US EPA, Municipal Environmental Research Laboratory, Cincinnati, OH
- Gagnon, C., Pelletier, É. and Maheu, S. 1993. Distribution of trace metals and some major constituents in sediments of the Saguenay Fjord, Canada. Mar. Pollut. Bull. **26** (2): 107-110.
- Gagnon, M. 1995. Bilan Régional - Secteur du Saguenay. Zones d'intervention prioritaire 22 et 23. Centre Saint-Laurent, Environnement Canada, Saint-Laurent Vision 2000.
- Gobeil, C. and Cossa, D. 1984. Profils des teneurs en mercure dans les sédiments et les eaux interstitielles du fjord du Saguenay (Québec): données acquises au cours de la période 1978-83. Rapport Technique Canadien Hydrographie et Sciences Océaniques: **53**.
- Héroux, M.-C. 2000. Rapport de mission AH9908. Projet Saguenay post-déluge. Rapport du GREGI no. ULSAGPD99-08. Département de géologie et génie géologique, Université Laval.
- Hickie, B. E., Kingsley, M. C. S., Hodson, P. V., Muir, D. C. G., Béland, P. and Mackay, D. 2000. A modelling-based perspective on the past, present, and future polychlorinated biphenyl contamination of the St. Lawrence beluga whale (*Delphinapterus leucas*) population. Can. J. Fish. Aquat. Sci. **57**(Suppl. 1): 101-112.
- Hoyt, E. 2000. Whale Watching 2000: Worldwide Tourism Numbers, Expenditures, and Expanding Socioeconomic Benefits. International Fund for Animal Welfare, Crowborough, UK.
- Le Groupe Type 1996. Documentation sur la méthode d'estimation de la fréquentation du Parc Marin du Saguenay-Saint-Laurent - saison estivale 1995, Parks Canada, September 1996, 43 pp. + appendices.
- Lesage, V. and Kinsley, C. S. 1998. Updated Status of the St Lawrence River Population of Beluga, *Delphinapterus leucas*, Can. Field Naturalist **112**(1): 98-114.
- Lepage, N., Hamel, P., Lefebvre, R., Therrien, R. and Blais, C. 1999. Decision analysis for leachate control at a fractured rock landfill. Ground Water Monit. Remed. **19**(3) : 157-170.
- Martineau, D., Lemberger, K., Dallaire, A., Labelle, P., Lipscomb, T.P., Michel, P. and Mikaelian, I. (2002). Cancer in Wildlife, a case study: Beluga from the St. Lawrence Estuary, Québec, Canada. *Environmental Health Perspectives*, **110**(3): 285-292.

- Massmann, J., Freeze, R. A., Smith, L., Sperling, T. and James, B. 1991. Hydrogeological decision analysis: 2. Applications to ground-water contamination. *Ground Water* **29**(4): 536-548.
- Morgan, M. G. and Herion, M. 1990. Uncertainty: A Guide to Dealing with Uncertainty in Quantitative Risk and Policy Analysis, Cambridge University Press, New York.
- Mucci, A., Guignard, C. and Olejczuk, P. 2000a. Mobility of metals and As in sediments following a large scale episodic sedimentation event. Proceedings of the 53th Canadian Geotechnical Conference, Montréal, 15-18 Oct. 2000, Vol. 1, pp. 169-175.
- Mucci, A., Richard, L.-F., Lucotte, M. and Guignard, C. 2000b. The differential geochemical behaviour of arsenic and phosphorous in the water column and sediments of the Saguenay fjord estuary, Canada. *Aquatic Geochem.* **6**: 293-324.
- Mucci, A., Boudreau, B. and Guignard C. 2003. Diagenetic mobility of trace elements in sediments covered by a flash flood deposit: Mn, Fe and As. *Applied Geochem.* **7**: 1011-1026.
- Muir, D. C. G., Ford, C. A., Stewart, R. E. A., Smith, T. G., Addison, R. F., Zink, M. E. and Béland, P. 1990. Organochlorine Contaminants in Belugas, *Delphinapterus leucas*, from Canadian waters. p. 165-190. In Smith, T. G., St. Aubin, D.J. and Geraci, J.R. (ed.) Advances in research on the beluga whale, *Delphinapterus leucas*. *Can. Bull. Fish. Aquat. Sci.* 224.
- Muris, M. 2001. Étude de la contamination des sédiments du fjord du Saguenay et évaluation de la rétention du cuivre, du plomb et du zinc. M. Sc. Thesis, Département de génie civil, Faculté des Sciences et Génie, Université Laval.
- Neville C. J., Ibaraki, M. and Sudicky, E. A. 2000. Solute transport with multiprocess nonequilibrium: a semi-analytical solution approach. *J. Cont. Hydr.* **44**: 141-159.
- Otero, X. L., Sanchez, J. M., and Macias F. 2000. Bioaccumulation of heavy metals in thionic fluvisols by a marine polychaete: The role of metal sulfides. *J. Environ. Qual.* **29**: 1133-1141.
- Palermo, M., Schroeder, P., Rivera, Y., Ruiz, C., Clarke, D., Galiani, J., Clausner, J., Hynes, M., Fredette, T., Tardy, B., Peyman-Dove, L. and Risko, A. 1999. Option for In-Situ Capping of Palos Verdes Shelf contaminated sediments. Technical Report EL-99-2, U.S. Army Engineer Waterways Experiment Station, Vicksburg, MS.

- Pelletier, É. and Canuel G. 1988. Trace metals in surface sediment of the Saguenay fjord, Canada. *Mar. Pollut. Bull.* **19**: 336-338.
- Pelletier, É., Deflandre, B., Nozais, C., Tita, G., Desrosiers, G., Gagné, J.-P. and Mucci, A. 1999. Crue éclair de juillet 1996 dans la région du Saguenay (Québec). 2. Impact sur les sédiments et biote de la baie des Ha! Ha! et du fjord du Saguenay. *Can. J. Fish. Aquat. Sci.* **56**: 2136-2147.
- Pelletier, É., Desrosiers, G., Locat, J., Mucci, A. and Tremblay, H. 2003. The origin and behavior of a catastrophic capping layer deposited on contaminated sediments of the Saguenay Fjord (Quebec). In: *Contaminated sediments: Characterization, Evaluation, Mitigation/Restoration and Management strategy Performance*, ASTM STP1442, J. Locat, R. Galvez-Cloutier, R. C. Chaney and K. Demars, Eds., ASTM International, West Conshohocken, PA, 2003, 3-18.
- Pippard, L. and Malcolm, H. 1978. White Whales (*Delphinapterus leucas*). Observations on their distributions, populations and critical habitats in the St. Lawrence and Saguenay rivers. Unpublished report prepared for Departement of Indian and Northern Affairs, Parks Canada, Ottawa, Ontario.
- Riisgard, H.U. 1989. Properties and energy cost of the muscular piston pump in the suspension feeding polychaete *Chaetopterus variopedatus*. *Mar. Ecol. Progr. Ser.* **56**: 157-168.
- Riisgard, H.U. 1991. Suspension feeding in the polychaete *Nereis diversicolor*. *Mar. Ecol. Progr. Ser.* **70**: 29-37.
- Saulnier, I. and Mucci, A. 2000. Trace Metal Remobilization Following the Resuspension of Estuarine Sediments: Saguenay Fjord, Canada. *Appl. Geochem.* **15**: 191-210.
- Sperling, T., Freeze, R. A., Massmann, J., Smith, L. and James, B. 1992. Hydrogeological Decision Analysis: 3. Application to Design of a Ground-Water Control System at an Open Pit Mine. *Ground Water* **30** (3): 376-389.
- Tremblay, G.-H. and Gobeil, C. 1990. Dissolved arsenic in the St Lawrence Estuary and the Saguenay Fjord, Canada. *Mar. Pollut. Bull.* **21**(10): 465-469.
- Vanysek, P. 2000. Ionic Conductivity and diffusion at infinite dilution. In *CRC handbook of chemistry and physics*, 81st edition, Cleveland, Ohio.
- Versteeg, H.K. and Malalasekera, W. 1995. An introduction to computational fluid dynamics: the finite volume method. Longman Scientific & Technical, Burnt Mill, Harlow, Essex.

- Vladykov, V.-D. 1946. Étude sur les mammifères marins IV. Nourriture du Marsouin Blanc ou Béluga (*Delphinapterus leucas*) du fleuve Saint-Laurent. Contrib. Dép. Pêches Québec, 14 : 191 pp.
- Wagemann, R., Stewart, R. E. A., Béland, P. and Desjardins, C. 1990. Heavy metals and selenium in tissues of beluga whales, *Delphinapterus leucas*, from the Canadian Arctic and the St. Lawrence Estuary. P. 191-206. In Smith, T. G., St. Aubin, D.J. and Geraci, J.R. (ed.) Advances in research on the beluga whale, *Delphinapterus leucas*. Can. Bull. Fish. Aquat. Sci. 224.
- Yan, Q.-L. and Wang W.-X. 2002. Metal exposure and bioavailability to a marine deposit-feeding Sipuncula, *Sipunculus nudus*. Environ. Sci. Technol. 36: 40-47.
- Zheng, C. and Bennett, G. D. 2002. Applied Contaminant Transport Modeling. 2<sup>nd</sup> Edition, John Wiley, New York.

# Conclusion

Cette étude a été réalisée dans le cadre global du Projet Saguenay Post-Déluge, dont le but était de déterminer l'efficacité à long terme de la couche de recouvrement naturelle, déposée dans le fjord du Saguenay suite à un événement de crue extrême, et de développer des outils pour la conception d'une telle couche. L'objectif spécifique de la présente étude était de développer un modèle numérique pour simuler le transport de contaminants dans une colonne de sédiments. Le modèle a ensuite été utilisé pour la conception d'une couche de recouvrement dans un cas hypothétique. L'étude a été subdivisée en trois volets:

1. Le développement d'un modèle numérique et calage avec des données de terrain.
2. L'analyse de sensibilité du modèle pour évaluer l'influence de certains paramètres sur la réponse.
3. L'application de la méthode d'analyse de décision pour la conception d'une couche de recouvrement hypothétique.

Le premier objectif était donc de développer un modèle numérique qui simule la migration verticale d'une composante dissoute à travers une couche de recouvrement. Dans le modèle le transport de masse est représenté d'une façon générale pour une composante dissoute, mais en raison de la disponibilité des données les simulations ont été adaptées au transport de l'arsenic et les résultats comparés avec des profils d'arsenic dissous mesurées à deux stations, deux ans après la déposition d'une couche de recouvrement naturelle dans le fjord du Saguenay. La bonne superposition des profils de concentrations simulées et mesurées a montré que le modèle est capable de représenter l'évolution d'un contaminant dissous à travers une couche de sédiments. L'arsenic n'est pas un contaminant dans le fjord du Saguenay, son origine étant naturelle. En outre, il réagit rapidement suite au passage d'un milieu réducteur à un milieu oxydant et il est plus facilement remobilisable que les métaux traces qui contaminent les sédiments du fjord du

Saguenay. On peut donc considérer que la simulation du transport de l'arsenic représente un cas particulièrement défavorable, comparativement aux autres métaux traces.

Idéalement, le modèle aurait dû être calé avec une séquence de profils de concentration de plusieurs contaminants dissous, mesurés pendant plusieurs années aux même stations et représentant donc l'évolution de la contamination dans les sédiments. Malheureusement la variabilité spatiale du milieu et les techniques d'échantillonnage n'ont pas permis d'obtenir une telle séquence de profils. Étant donnée la profondeur moyenne du fjord d'environ 150 m, les échantillons peuvent difficilement être pris à un endroit précis, mais sont plutôt prélevés à l'intérieur d'un périmètre de quelques mètres, tout dépendant de l'intensité des courants qui déplacent le carottier dans sa descente vers le fond. Ainsi les profils qui ont été mesurés à la même station pendant plusieurs années montrent des épaisseurs de turbidite variables et la distribution de contaminants est difficile à corrélérer d'un profil à l'autre. Il n'est donc pas possible d'utiliser une séquence de profils pour valider l'évolution de la contamination représentée par le modèle.

Dans le cadre du Projet Saguenay Post-Déluge un grand nombre d'échantillons de sédiments a été prélevé et analysé. L'ensemble des données montre que certaines propriétés des sédiments sont très variables d'une station à l'autre et même à l'intérieur d'une même station d'échantillonnage. En particulier, on a constaté une variabilité qui concerne surtout la quantité et profondeur des tubes de vers, ainsi que l'épaisseur de la couche de turbidite. Afin d'évaluer l'effet de la variabilité des paramètres sur la réponse du modèle, nous avons réalisé une première série de simulations pour des profondeurs de bio-irrigation et des épaisseurs de la couche variables. Ces simulations considèrent deux types de contaminants: les contaminants réactifs, qui peuvent être remobilisés et pour lesquels il peut y avoir ajout de masse en solution, et les contaminants non-réactifs. Les contaminants réactifs sont des composantes qui, comme l'As, sont associées au FeS et piégées dans les sédiments sous forme solide. Ces composantes (e.g. Ni, Cu, Co, Hg, Pb) peuvent être remobilisées suite à l'oxydation du FeS causé par l'apport d'eau riche en oxygène dans les trous de vers (bio-irrigation). Le modèle a été utilisé pour calculer la variation des profils de contaminants dans le temps ainsi que la masse totale de

contaminant relarguée par la limite supérieure des sédiments à la fin de la simulation. Le résultat des simulations montre que pour un contaminant réactif, la profondeur de bio-irrigation a une influence plus importante que l'épaisseur de la couche sur le relargage de contaminant. La dissolution qui a lieu à l'intérieur des tubes de vers est donc le processus qui régit le relargage d'une composante réactive. Par contre, pour un contaminant non réactif, le relargage dépend du rapport entre la profondeur de bio-irrigation et l'épaisseur de la couche. Le contaminant non-réactif sera relargué seulement si les tubes de vers atteignent les sédiments contaminés. Dans les deux cas, réactif et non-réactif, les simulations ont montré l'importance de la profondeur de bio-irrigation.

D'un point de vue environnemental les concentrations d'As dissous calculées par le modèle pour la couche de surface des sédiments du Saguenay ne dépassent pas le Critère de Concentration Continue pour l'eau salée recommandé par l'USEPA (USEPA 1999). Ce critère représente la concentration maximale à laquelle une communauté aquatique peut être soumise à temps indéterminé sans avoir des conséquences inacceptables. D'ailleurs le modèle ne tient pas compte du fait qu'une fraction significative de l'As remobilisée par l'oxydation du FeS sera adsorbée par des oxydes de fer ou de manganèse dans sa migration vers la surface des sédiments et donc que la concentration sera ultérieurement réduite. Par conséquent, seulement une très petite partie sera effectivement relarguée par la limite supérieure et lorsque la composante atteindra la colonne d'eau au-dessus des sédiments, elle sera mélangée et diluée dans l'eau par effet des courants de fond. Les sédiments du site à l'étude ne présentent donc pas de danger pour l'écosystème en ce qui concerne la présence d'As dissous. Néanmoins, la modélisation du transport de contaminants dissous dans les sédiments du fjord du Saguenay s'est avéré un exercice intéressant et instructif, puisqu'il a permis d'utiliser le modèle avec des données réelles et d'évaluer l'importance de la bio-irrigation et de l'épaisseur de la couche pour l'efficacité de la couche de recouvrement dans un cas concret. Même si le nombre de données pouvant être utilisé pour le calage du modèle était limité par la variabilité du milieu et les problèmes de corrélation des profils, le site représente une bonne occasion pour utiliser un tel modèle et évaluer l'importance des différents paramètres d'entrée pour le transport de contaminant.

Afin de mieux comprendre le système et ses interactions ainsi que l'effet de la variabilité et de l'incertitude qui caractérisent certains paramètres d'entrée nous avons réalisé une analyse de sensibilité détaillée, basée sur la méthode du design factoriel. La méthode permet de déterminer de façon systématique les facteurs ayant un effet significatif sur la réponse du modèle. Deux types de réponses ont été considérés pour l'analyse de sensibilité: la masse cumulative de contaminant qui sort du système par la limite supérieure (interface sédiments/eau) dans les 10 ans suivant la mise en place du recouvrement et la concentration finale du contaminant à la surface de la couche de recouvrement 10 ans après le recouvrement. Les deux réponses ont été choisies parce qu'elles représentent deux voies à travers lesquelles les contaminants peuvent atteindre la faune aquatique et avoir des effets néfastes sur l'environnement. Les résultats de l'analyse de sensibilité ont montré que pour les conditions retrouvées dans le fjord du Saguenay, les facteurs ayant un effet significatif varient en fonction de la réponse étudiée, le type de contaminant (réactif ou non) et dans certains cas l'épaisseur de la couche. En général les paramètres de bio-irrigation sont important dans presque tous les cas. Le coefficient de dissolution est cependant critique uniquement pour la concentration de contaminant à la surface du sédiment.

Les résultats obtenus nous indiquent que les paramètres liés à la bio-irrigation doivent être caractérisés avec soin pour obtenir des résultats de modélisation valables. Il faut cependant reconnaître que même une caractérisation très détaillée des sédiments ne pourra jamais déterminer la globalité des variations spatiales des paramètres d'entrée et les représenter dans un modèle. Par conséquent il y aura toujours une marge d'imprécision dans la réponse du modèle et de l'incertitude vis à vis de la fiabilité de la réponse.

Afin de pouvoir évaluer l'impact de l'incertitude des paramètres d'entrée sur la réponse, nous avons réalisé une analyse d'incertitude avec la méthode Monte Carlo. Cette analyse fournit la distribution de la réponse du modèle en fonction de la variation des paramètres d'entrée. Les résultats de l'analyse d'incertitude ont été ensuite intégrés dans une approche d'analyse de décision qui a été appliquée au dimensionnement d'une couche

de recouvrement dans un cas hypothétique de réhabilitation de sédiments contaminés. Le cas qui a été choisi pour illustrer la méthode s'inspire de la réalité et concerne la réhabilitation d'un site contaminé qui est fréquenté régulièrement par les bélugas et qui est soupçonné d'avoir un effet nocif sur la santé de ces mammifères marins. Le site se trouve à l'embouchure du fjord du Saguenay, à Baie-Ste-Catherine et n'a pas subi les conséquences de la crue de 1996.

L'épaisseur optimale de la couche a été calculée avec la méthode de l'analyse de décision qui unit la probabilité que la structure mise en place puisse satisfaire les critères de réussite du projet avec l'aspect économique. L'avantage de la méthode est dans la comparaison systématique des différentes alternatives sur la base du coût et des risques associés au projet et dans la représentation simple et efficace des résultats. Afin de considérer également les contaminants peu solubles, comme certain contaminants organiques présents dans les sédiments du site à l'étude, la probabilité que ces derniers traversent la couche a été évaluée en utilisant la distribution de la profondeur de bioturbation.

Dans le développement du modèle nous avons simplifié la représentation du système à l'étude et des processus, dans le but d'avoir un code simple nécessitant un nombre minimal de paramètres d'entrée. Nous avons essayé de faire la distinction entre les processus fondamentaux, comme l'advection, la diffusion, la bio-irrigation, qui sont essentiels à la description de la migration des composantes dissoutes et les processus secondaires, comme les réactions, différents et typiques pour chaque composante. Un des objectifs de l'étude était de mieux comprendre le fonctionnement d'une couche de recouvrement et d'identifier les facteurs importants qui définissent son efficacité en utilisant les données recueillies dans le cadre du Projet Saguenay Post-Déluge. Dans un système complexe, influencé par un très grand nombre de paramètres, ayant une incertitude assez élevée, il est plus difficile de saisir les paramètres qui ont une influence majeure sur le résultat du système. De plus, l'avantage principal d'avoir un code simple est que le temps de simulation est court ce qui permet de l'utiliser pour réaliser des séries de simulations Monte Carlo en un laps de temps raisonnable.

L'application du modèle se limite aux contaminants qui sont dissous ou qui peuvent être remobilisés suite à l'oxydation des sulfures. Il n'est par contre pas adapté à la simulation de la migration de contaminants très peu solubles et liés aux particules, tels les HAP et d'autres organiques. Ces contaminants peuvent éventuellement "migrer" vers la surface par effet du remaniement des sédiments causé par la bioturbation, un processus qui n'est pas représenté dans le modèle. Il faut aussi noter que les mécanismes de remobilisation considérés présentement dans le modèle ne sont pas représentatifs d'un milieu lacustre, dans lequel les sulfures sont beaucoup moins abondants.

Le modèle pourrait être amélioré, en intégrant d'une façon plus détaillée les réactions chimiques. Cela n'a pas été fait dans le cadre de la thèse pour éviter d'introduire également une très grande incertitude concernant la cinétique des réactions, les concentrations initiales des différentes composantes, etc. qui aurait pu masquer l'importance d'autres processus, avec une incertitude mineure. Une autre raison est le manque de données adéquates pour caler un tel modèle.

Afin de considérer les variations spatiales des sédiments le modèle pourrait être modifié pour représenter le cas 3D. En outre, il pourrait éventuellement intégrer les phénomènes de sédimentation et d'érosion à la surface de la couche de recouvrement. Dans l'étude ce dernier aspect n'a pas été considéré car dans le fjord du Saguenay le taux de sédimentation est assez limité, sauf dans zones proches de l'embouchure des rivières.

Enfin, l'analyse de sensibilité pourrait être réalisée dans un contexte plus général, afin de considérer d'autres conditions que celles observées dans les sédiments du fjord du Saguenay. Le modèle pourrait donc être utilisé pour évaluer l'effet de paramètres qui n'ont pas été considérés jusqu'ici, comme le taux d'accumulation ou la vitesse d'écoulement.

## Bibliographie

- Aggett, J. et O'Brien, G. A. 1985. Detailed model for the mobility of arsenic in lacustrine sediments based on measurements in Lake Ohakuri. Environ. Sci. Technol. **19**: 231-238.
- Allan, R. J. 1990. The Saguenay Fjord: A third factor in the toxic chemical contamination of the St. Lawrence river estuary. Wat. Poll. Res. J. Canada. **25**(1): 1-14.
- Aller, R. C. 1980. Quantifying solute distributions in the biotubated zone of marine sediments by defining an average microenvironment. Geochim. Cosmochim. Acta **44**: 1955-1965.
- Aller, R. C. et Aller, J. Y. 1998. The effect of biogenic irrigation intensity and solute exchange on diagenetic reaction rates in marine sediments. J. Mar. Res. **56**: 905-936.
- Aller, R. C. et Yingst, J. Y. 1978. Biogeochemistry of tube-dwellings: A study of the sedentary polychaete *Amphitrite ornata* (Leidy). J. Mar. Res. **36**(2): 201-254.
- Aller, R. C. et Yingst, J. Y. 1985. Effects of the marine deposit-feeders *Heteromastus filiformis* (Polychaeta), *Macoma balthica* (Bivalvia), and *Tellina texana* (Bivalvia) on averaged sedimentary solute transport, reaction rates, and microbial distributions. J. Mar. Res. **43**: 615-645.
- Archer, D. et Devol, A. 1992. Benthic oxygen fluxes on the Washington shelf and slope: A comparison of in situ microelectrode and chamber flux measurements. Limn. Oceanogr. **37**(3): 614-629.
- Barbeau, C., Bougie, R. et Côté, J.-E. 1981a. Variations spatiales et temporelles du césium-137 et du carbone dans les sédiments du fjord du Saguenay. Can. J. Earth Sci. **18**: 1004-1011.
- Barbeau, C., Bougie, R. et Côté, J.-E. 1981b. Temporal and spatial variations of mercury, lead, zinc and copper in sediments of the Saguenay fjord. Can. J. Earth Sci. **18**: 1065-1074.
- Belzile, N. et Tessier, A. 1990. Interactions between arsenic and iron oxyhydroxides in lacustrine sediments. Geochim. Cosmochim. Acta **54**: 103-109.
- Boudreau, B. P. 1984. On the equivalence of nonlocal and radial diffusion models for porewater irrigation. J. Mar. Res. **42**: 731-735.

- Boudreau, B. P. 1997. Diagenetic Models and Their Implementation: Modelling Transport and Reactions in Aquatic Sediments. Springer-Verlag, Berlin Heidelberg.
- Boudreau, B. P. 1999. Metals and models: Diagenetic modelling in freshwater lacustrine sediments. *J. Paleolimn.* **22**: 227-251.
- Box, G. E. P., Hunter, W. G. et Hunter, J. S. 1978. Statistics for Experimenters: an Introduction to Design, Data Analysis, and Model Building. John Wiley, New York.
- Boyer, J. M., Chapra, S. C., Ruiz, C. E. et Dortch, M. S. 1994. RECOVERY, a mathematical model to predict the temporal response of surface water to contaminated sediments. Technical report W-94-4, U.S. Army Engineer Waterways Experiment Station, Vicksburg, MS.
- Bourg, C. 2002. Étude du transport de métaux lourds par advection et diffusion dans des sédiments de la couche de 1996 au Saguenay (Québec). Mémoire de maîtrise, Département de génie civil, Faculté des Sciences et Génie, Université Laval.
- Coakley, J. P. et Poulton, D. J. 1993. Source-related classification of St. Lawrence estuary sediments based on spatial distribution of adsorbed contaminants. *Estuaries* **16**(4): 873-886.
- Comité multipartite sur les sites contaminés pouvant affecter le béluga du Saint-Laurent 1998. Sites contaminés du Saint-Laurent susceptibles d'avoir un impact sur le béluga. Rapport présenté au comité de gestion de l'entente du Plan d'action Saint-Laurent Vision 2000. Environnement Canada, Pêches et Océans Canada, Patrimoine canadien et Ministère de l'Environnement et de la Faune du Québec. 26 p.
- Cossa, D. 1990. Chemical contaminants in the St. Lawrence Estuary and Saguenay Fjord. In: El-Sabh, M. I., Silverberg, N. (Eds.), Oceanography of a large scale estuarine system, The St. Lawrence. Coastal and Estuarine Studies **39**: 239-268, Springer Verlag.
- Dakins, M. E., Toll, J. E. et Small, M. J. (1994). Risk-based environmental remediation: decision framework and role of uncertainty. *Environ. Toxicol. and Chem.*, **13**(12): 1907-1915.
- De Montety, L., Long, B., Desrosiers, G., Crémer, J.-F. and Locat, J. 2000. Quantification des structures biogènes en fonction d'un gradient de perturbation dans la baie des Ha! Ha! à l'aide de la tomodensitométrie axiale. Proceedings of the 53th Canadian Geotechnical Conference, Montréal, 15-18 Oct. 2000, Vol. 1, pp. 131-135.

- Domenico, P. A. et Schwartz, F. W. 1998. Physical and chemical hydrogeology. Wiley, New York.
- Dueri, S. et Therrien, R. 2003. Factors controlling contaminant transport through the flood sediments of the Saguenay Fjord: Numerical sensitivity analysis. In: Contaminated sediments: Characterization, Evaluation, Mitigation/Restoration and Management strategy Performance, ASTM STP1442, J. Locat, R. Galvez-Cloutier, R.C. Chaney, and K.R. Demars, Eds. ASTM International, West Conshohocken, PA, 167-182.
- Dueri, S., Therrien, R. et Locat, J. (Sous presse). Numerical modeling of the migration of dissolved contaminants through a subaqueous capping layer. *J. Environ. Eng. Sci.*
- Elliott, M., Zheng, Y. et Bagley, D. M. 2000. Determining Significant Anaerobic Kinetic Parameters Using Simulation. *Environ. Technol.* **21**: 1181-1191.
- Emerson, S., Jahnke, R. et Heggie, D. 1984. Sediment-water exchange in shallow water estuarine sediments. *J. Mar. Res.* **42**: 709-730.
- Forster, S. et Graf, G. 1995. Impact of irrigation on oxygen flux into the sediment: intermittent pumping by Callianassa subterranea and "piston-pumping" by Lanice conchilega. *Mar. Biol.* **123**: 335-346.
- Freeze, R. A., Massmann, J., Smith, L., Sperling, T. et James, B. 1990. Hydrogeological decision analysis: 1. A framework. *Ground Water* **28**(5): 738-766.
- Fuller, W. H. 1978. Investigation of landfill leachate pollutant attenuation by soils. US EPA, Municipal Environmental Research Laboratory, Cincinnati, OH.
- Furukawa, Y., Bentley, S. J., Shiller, A. M., Lavoie, D. L. et Van Cappellen, P. 2000. The role of biologically-enhanced pore water transport in early diagenesis: an example from carbonate sediments in the vicinity of North Key Harbor, Dry Tortugas National Park, Florida. *J. Mar. Res.* **58**: 493-522.
- Furukawa, Y., Bentley, S. J. et Lavoie, D. L. (2001). Bioirrigation modeling in experimental benthic mesocosms. *J. Mar. Res.* **59**: 417-452.
- Gagnon, C., Pelletier, É. et Maheu, S. 1993. Distribution of trace metals and some major constituents in sediments of the Saguenay Fjord, Canada. *Mar. Pollut. Bull.* **26** (2): 107-110.
- Gagnon, C., Mucci, A. et Pelletier, É. 1995. Anomalous accumulation of acid-volatile sulphides (AVS) in a coastal marine sediment, Saguenay Fjord, Canada. *Geochim. Cosmochim. Acta*. **59**(13): 2663-2675.

- Gagnon, M. 1995. Bilan Régional - Secteur du Saguenay. Zones d'intervention prioritaire 22 et 23. Centre Saint-Laurent, Environnement Canada, Saint-Laurent Vision 2000.
- Gobeil C. et Cossa D. 1984. Profils des teneurs en mercure dans les sédiments et les eaux interstitielles du fjord du Saguenay (Québec): données acquises au cours de la période 1978-83. Rapport Technique Canadien Hydrographie et Sciences Océaniques: **53**.
- Guinasso, N. L. et Schink, D. R. 1975. Quantitative estimates of biological mixing rates in abyssal sediments. *J. Geoph. Res.* **80**: 3032-3043.
- Héroux, M.-C. 2000. Rapport de mission AH9908. Projet Saguenay post-déluge. Rapport du GREGI no. ULSAGPD99-08. Département de géologie et génie géologique, Université Laval.
- Hickie, B. E., Kingsley, M. C. S., Hodson, P. V., Muir, D. C. G., Béland, P. et Mackay, D. 2000. A modelling-based perspective on the past, present, and future polychlorinated biphenyl contamination of the St. Lawrence beluga whale (*Delphinapterus leucas*) population. *Can. J. Fish. Aquat. Sci.* **57**(Suppl. 1): 101-112.
- Hoyt, E. 2000. Whale Watching 2000: Worldwide Tourism Numbers, Expenditures, and Expanding Socioeconomic Benefits. International Fund for Animal Welfare, Crowborough, UK.
- Huerta-Diaz, M. A., Tessier, A. et Carignan, R. 1998. Geochemistry of trace metals associated with reduced sulfur in freshwater sediments. *Appl. Geochem.* **13**: 213-233.
- Jorgensen, B. B. et Revsbech, N. P. 1985. Diffusive boundary layers and the oxygen uptake of sediments and detritus. *Limn. Oceanogr.* **30**(1): 111-122.
- Kabala, Z. J. 2001. Sensitivity Analysis of a Pumping Test on a Well with Wellbore Storage and Skin. *Adv. Wat. Res.* **24**: 483-504.
- Lapointe, M. F., Secretan, Y., Driscoll, S. N., Bergeron, N et Leclerc, M 1998. Response of the Ha! Ha! River to the flood of July 1996 in the Saguenay Region of Quebec: Large-scale avulsion in a glaciated valley. *Wat. Res. Res.* **34**(9): 2383-2392.
- Leclerc, A., Gagnon, M. J., Côté, R. et Rami, A. 1986. Compaction and movement of interstitial water in bottom sediments of the Saguenay Fjord, Québec, Canada. *Sedim. Geol.* **46**: 213-230.

Le Groupe Type 1996. Documentation sur la méthode d'estimation de la fréquentation du Parc Marin du Saguenay-Saint-Laurent - saison estivale 1995, Parks Canada, September 1996.

Lesage, V. et Kinsley, C. S. 1998. Updated Status of the St Lawrence River Population of Beluga, *Delphinapterus leucas*, Can. Field Nat. **112**(1): 98-114.

Lepage, N., Hamel, P., Lefebvre, R., Therrien, R. et Blais, C. 1999. Decision analysis for leachate control at a fractured rock landfill. Ground Water Monit. Remed. **19**(3): 157-170.

Locat, J. et Leroueil, S. 1987. Physicochemical and geotechnical characteristics of recent Saguenay Fjord sediments. Can. Geotech. J. **25**: 382-388.

Marinelli, R. L. et Boudreau, B. P. 1996. An experimental and modeling study of pH and related solutes in an irrigated anoxic coastal sediment. J. Mar. Res. **54**: 939-966.

Martin, W. R. et Banta, G. T. 1992. The measurement of sediment irrigation rates: A comparison of the  $\text{BR}^-$  tracer and  $^{222}\text{RN}/^{226}\text{RA}$  disequilibrium techniques. J. Mar. Res. **50**: 125-154.

Martineau, D., Lemberger, K., Dallaire, A., Labelle, P., Lipscomb, T.P., Michel, P. et Mikaelian, I. (2002). Cancer in Wildlife, a case study: Beluga from the St. Lawrence Estuary, Québec, Canada. Environmental Health Perspectives, **110**(3): 285-292.

Massmann, J., Freeze, R. A., Smith, L., Sperling, T. et James, B. 1991. Hydrogeological decision analysis: 2. Applications to ground-water contamination. Ground Water **29**(4): 536-548.

Matisoff, G. et Wang, X. 1998. Solute transport in sediment by freshwater infaunal bioirrigators. Limn. Oceanogr. **43**(7): 1487-1499.

Maurice, F. 2000. Caractéristiques géotechniques et évolution de la couche de sédiment déposée lors du déluge de 1996 dans la Baie des Ha! Ha! (Fjord du Saguenay, Québec). Mémoire de maîtrise, Université Laval.

McCaffrey, R. J., Myers, A. C., Davey, E., Morrison, G., Bender, M., Luedtke, N., Cullen, D., Froelich, P. et Klinkhammer, G. 1980. The relation between pore water chemistry and benthic fluxes of nutrients and manganese in Narragansett Bay, Rhode Island. Limn. Oceanogr. **25**(1): 31-44.

Meyers, M. B., Fossing, H. et Powell, E. N. 1987. Microdistribution of interstitial meiofauna, oxygen and sulfide gradients, and the tubes of macro-infauna. Mar. Ecol. Progr. Ser. **35**: 223-241.

- Mohan, R. K., Mageau, D. W. et Brown, M. P. 1999. Modeling the geophysical impacts of underwater in-situ cap construction. *Mar. Tech. Soc. J.* **33**(3): 80-87.
- Mohan, R. K., Brown, M. P. et Barnes, C. R. 2000. Design criteria and theoretical basis for capping contaminated marine sediments. *Appl. Ocean Res.* **22**: 85-93.
- Morgan, M. G. et Herion, M. 1990. Uncertainty: A Guide to Dealing with Uncertainty in Quantitative Risk and Policy Analysis, Cambrige University Press, New York.
- Morse, J.W. 1994. Interactions of trace metals with authigenic sulfide minerals: implications for their bioavailability. *Mar. Chem.* **46**: 1-6.
- Mucci, A. et Edenborn, H. M. 1992. Influence of an organic-poor landslide deposit on the early diagenesis of iron and manganese in coastal marine sediment. *Geochim. Cosmochim. Acta* **56**: 3909-3921.
- Mucci, A., Guignard, C. and Olejczuk, P. 2000a. Mobility of metals and As in sediments following a large scale episodic sedimentation event. Proceedings of the 53th Canadian Geotechnical Conference, Montréal, 15-18 Oct. 2000, Vol. 1, pp. 169-175.
- Mucci, A., Richard, L.-F., Lucotte, M. et Guignard, C. 2000b. The differential geochemical behaviour of arsenic and phosphorous in the water column and sediments of the Saguenay fjord estuary, Canada. *Aquatic Geochem.* **6**: 293-324.
- Mucci, A., Boudreau, B. et Guignard C. 2003. Diagenetic mobility of trace elements in sediments covered by a flash flood deposit: Mn, Fe and As. *Applied Geochem.* **7**: 1011-1026.
- Muir, D. C. G., Ford, C. A., Stewart, R. E. A., Smith, T. G., Addison, R. F., Zink, M. E. et Béland, P. 1990. Organochlorine Contaminants in Belugas, *Delphinapterus leucas*, from Canadian waters. p. 165-190. In Smith, T. G., St. Aubin, D. J. and Geraci, J. R. (ed.) Advances in research on the beluga whale, *Delphinapterus leucas*. *Can. Bull. Fish. Aquat. Sci.* 224.
- Muris, M. 2001. Étude de la contamination des sédiments du fjord du Saguenay et évaluation de la rétention du cuivre, du plomb et du zinc. Mémoire de maîtrise, Département de génie civil, Faculté des Sciences et Génie, Université Laval.
- Neville C. J., Ibaraki, M. et Sudicky, E. A. 2000. Solute transport with multiprocess nonequilibrium: a semi-analytical solution approach. *J. Cont. Hydr.* **44**: 141-159.
- Otero, X. L., Sanchez, J. M. et Macias F. 2000. Bioaccumulation of heavy metals in thionic fluvisols by a marine polychaete: The role of metal sulfides. *J. Environ. Qual.* **29**: 1133-1141.

- O'Day, P. A., Carroll, S. A., Randall, S., Martinelli, R. E., Anderson, S. L., Jelinski, J. et Knezovich, J. P. 2000. Metal speciation and bioavailability in contaminated estuary sediments, Alameda Naval Air Station, California. *Environ. Sci. Technol.* **34**: 3665-3673.
- Palermo, M., Schroeder, P., Rivera, Y., Ruiz, C., Clarke, D., Gailani, J., Clausner, J., Hynes, M., Fredette, T., Tardy, B., Peyman-Dove, L. et Risko, A. 1999. Options for In Situ Capping of Palos Verdes Shelf Contaminated Sediments. Technical Report EL-99-2, US Army Engineer Waterways Experiment Station, Vicksburg, MS.
- Park, S. S. et Jaffé P. R. 1996. Development of a sediment redox potential model for the assessment of postdepositional metal mobility. *Ecol. Model.* **91**: 169-181.
- Pelletier, É. et Canuel G. 1988. Trace metals in surface sediment of the Saguenay fjord, Canada. *Mar. Pollut. Bull.* **19**: 336-338.
- Pelletier, É., Deflandre, B., Nozais, C., Tita, G., Desrosiers, G., Gagné, J.-P. et Mucci, A. 1999. Crue éclair de juillet 1996 dans la région du Saguenay (Québec). 2. Impact sur les sédiments et biote de la baie des Ha! Ha! et du fjord du Saguenay. *Can. J. Fish. Aquat. Sci.* **56**: 2136-2147.
- Pelletier, É., Desrosiers, G., Locat, J., Mucci, A. et Tremblay, H. 2003. The origin and behavior of a catastrophic capping layer deposited on contaminated sediments of the Saguenay Fjord (Quebec). In: *Contaminated sediments: Characterization, Evaluation, Mitigation/Restoration and Management strategy Performance*, ASTM STP1442, J. Locat, R. Galvez-Cloutier, R. C. Chaney and K. Demars, Eds., ASTM International, West Conshohocken, PA, 2003, 3-18.
- Perret, D. 1995. Diagenèse mécanique précoce des sédiments fins du fjord du Saguenay. Thèse de doctorat, Université Laval.
- Petersen, W., Willer, E. et Willamowski, C. 1997. Remobilization of trace elements from polluted anoxic sediments after resuspension in oxic water. *Wat. Air Soil Poll.* **99**: 515-522.
- Petersen, K., Kristensen, E. et Bjerregaard, P. 1998. Influence of bioturbating animals on flux of cadmium into estuarine sediment. *Mar. Environ. Res.* **45**(4/5): 403-415.
- Pippard L. et Malcolm H. 1978. White Whales (*Delphinapterus leucas*). Observations on their distributions, populations and critical habitats in the St. Lawrence and Saguenay rivers. Unpublished report prepared for Departement of Indian and Northern Affairs, Parks Canada, Ottawa, Ontario.

- Reible, D. D., Popov, V., Valsaraj, K. T., Thibodeaux, L. J., Lin, F., Dikshit, M., Todaro, M. A. et Fleeger, J. W. 1996. Contaminant fluxes from sediment due to tubificid oligochaete bioturbation. *Wat. Res.* **30** (3): 704-714.
- Riedel, G. F., Sanders, J. G. et Osman, R. W. 1987. The effect of biological and physical disturbances on the transport of arsenic from contaminated estuarine sediments. *Estuarine Coast. Shelf Sci.* **25**: 693-706.
- Riisgard, H. U. 1989. Properties and Energy Cost of the Muscular Piston Pump in the Suspension Feeding Polychaete *Chaetopterus Varioipedatus*. *Mar. Ecol. Progr. Ser.* **56**: 157-168.
- Riisgard, H. U. 1991. Suspension Feeding in the Polychaete *Nereis Diversicolor*. *Mar. Ecol. Progr. Ser.* **70**: 29-37.
- Riisgard, H. U., Vedel, A., Boye, H. et Larsen, P. S. 1992. Filter-net structure and pumping activity in the polychaete *Nereis diversicolor*: effects of temperature and pump-modelling. *Mar. Ecol. Progr. Ser.* **83**: 79-89.
- Rivera-Duarte, I. et Flegal, A. R. 1994. Benthic lead fluxes in San Francisco Bay, California, USA. *Geochim. Cosmochim. Acta* **58**: 3307-3313.
- Ruiz, C. E., Schroeder, P. R. et Aziz, N. M. 2000. RECOVERY: A contaminant sediment-water interaction model. ERDC/EL SR-D-00-1, U.S. Army Engineer Research and Development Center, Waterways Experiment Station, Vicksburg, MS.
- Saulnier, I. et Mucci, A. 2000. Trace Metal Remobilization Following the Resuspension of Estuarine Sediments: Saguenay Fjord, Canada. *Appl. Geochem.* **15**: 191-210.
- Schafer, C. T., Smith, J. N. et Loring, D. H. 1980. Recent sedimentation events at the head of Saguenay Fjord, Canada. *Environ. Geol.* **3**: 139-150.
- Schafer, C. T., Smith, J. N. et Côté, R. 1990. The Saguenay fiord: a major tributary to the St. Lawrence Estuary. In: El-Sabh, M. I., Silverberg, N. (Eds.), *Oceanography of a large scale estuarine system, The St. Lawrence. Coastal and Estuarine Studies.* **39**: 378-419, Springer Verlag.
- Simpson, S. L., Rosner, J. et Ellis, J. 2000. Competitive displacement reactions of cadmium, copper, and zinc added to a polluted, sulfidic estuarine sediment. *Environ. Toxicol. Chem.* **19**: 1992-1999.
- Soetaert, K., Herman, P. M. J. et Middelburg J. J. 1996. A model of early diagenetic processes from the shelf to abyssal depths. *Geochim. Cosmochim. Acta*. **60**(6): 1019-1040.

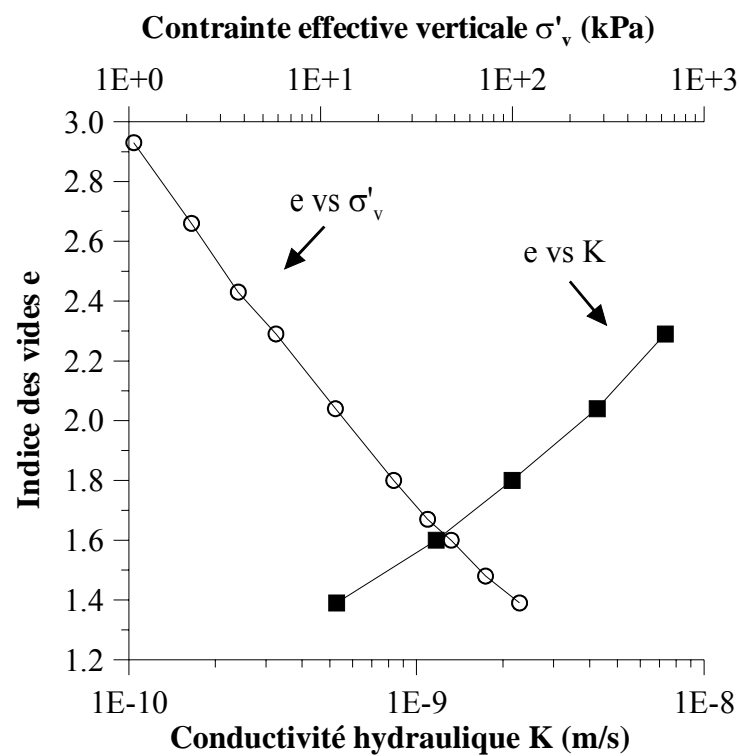
- Sperling, T., Freeze, R. A., Massmann, J., Smith, L. et James, B. 1992. Hydrogeological Decision Analysis: 3. Application to Design of a Ground-Water Control System at an Open Pit Mine. *Ground Water* **30** (3): 376-389.
- Syvitski J. P. M., Burrel, D. C. et Skei, J.M. 1987. Fjords: processes and products. Ed. New York, Springer-Verlag.
- Tremblay, G.-H. et Gobeil, C. 1990. Dissolved arsenic in the St Lawrence Estuary and the Saguenay Fjord, Canada. *Mar. Pollut. Bull.* **21**(10): 465-469.
- Tremblay, H., Desrosiers, G., Locat, J., Mucci, A. et Pelletier, É. 2003. Characterization of a catastrophic flood sediment layer: geological, geotechnical, biological, and geochemical signatures. In: Contaminated sediments: Characterization, Evaluation, Mitigation/Restoration and Management strategy Performance, ASTM STP1442, J. Locat, R. Galvez-Cloutier, R.C. Chaney, and K.R. Demars, Eds. ASTM International, West Conshohocken, PA, 87-101.
- USEPA 1994. ARCS Remediation Guidance Document. EPA 905-B94-003, Great Lakes National Program Office, Chicago, IL.
- USEPA 1999. National recommended water quality criteria - Correction. United States Environmental Protection Agency, Office of Water 4304. EPA 822-Z-99-001.
- Vanysek P. 2000. Ionic Conductivity and diffusion at infinite dilution. In CRC handbook of chemistry and physics, 81st edition, Cleveland, Ohio.
- Versteeg, H. K. et Malalasekera, W. 1995. An introduction to computational fluid dynamics : the finite volume method. Longman Scientific & Technical, Burnt Mill, Harlow, Essex.
- Vladykov, V.-D. 1946. Étude sur les mammifères marins IV. Nourriture du Marsouin Blanc ou Béluga (*Delphinapterus leucas*) du fleuve Saint-Laurent. Contrib. Dép. Pêches Québec, 14 : 191 pp.
- Wagemann, R., Stewart, R.E.A., Béland, P. et Desjardins, C. 1990. Heavy metals and selenium in tissues of beluga whales, *Delphinapterus leucas*, from the Canadian Arctic and the St. Lawrence Estuary. P. 191-206. In Smith, T. G., St. Aubin, D.J. and Geraci, J.R. (ed.) Advances in research on the beluga whale, *Delphinapterus leucas*. *Can. Bull. Fish. Aquat. Sci.* 224.
- Wang, X. et Matisoff, G. 1997. Solute transport in sediments by a large fresh water oligochaete, *Brachiura sowerbyi*. *Environ. Sci. Technol.* **31**: 1926-1933.
- Wang, Y. et Van Cappellen, P. 1996. A multicomponent reactive transport model of early diagenesis: application to redox cycling in coastal marine sediments. *Geochim. Cosmochim. Acta* **60**(16): 2993-3014.

- Yan, Q.-L. et Wang W.-X. 2002. Metal exposure and bioavailability to a marine deposit-feeding Sipuncula, *Sipunculus nudus*. Environ. Sci. Technol. **36**: 40-47.
- Zeman, A. J. 1994. Subaqueous capping of very soft contaminated sediments. Can. Geotech. J. **31**: 570-577.
- Zheng, C. et Bennett, G. D. 2002. Applied Contaminant Transport Modeling. 2<sup>nd</sup> edition, John Wiley, New York.

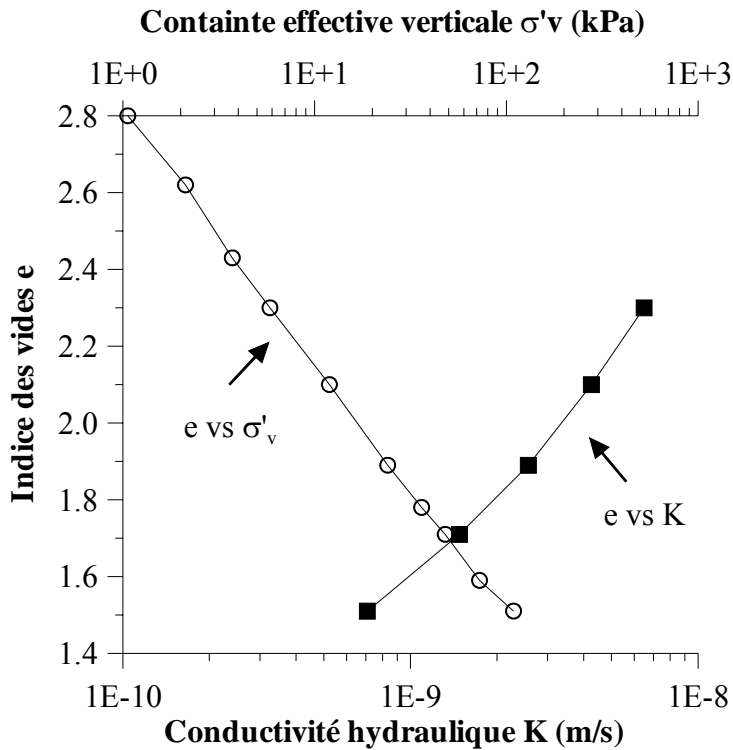
## Annexe 1: Essais oedométriques

Les résultats des essais oedométriques sont présentés ici sous forme de graphiques, illustrant les relations entre l'indice des vides, la conductivité hydraulique et la contrainte effective verticale (charge imposée sur l'échantillon).

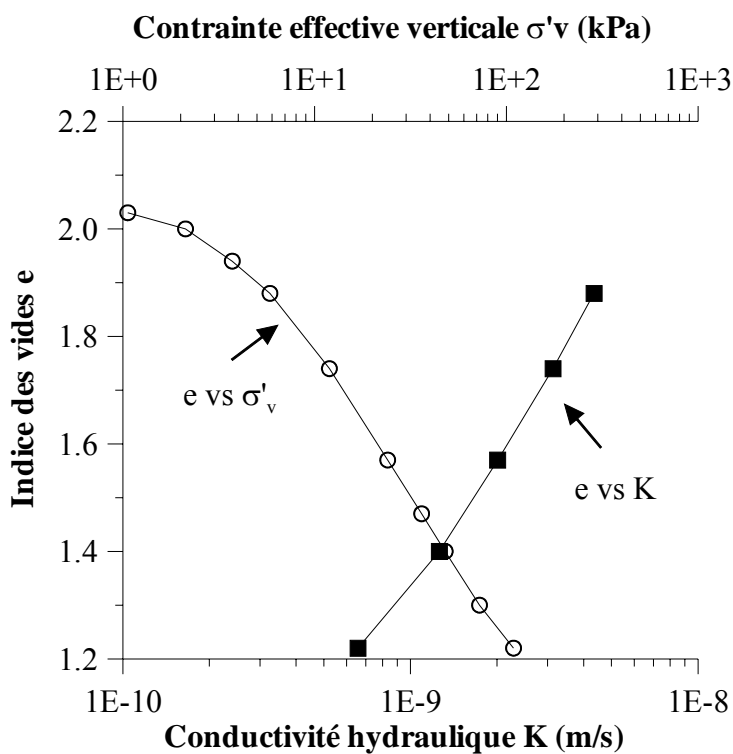
### Essai 1



### Essai 2

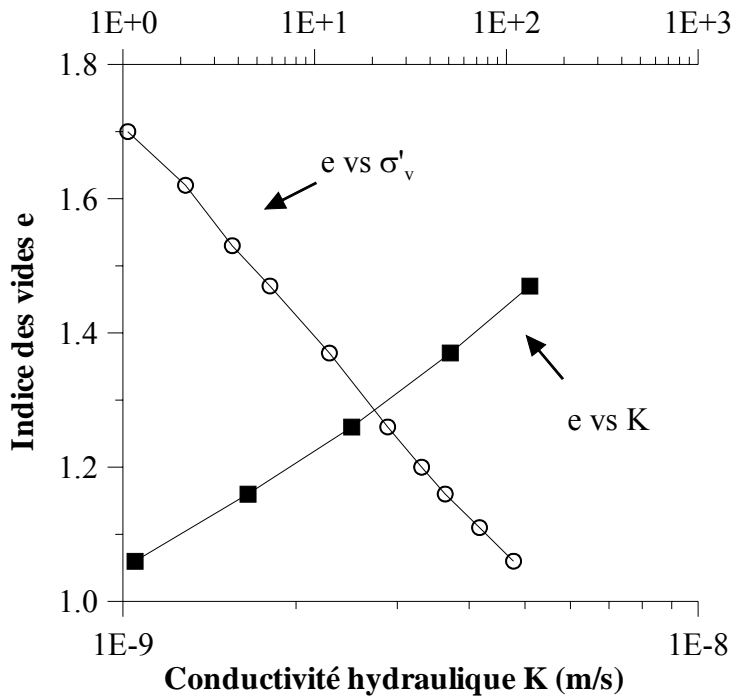


### Essai 3



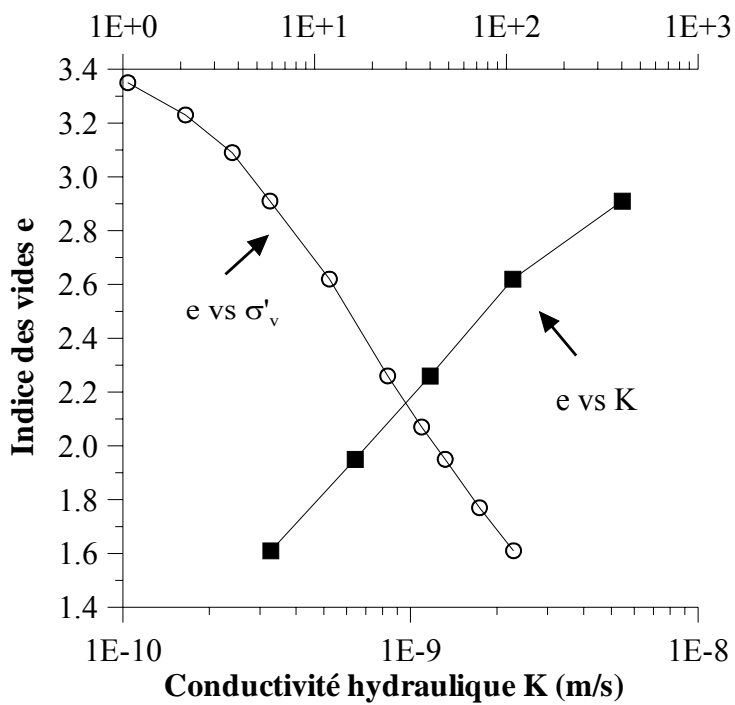
### Essai 4

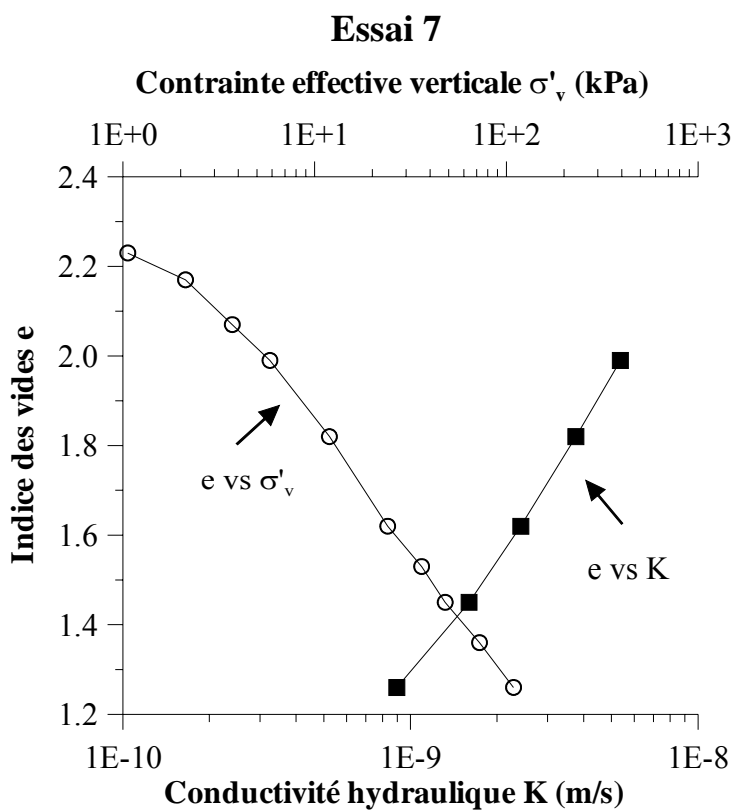
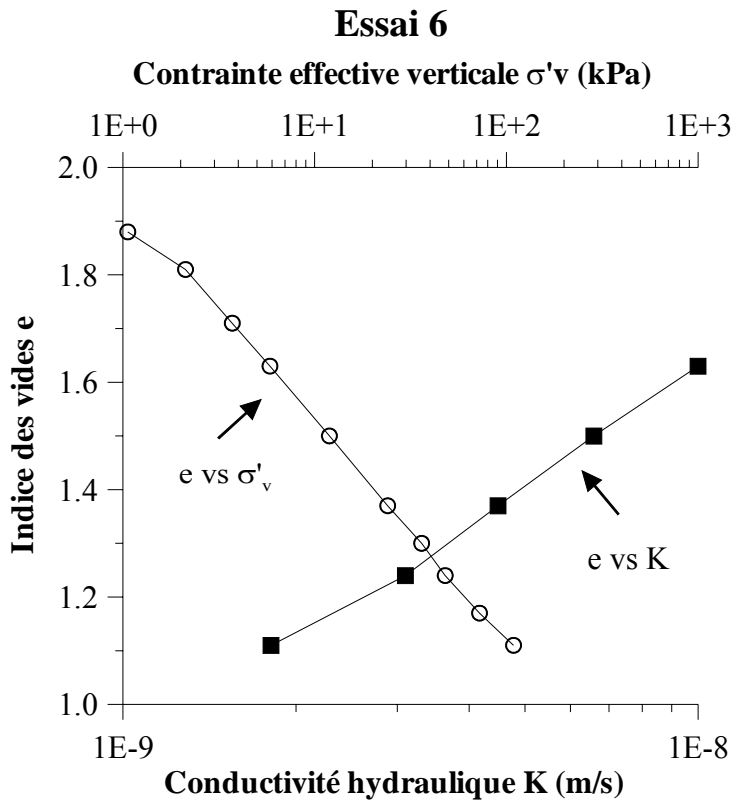
Contrainte effective verticale  $\sigma'_v$  (kPa)



### Essai 5

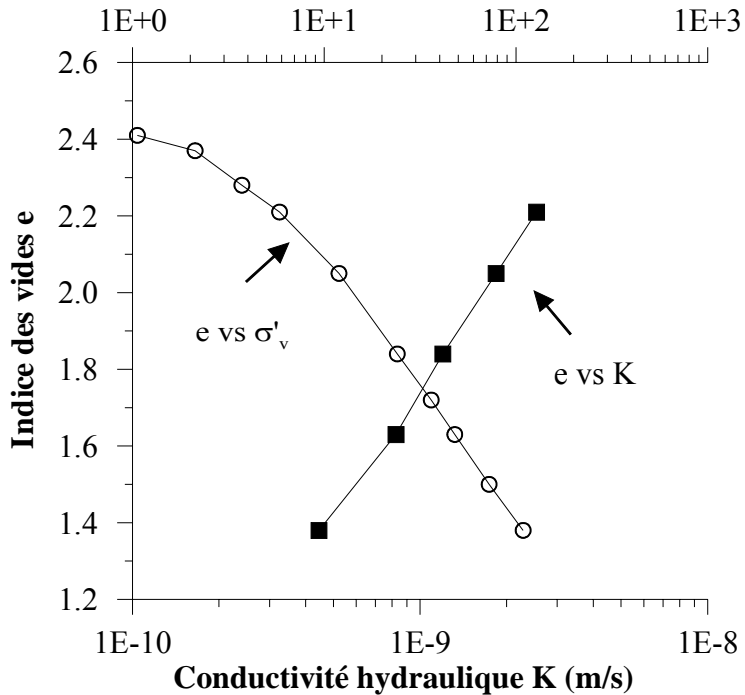
Contrainte effective verticale  $\sigma'_v$  (kPa)





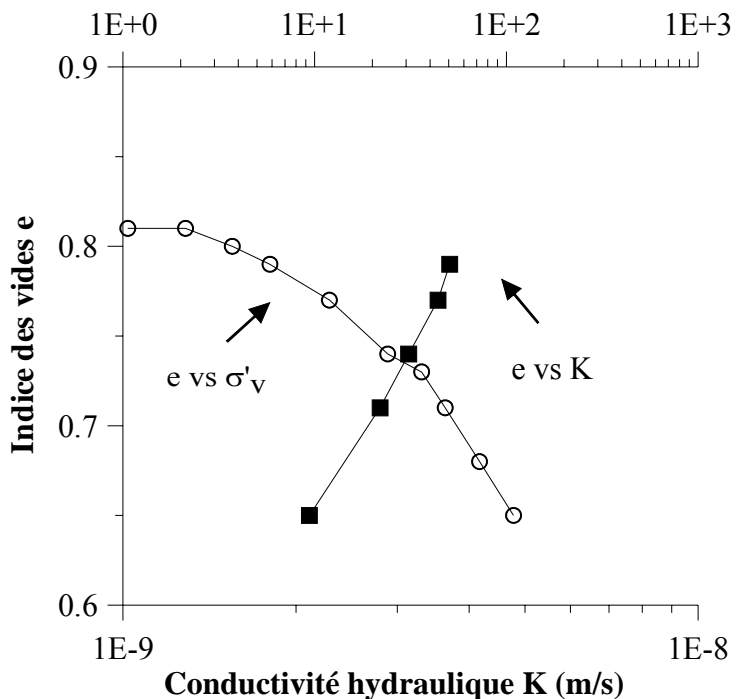
### Essai 8

Contrainte effective verticale  $\sigma'_v$  (kPa)



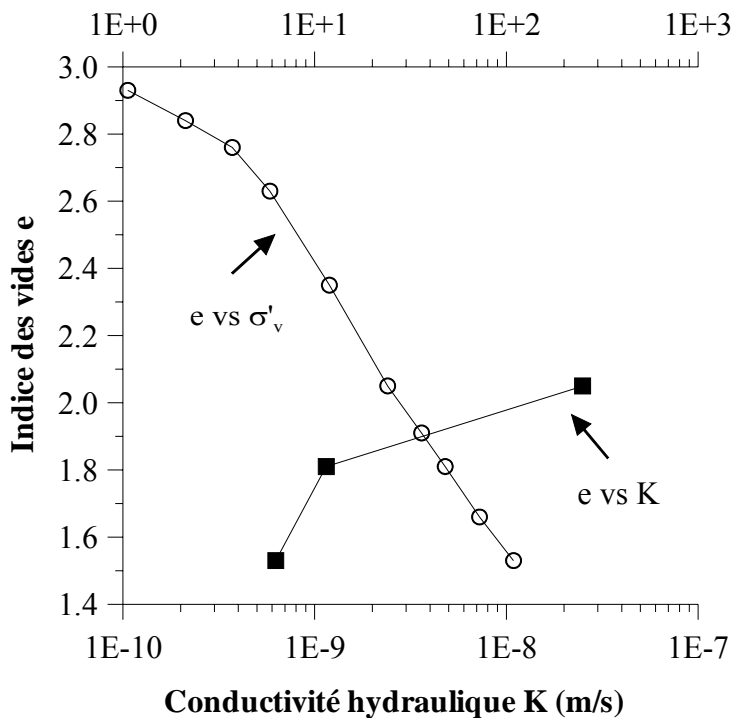
### Essai 9

Contrainte effective verticale  $\sigma'_v$  (kPa)



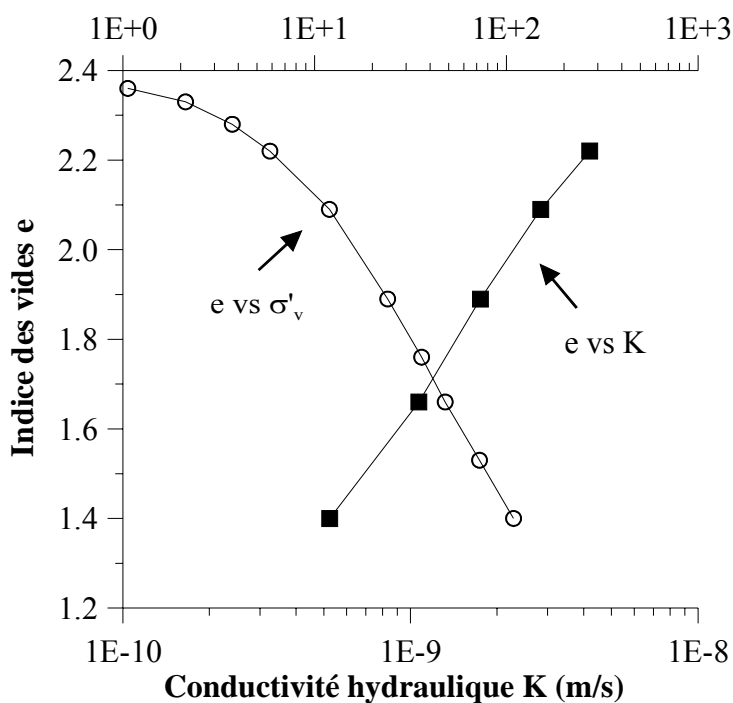
### Essai 11

Contrainte effective verticale  $\sigma'_v$



### Essai 12

Contrainte effective verticale  $\sigma'_v$  (kPa)



## Annexe 2: Discrétisation des équations du modèle

Le transport dans les sédiments est décrit par l'équation:

$$n_s \frac{\partial C_s}{\partial t} = n_s \cdot \frac{D_s}{R} \left( \frac{\partial^2 C_s}{\partial z^2} \right) - n_s \cdot \frac{v_s}{R} \cdot \frac{\partial C_s}{\partial z} - \beta(C_s - C_T)$$

et le transport dans les tubes est représenté par:

$$n_T \frac{\partial C_T}{\partial t} = n_T D_m \frac{\partial^2 C_T}{\partial z^2} - n_T v_T \frac{\partial C_T}{\partial z} + \beta(C_s - C_T) + S$$

Chaque équation est intégrée sur un volume de contrôle d'une dimension de  $\Delta z$  et un pas de temps fini de  $\Delta t$ . Étant donné que le transport dans les tubes est dominé par l'advection (bio-irrigation) vers la limite supérieure, nous utilisons la pondération en amont pour le terme advectif de l'équation des tubes. Le terme advectif de l'équation des sédiments est discrétisé en utilisant la pondération hybride ce qui signifie que si le nombre de Peclet est plus grand que 2 ( $Pe > 2$ ) le modèle choisi automatiquement la pondération en amont et dans le cas contraire ( $Pe \leq 2$ ) la pondération centrale. Le terme diffusif de l'équation des sédiments et des tubes sont discrétisés en utilisant la pondération centrale. La méthode des différences finies est utilisée pour évaluer l'intégral dans le temps. Si nous utilisons une méthode de résolution complètement implicite le facteur de pondération,  $f$ , est égal à 1, tandis que la méthode explicite est obtenue par une valeur de  $f$  égale à 0.

Pour  $Pe \leq 2$  l'équation discrétisée pour les sédiments prend la forme de:

$$\left\{ n_S \frac{\Delta z}{\Delta t} + f \left[ \frac{n_S}{R} \left( \frac{2D_S}{\Delta z} \right) + \beta \Delta z \right] \right\} C'_{SP} = \\ f \frac{n_S}{R} \left( \frac{Ds}{\Delta z} + \frac{v_S}{2} \right) C'_{SB} + (1-f) \frac{n_S}{R} \left( \frac{Ds}{\Delta z} + \frac{v_S}{2} \right) C^o_{SB} + f \frac{n_S}{R} \left( \frac{Ds}{\Delta z} - \frac{v_S}{2} \right) C'_{SH} + (1-f) \frac{n_S}{R} \left( \frac{Ds}{\Delta z} - \frac{v_S}{2} \right) C^o_{SH} + \\ \left\{ n_S \frac{\Delta z}{\Delta t} - (1-f) \left[ \frac{n_S}{R} \left( \frac{2D_S}{\Delta z} \right) + \beta \Delta z \right] \right\} C^o_{SP} + f \cdot \beta \cdot \Delta z \cdot C'_{TP} + (1-f) \beta \cdot \Delta z \cdot C^o_{TP}$$

Tandis que pour  $Pe > 2$  elle est représentée par:

$$\left\{ n_S \frac{\Delta z}{\Delta t} + f \left[ \frac{n_S}{R} \left( \frac{2D_S}{\Delta z} \right) + n_S v_S + \beta \Delta z \right] \right\} C'_{SP} = \\ f \frac{n_S}{R} \left( \frac{Ds}{\Delta z} + \frac{v_S}{2} \right) C'_{SB} + (1-f) \frac{n_S}{R} \left( \frac{Ds}{\Delta z} + \frac{v_S}{2} \right) C^o_{SB} + f \frac{n_S}{R} \left( \frac{Ds}{\Delta z} - \frac{v_S}{2} \right) C'_{SH} + (1-f) \frac{n_S}{R} \left( \frac{Ds}{\Delta z} - \frac{v_S}{2} \right) C^o_{SH} + \\ \left\{ n_S \frac{\Delta z}{\Delta t} - (1-f) \left[ \frac{n_S}{R} \left( \frac{2D_S}{\Delta z} \right) + n_S v_S + \beta \Delta z \right] \right\} C^o_{SP} + f \cdot \beta \cdot \Delta z \cdot C'_{TP} + (1-f) \beta \cdot \Delta z \cdot C^o_{TP}$$

L'équation discrétisée pour les tubes est:

$$\left\{ n_{TP} \frac{\Delta z}{\Delta t} + f \left[ n_{TP} v_T + n_{TP} \left( \frac{2D_m}{\Delta z} \right) + \beta \Delta z \right] \right\} C'_{TP} = \\ f \cdot n_{TB} \left( \frac{D_m}{\Delta z} + v_T \right) C'_{TB} + (1-f) \cdot n_{TB} \left( \frac{D_m}{\Delta z} + v_T \right) C^o_{TB} + f \cdot n_{TH} \left( \frac{D_m}{\Delta z} \right) C'_{TH} + (1-f) n_{TH} \left( \frac{D_m}{\Delta z} \right) C^o_{TH} + \\ \left\{ n_{TP} \frac{\Delta z}{\Delta t} - (1-f) \left[ n_{TP} v_T + \left( \frac{2D_m}{\Delta z} \right) + \beta \Delta z \right] \right\} C^o_{TP} + f \cdot \beta \cdot \Delta z \cdot C'_{SP} + (1-f) \beta \cdot \Delta z \cdot C^o_{SP} + S$$

Les indices H, B et P indiquent la position (H = haut, B= bas) du volume auquel se réfère le paramètre, par rapport au volume pour lequel on calcule le flux (P) (Figure A.1).

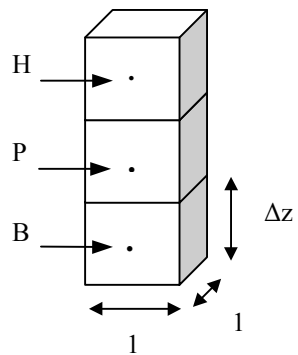


Figure A.1: *Représentation graphique de la discréétisation en volumes finis.*

## Annexe 3: Code

Cette annexe présente le code du modèle numérique TRANSCAP-1D ainsi que le cadre qui permet de réaliser les simulations Monte Carlo. Le modèle a été compilé avec le compilateur FORTRAN 90. Le transport de contaminant dans les sédiments est calculé avec la sousroutine "solution". Cette sousroutine est appelé par le cadre du programme "Monte Carlo", qui permet de réaliser des séries simulations stochastiques. Par la suite nous présentons le code de la sousroutine qui choisi les nombres aléatoires.

```
!
!*****TRANSCAP-1D Finite volume solution of the 1D transport equation in bio-irrigated
!sediments
!
!*****Arrays
!
! a : global left-hand-side matrix
! alfa: vector of irrigation coefficient (input)
! c : vector of nodal concentrations (ug/m**3)
! cfes : vector of concentration of FeS (umol/g)
! d1 : vector with the values of the left diagonal blocks of matrix A
! d2 : vector with the values of the middle diagonal blocks of matrix A
! d3 : vector with the values of the right diagonal blocks of matrix A
! f : global vector of known values (right hand side)
! port: vector of tube porosity
! r : right hand side matrix
! s : right hand side vector (Stu)
! twant : vector of desired time(s) for output
! x : vector of nodal coordinates (m)
!
! Variables
!
! Real
!
! alfa1, alfa2: irrigation coefficients (1/day & 1/m)
!           alfa = alfa1*exp(alfa2*(x-xmax))
! area : column area (m**2)
! biox : maximum depth of bioturbation (m) (has to be a multiple of dx!)
```

```

! k1, k2 : coefficients of linear dissolution equation
! conc : concentration at the water/sediment interface (ug/m**3)
! cour : courant number
! diff : effective diffusion coefficient (m**2/day)
! ds : diffusion/dispersion coefficient in sediment (m**2/day) d = v*disp+diff
! dm : molecular diffusion
! disp : dispersivity (m)
! dt : time increment (day)
! dx : distance increment (m)      (homogeneous grid!)
! epsil : time weighting factor (normally =1)
! fluxlo : flux through lower boundary
! fluxup : flux through upper boundary
! gamma : cinetic coefficient for dissolution reaction
! mins : mass of dissolved contaminant before simulation in sediment
! mint : mass of dissolved contaminant before simulation in tube
! mdiss : mass entering the system by dissolution (tube)
! mends : mass inside the column after simulation in sediment
! mendt : mass inside the column after simulation in tube
! mex: mass exchanged between sediment and tube
! mouts : mass leaving from the boundaries (sediment)
! moutt : mass leaving from the boundaries (tube)
! pec : peclet number
! pors : sediment porosity
! porscap : cap sediment porosity
! port0 : tube porosity at the surface of the sediment
!           port=port0*exp(alfa2*(x-xmax))
! qs : advective flow in sediment (m**3/day)
! qq : flux contribution for the inflow boundary equation
! retard : retardation coefficient           retard = 1+rho*xkd/pors
! tmax : maximum simulation time (day)
! vs : average water velocity in sediment (m/day)      vs = qs/(area*pors)
! vt : average water velocity in tube (m/day)
! xmax : lenght of column (m)

!
!

! Integer

!
!

! nn : number of nodes
! neq : number of equations per node (tube + sediment)
! nunk : number of unknowns
! ntwant : number of desired time output
!
!
!
*****...define the types of the variables
!
```

```

!
! subroutine solution(x, cfes, cs, ct, twant)
!
! USE PORTLIB
!
common alfa1, alfa2, area, biox,      capdx,          &
      k1, k2, conc, dm, disp, diff, dp, dt, dx, epsil,&
      gamma, pors, porscap, port0, qs, retard,        &
      tmax, vt, xmax
double precision alfa1, alfa2, area, biox, capdx,          &
      k1, k2, conc, dm, disp, diff, dp, dt, dx, epsil,  &
      gamma, pors, porscap, port0, qs, retard,        &
      tmax, vt, xmax
common sim, nsim, ntwant, nn, AllocateStatus
      integer sim, nsim, ntwant, nn, AllocateStatus
common title
character *80 title
!
double precision b, balsed, baltub, cours, courscap, court,    &
      csurf, ds, dscap, dscheck, dscapcheck, dxmax,       &
      fluxlos, fluxlot, fluxups, fluxupt, mdiss, mends, mendt, &
      mex, mins, mint, mouts, moutt, pecs, pecscap, pect, qq, &
      sumex, sumlos, sumlot, sumup, sumups, sumupt, sumdiss, &
      tcheck, ttime, vs, vscap, vscheck, vscapcheck
double precision x(nn), cs(nn), ct(nn), cfes(nn), twant(ntwant)
double precision, dimension(:, ), allocatable :: alfa, c,          &
      f, port, s, d1, d2, d3
double precision, dimension (:,:), allocatable :: a, r
integer cap, i, ii, j, jj, n, neq, nprint, nunk, nunk2, ucap
parameter (neq=2)
character *1 tab
      character(8) whatimeisit
      tab=char(9)
!
! ...open the working files
!
open(4, file='mcflux.out')
open(5, file='mcoutput.out')
open(6, file='mccsurf.out')
!
! ...calculate total number of unknown
!
nunk = neq*nn
nunk2 = neq*nunk
!
! ...allocate the memory for the arrays

```

```

!
if (sim.eq.1) then
allocate(c(nunk), alfa(nn), port(nn), f(nunk), s(nunk),
        d1(nunk2), d2(nunk2), d3(nunk2), stat = AllocateStatus) &
if (AllocateStatus /= 0) stop "***Not enough memory***"
allocate(a(nunk,5), r(nunk,5),stat = AllocateStatus)
if (AllocateStatus /= 0) stop "***Not enough memory***"
endif

!
! ...find the maximum dx to use for the Peclet and Courant
! numbers
!
dxmax = -1.0d30
if(dx.gt.dxmax) dxmax = dx
!
! ...calculate number of nodes corresponding to the capping layer (cap)
! and number of nodes under the capping layer (ucap)
!
cap=int(capdx/dx)
ucap=nn-cap
!
! ...echo back output
!
405 write(5,405) sim,nn,xmax,area,tmax,dt,epsil,dp,biox,capdx
format(//,60('*'),/5x,'Simulation', t20 ,i4,/60('*'),//,5x,
'Number of nodes:',t55,i5,/5x, &
'Length of the column (m):',t48,d12.5, &
/,5x,'Area of the column (m**2):',t48,d12.5, &
/,5x,'Maximum simulation time (day):',t48,d12.5, &
/,5x,'Time step (day):', t48, d12.5, &
/,5x,'Time weighting factor:',t48,d12.5, &
/,5x,'(DP) Depth of bioirrigation (m):',t48,d12.5, &
/,5x,'(INT) Depth of bioirrigation (m):',t48,d12.5, &
/,5x,'Depth of the capping layer (m):',t48,d12.5) &
write(5,406) qs, vt, pors, porscap, port0, dm, diff, disp
406 format(5x, 'Advection flow in sediment(m**3/day):',t48,d12.5, &
/,5x,'Irrigation velocity (m/day):',t48,d12.5, &
/,5x,'Sediment porosity:',t48,d12.5, &
/,5x,'Capping layer porosity:',t48,d12.5, &
/,5x,'Tube porosity at surface:',t48,d12.5, &
/,5x,'Molecular diffusion (m**2/day):',t48,d12.5, &
/,5x,'Effective diffusion coefficient (m**2/day):',t48,d12.5, &
/,5x,'Dispersivity (m):',t48,d12.5)
write(5,407) k1, k2, gamma, alfa1, alfa2, conc
407 format(5x,'Lin. dissolution eq. coeff. b1 & b2:',t48,
d12.5,3x,d12.5, &
&

```

```

/,5x,'Cinetic coeff for dissolution (1/day):',t48,d12.5,      &
/,5x,'Irrigation coefficient alfa1 (1/day):',t48,d12.5,      &
/,5x,'Irrigation coefficient alfa2 (1/m):',t48,d12.5,      &
//,5x,'Conc. at wat./sed. interface (ug/m**3) = ',t48,d12.5)
!
! ...calculate alfa coefficients and tube porosity at each node
!
do 16 i=1,nn
  alfa(i)=0.0d0
  port(i)=0.0d0
  b = xmax - x(i)
  if(b.le.biox) then
    alfa(i) = alfa1*DEXP(alfa2*(x(i)-xmax))
    port(i) = port0*DEXP(alfa2*(x(i)-xmax))
  endif
16  continue

!
! ...Calculate mass inside the column (sediment and tubes)
! at the beginning of the simulation
!
mins=0.0d0
mint=0.0d0
do 8 i=1,nn
  nc=ucap-i
  if (nc.ge.0) then
    mins=mins+(cs(i)*pors)*area*dx
  elseif (nc.lt.0) then
    mins=mins+(cs(i)*porscap)*area*dx
  endif
  mint=mint+(ct(i)*port(i))*area*dx
8   continue

!
! ...assemble concentration vector c
!
do 12 i=1,nn
  j= 2*i-1
  n= 2*i
  c(j)=cs(i)
  c(n)=ct(i)
12  continue

!
! ...compute constants
!
vs = qs/(area*pors)
vscap = qs/(area*porscap)

```

```

ds = vs*disp + diff
dscap = vscap*disp + diff
!
! ...echo back calculated parameters
!
! write(5,409) vs, vscap, ds, dscap, retard
409 format(/,5x, 'In sediment:',/, &
      5x,'Unretarded average linear vel. (in sed.) (m/day):',t48,d12.5,/, &
      5x,'Unretarded average linear vel. (in cap) (m/day):',t48,d12.5,/, &
      5x,'Unretarded diff./disp. coeff. (in sed.) (m2/day):',t48,d12.5,/, &
      5x,'Unretarded diff./disp. coeff. (in cap) (m2/day):',t48,d12.5,/, &
      5x,'Retardation coefficient:',t48, d12.5)
!
! ...calculate retarded constants for the sediment
! to check and print Peclet and Courant
!
if(vs.eq.0.0) then
  write(5,410)
410 format (/,5x, 'No advection in sediment')
else
  vscheck=vs/retard
  vscapcheck=vscap/retard
  dscheck=ds/retard
  dscapcheck=dscap/retard
  pecs=vscheck*dxmax/dscheck
  pecscap=vscapcheck*dxmax/dscapcheck
  cours=vscheck*dt/dxmax
  courscap=vscapcheck*dt/dxmax
  write(5,411) pecs, pecscap, cours, courscap
411 format(/,5x,'Maximum Peclet number:',t48,d12.5, &
      /,5x,'Maximum Peclet number in cap:',t48,d12.5, &
      /,5x, 'Maximum Courant number in sediment:', t48,d12.5 &
      /,5x, 'Maximum Courant number in cap:', t48,d12.5)
endif
!
! ...calculate retarded constants for the tube
! to check and print Peclet and Courant
!
if(vt.eq.0.0) then
  write(5,412)
412 format (/,5x, 'No advection in tube')
else
  pect=vt*dxmax/dm
  court=vt*dt/dxmax
  write(5,413) pect,court
413 format(/,5x,'Maximum Peclet number for tube:',t48,d12.5, &

```

```

    /,5x, 'Maximum Courant number for tube:', t48,d12.5)
endif
!
! ...assemble the first row of the A matrix (sediment)
!
if (ucap .gt. 1)      then
    a(1,1)= 0.0d0
    a(1,2)= 0.0d0
    a(1,3)= pors*dx/dt+epsil*(pors*(vs/retard)+alfa(1)*dx)
    a(1,4)= -epsil*alfa(1)*dx
    a(1,5)= 0.0d0
elseif (ucap .eq. 1)   then
    a(1,1)= 0.0d0
    a(1,2)= 0.0d0
    a(1,3)= pors*dx/dt+epsil*(pors*(vs+vscap)/2/retard+alfa(1)*dx)
    a(1,4)= -epsil*alfa(1)*dx
    a(1,5)= 0.0d0
elseif (ucap.eq.0) then
    a(1,1)= 0.0d0
    a(1,2)= 0.0d0
    a(1,3)= porscap*dx/dt+epsil*(porscap*(vscap/retard)+alfa(1)*dx)
    a(1,4)= -epsil*alfa(1)*dx
    a(1,5)= 0.0d0
endif

!
! ...assemble the second row of the A matrix (tube)
!
if (alfa(1) .eq. 0.0d0) then
    a(2,1) = 0.0d0
    a(2,2) = 0.0d0
    a(2,3) = 1.0d0
    a(2,4) = 0.0d0
    a(2,5) = 0.0d0
else
    a(2,1)= 0.0d0
    a(2,2)= -epsil*alfa(1)*dx
    a(2,3)= port(1)*dx/dt+epsil*(port(1)*vt+(alfa(1)*dx))+gamma*dx
    a(2,4)= 0.0d0
    a(2,5)= 0.0d0
endif

!
! ...assemble middle nodes of A matrix (sediment)
!
if (pecs.gt.2.0) then
!
```

```

!      ...if Peclet number is greater than 2 then use upwind weighting
!
do 52 i=3,nunk-3,2
  n=(i+1)/2
  nc=ucap-n
  if (nc.gt.0) then
    a(i,1)= -epsil*pors*(ds/retard/dx+vs/retard)
    a(i,2)= 0.0d0
    a(i,3)= pors*dx/dt+epsil*(pors*2*ds/retard/dx+pors*vs/retard+alfa(n)*dx)
    a(i,4)= -epsil*alfa(n)*dx
    a(i,5)= -epsil*pors*(ds/retard/dx)
  elseif (nc.eq.0) then
    a(i,1)= -epsil*pors*(ds/retard/dx+vs/retard)
    a(i,2)= 0.0d0
    a(i,3)= pors*dx/dt+epsil*(pors*(ds+(ds+dscap)/2)/
                                retard/dx+pors* (vs+vscap)/2/retard+alfa(n)*dx)
    a(i,4)= -epsil*alfa(n)*dx
    a(i,5)= -epsil*porscap*((ds+dscap)/2/retard/dx)
  elseif (nc.eq.-1)  then
    a(i,1)= -epsil*pors*((ds+dscap)/2/retard/dx+(vs+vscap)/2/retard)
    a(i,2)= 0.0d0
    a(i,3)= porscap*dx/dt+epsil*(porscap*(dscap+(ds+dscap)/2) /
                                retard/dx+porscap*vscap/retard+alfa(n)*dx)
    a(i,4)= -epsil*alfa(n)*dx
    a(i,5)= -epsil*porscap*(dscap/retard/dx)
  elseif (nc.lt.-1) then
    a(i,1)= -epsil*porscap*(dscap/retard/dx+vscap/retard)
    a(i,2)= 0.0d0
    a(i,3)= porscap*dx/dt+epsil*
              (porscap*2*dscap/retard/dx+porscap*vscap/retard+alfa(n)*dx)
    a(i,4)= -epsil*alfa(n)*dx
    a(i,5)= -epsil*porscap*(dscap/retard/dx)
  endif
52  continue
  else
!
!      ...else use central weighting
!
do 54 i=3,nunk-3,2
  n=(i+1)/2
  nc=ucap-n
  if (nc.gt.0) then
    a(i,1)= -epsil*pors*(ds/retard/dx+vs/retard/2)
    a(i,2)= 0.0d0
    a(i,3)= pors*dx/dt+epsil*(pors*2*ds/retard/dx+alfa(n)*dx)
    a(i,4)= -epsil*alfa(n)*dx

```

```

      a(i,5)= -epsil*pors*(ds/retard/dx-vs/retard/2)
      elseif (nc.eq.0) then
        a(i,1)= -epsil*pors*(ds/retard/dx+vs/retard/2)
        a(i,2)= 0.0d0
        a(i,3)= pors*dx/dt+epsil*(pors*(ds+(ds+dscap)/2)/
          retard/dx+pors*((vs+vscap)/2-vs)/2/retard+alfa(n)*dx)
        a(i,4)= -epsil*alfa(n)*dx
        a(i,5)= -epsil*porscap*((ds+dscap)/2/retard/dx-(vs+vscap)/2/retard/2)
      elseif (nc.eq.-1) then
        a(i,1)= -epsil*pors*((ds+dscap)/2/retard/dx+(vs+vscap)/2/retard/2)
        a(i,2)= 0.0d0
        a(i,3)= porscap*dx/dt+epsil*(porscap*(dscap+(ds+dscap)/2)/
          retard/dx+porscap*(vscap-(vs+vscap)/2)/2/retard+alfa(n)*dx)
        a(i,4)= -epsil*alfa(n)*dx
        a(i,5)= -epsil*porscap*(dscap/retard/dx-vscap/retard/2)
      elseif (nc.lt.-1) then
        a(i,1)= -epsil*porscap*(dscap/retard/dx+vscap/retard/2)
        a(i,2)= 0.0d0
        a(i,3)= porscap*dx/dt+epsil*(porscap*2*dscap/retard/dx+alfa(n)*dx)
        a(i,4)= -epsil*alfa(n)*dx
        a(i,5)= -epsil*porscap*(dscap/retard/dx-vscap/retard/2)
      endif
54  continue
      endif
!
! ...assemble middle rows of A matrix (tube)
!
do 56 i=4,nunk-2,2
  n=i/2
  if (alfa(n) .eq. 0.0d0) then
    a(i,1) = 0.0d0
    a(i,2) = 0.0d0
    a(i,3) = 1.0d0
    a(i,4) = 0.0d0
    a(i,5) = 0.0d0
  else
    a(i,1) = -epsil*port(n-1)*(dm/dx+vt)
    a(i,2) = -epsil*(alfa(n)*dx)
    a(i,3) = port(n)*dx/dt+epsil*
      (dm*2*port(n)/dx+port(n)*vt+alfa(n)*dx)+gamma*dx
    a(i,4) = 0.0d0
    a(i,5) = -epsil*port(n+1)*(dm/dx)
  endif
56 continue
!
! ...set up first-type boundary condition at outlow

```

```

! Trick for Dirichlet:
! set the diagonal term of the L.H.S coefficient matrix to a very
! high number and set the flux contribution (qq) in order tu ensure
! that c(nn) goes to the desired value
!
    a(nunk-1,1)=0.0d0
    a(nunk-1,2)=0.0d0
    a(nunk-1,3)=1.0d35
    a(nunk-1,4)=0.0d0
    a(nunk-1,5)=0.0d0
    a(nunk,1)=0.0d0
    a(nunk,2)=0.0d0
    a(nunk,3)=1.0d35
    a(nunk,4)=0.0d0
    a(nunk,5)=0.0d0
    qq=1.0d35*conc
!
! ...Assemble first row of R matrix (sediment)
!
    if (ucap .gt. 1) then
        r(1,1)= 0.0d0
        r(1,2)= 0.0d0
        r(1,3)= pors*dx/dt-(1-epsil)*(pors*vs/retard+alfa(1)*dx)
        r(1,4)= (1-epsil)*alfa(1)*dx
        r(1,5)= 0.0d0
    elseif (ucap.eq.1) then
        r(1,1)= 0.0d0
        r(1,2)= 0.0d0
        r(1,3)= pors*dx/dt-(1-epsil)*(pors*(vs+vscap)/2/retard+alfa(1)*dx)
        r(1,4)= (1-epsil)*alfa(1)*dx
        r(1,5)= 0.0d0
    elseif (ucap.eq.0) then
        r(1,1)= 0.0d0
        r(1,2)= 0.0d0
        r(1,3)= porscap*dx/dt-(1-epsil)*(porscap*vscap/retard+alfa(1)*dx)
        r(1,4)= (1-epsil)*alfa(1)*dx
        r(1,5)= 0.0d0
    endif
!
! ...assemble the second row of the R matrix (tube)
!
    r(2,1)= 0.0d0
    r(2,2)= (1-epsil)*alfa(1)*dx
    r(2,3)= port(1)*dx/dt-(1-epsil)*(port(1)*vt+alfa(1)*dx)
    r(2,4)= 0.0d0
    r(2,5)= 0.0d0

```

```

!
! ...assemble middle rows of R matrix (sediment)
!
! if (pecs.gt.2.0) then
!
! ...upwind weighting
!
do 60 i=3,nunk-3,2
  n=(i+1)/2
  nc=ucap-n
  if (nc.gt.0) then
    r(i,1)= (1-epsil)*pors*(ds/retard/dx+vs/retard)
    r(i,2)= 0.0d0
    r(i,3)= pors*dx/dt-(1-epsil)*(pors*(2*ds/retard/dx+vs/retard)+alfa(n)*dx)
    r(i,4)= (1-epsil)*alfa(n)*dx
    r(i,5)= (1-epsil)*pors*(ds/retard/dx)
  elseif (nc.eq.0) then
    r(i,1)= (1-epsil)*pors*(ds/retard/dx+vs/retard)
    r(i,2)= 0.0d0
    r(i,3)= pors*dx/dt-(1-epsil)*(pors*((ds+(ds+dscap)/2)/
      retard/dx+(vs+vscap)/2/retard)+alfa(n)*dx)
    r(i,4)= (1-epsil)*alfa(n)*dx
    r(i,5)= (1-epsil)*porscap*((ds+dscap)/2/retard/dx)
  elseif (nc.eq.-1) then
    r(i,1)= (1-epsil)*pors*((ds+dscap)/2/retard/dx+(vs+vscap)/2/retard)
    r(i,2)= 0.0d0
    r(i,3)= porscap*dx/dt-(1-epsil)*(porscap*((dscap+(ds+dscap)/2)/
      retard/dx+vscap/retard)+alfa(n)*dx)
    r(i,4)= (1-epsil)*alfa(n)*dx
    r(i,5)= (1-epsil)*porscap*(dscap/retard/dx)
  elseif (nc.lt.-1) then
    r(i,1)= (1-epsil)*porscap*(dscap/retard/dx+vscap/retard)
    r(i,2)= 0.0d0
    r(i,3)= porscap*dx/dt-(1-epsil)*(porscap*(2*dscap/retard/dx+vscap/retard)
      +alfa(n)*dx)
    r(i,4)= (1-epsil)*alfa(n)*dx
    r(i,5)= (1-epsil)*porscap*(dscap/retard/dx)
  endif
60 continue
else
!
! ...central weighting
!
do 72 i=3,nunk-3,2
  n=(i+1)/2
  nc=ucap-n

```

```

if (nc.gt.0) then
  r(i,1)= (1-epsil)*pors*(ds/retard/dx+vs/retard/2)
  r(i,2)= 0.0d0
  r(i,3)= pors*dx/dt-(1-epsil)*((pors*2*ds/retard/dx)+alfa(n)*dx)
  r(i,4)= (1-epsil)*alfa(n)*dx
  r(i,5)= (1-epsil)*pors*(ds/retard/dx-vs/retard/2)
elseif (nc.eq.0) then
  r(i,1)= (1-epsil)*pors*(ds/retard/dx+vs/retard/2)
  r(i,2)= 0.0d0
  r(i,3)= pors*dx/dt-(1-epsil)*((pors*(ds+(ds+dscap)/2)/retard/dx)-
    pors*((vs+vscap)/2-vs)/2/retard+alfa(n)*dx)
  r(i,4)= (1-epsil)*alfa(n)*dx
  r(i,5)= (1-epsil)*porscap*((ds+dscap)/2/retard/dx-(vs+vscap)/2/retard/2)
elseif (nc.eq.-1) then
  r(i,1)= (1-epsil)*pors*((ds+dscap)/2/retard/dx+(vs+vscap)/2/retard/2)
  r(i,2)= 0.0d0
  r(i,3)= porscap*dx/dt-(1-epsil)*((porscap*(dscap+(ds+dscap)/2)/retard/dx)-
    +porscap*(vscap-(vs+vscap)/2)/2/retard+alfa(n)*dx)
  r(i,4)= (1-epsil)*alfa(n)*dx
  r(i,5)= (1-epsil)*porscap*(dscap/retard/dx-vscap/retard/2)
elseif (nc.lt.-1) then
  r(i,1)= (1-epsil)*porscap*(dscap/retard/dx+vscap/retard/2)
  r(i,2)= 0.0d0
  r(i,3)= porscap*dx/dt-(1-epsil)*((porscap*2*dscap/retard/dx)+alfa(n)*dx)
  r(i,4)= (1-epsil)*alfa(n)*dx
  r(i,5)= (1-epsil)*porscap*(dscap/retard/dx-vscap/retard/2)
endif

72  continue
endif
!
! ...assemble middle rows of R matrix (tube)
!
do 62 i=4,nunk-2,2
  n=i/2
  r(i,1)= (1-epsil)*port(n-1)*(dm/dx+vt)
  r(i,2)= (1-epsil)*(alfa(n)*dx)
  r(i,3)= port(n)*dx/dt-(1-epsil)*(2*dm*port(n)/dx+port(n)*vt+alfa(n)*dx)
  r(i,4)= 0.0d0
  r(i,5)= (1-epsil)*port(n+1)*(dm/dx)
62  continue
!
! ...assemble last rows of R matrix for Dirichlet condition
!
do 64 j=1,5
  r(nunk-1,j)=0.0d0

```

```

      r(nunk,j)=0.0d0
64 continue
!
! ...Assemble s vector
!
do 66 i=1,nunk-1,2
  n=(i+1)/2
  b = xmax - x(n)
  s(i)=0.0d0
  s(i+1)=0.0d0
  if(b.le.biox) then
    s(i+1)=gamma*1.0d3*(k1*cfes(n)+k2)*dx
  endif
66 continue
!
! ...Decompose A matrix in 3 vectors of lenght neq*nn
!
!
do 68 ii=1,nn
  i=ii*4-3
  j=ii*2-1
  d1 (i) = a(j,1)
  d1 (i+1) = a(j,2)
  d1 (i+2) = 0.0d0
  d1 (i+3) = a(j+1,1)
  d2 (i) = a(j,3)
  d2 (i+1)= a(j,4)
  d2 (i+2)= a(j+1,2)
  d2 (i+3)= a(j+1,3)
  d3 (i) = a(j,5)
  d3 (i+1) = 0.0d0
  d3 (i+2) = a(j+1,4)
  d3 (i+3) = a(j+1,5)
68 continue
!
! ...start loop over time
!
ttime=0.0d0
sumups=0.0d0
sumlos=0.0d0
sumupt=0.0d0
sumlot=0.0d0
mdiss=0.0d0
mex=0.0d0
500 ttime=ttime+dt
tcheck=ttime-tmax

```

```

!
! ...if time > maximum time then stop
!
! if(tcheck.gt.1.0d-3) goto 999
!
! ...multiply out right-hand side to form the vector of knowns
!
! ...First node
!
f(1)=r(1,3)*c(1)+r(1,4)*c(2)+r(1,5)*c(3)+s(1)
if (alfa(1) .eq. 0.0d0) then
  f(2)=0.0d0
else
  f(2)=r(2,2)*c(1)+r(2,3)*c(2)+r(2,5)*c(4)+s(2)
endif
!
! Middle nodes
!
do 70 i=3,nunk-3,2
  n=(i+1)/2
  f(i)=r(i,1)*c(i-2)+r(i,2)*c(i-1)+r(i,3)*c(i)+      &
    r(i,4)*c(i+1)+r(i,5)*c(i+2)+s(i)
  if (alfa(n) .eq. 0.0d0) then
    f(i+1) = 0.0d0
  else
    f(i+1)=r(i+1,1)*c(i-1)+r(i+1,2)*c(i)+r(i+1,3)*c(i+1)+      &
      r(i+1,4)*c(i+2)+r(i+1,5)*c(i+3)+s(i+1)
  endif
70 continue
f(nunk-1)=qq
f(nunk)=qq
!
! ...solve the matrix
!
call Thomas(d2,d3,d1,f,c,neq,nn,nunk,nunk2)
!
! ...Calculate contaminant flux through upper boundary of sediment
! depending on the Peclet number
!
if (pecs.gt.2.0) then
  if (cap.eq.0) then
    fluxups=pors*(vs/retard*(c(nunk-3))-ds/retard*(c(nunk-1)-c(nunk-3))/dx)
  elseif (cap.eq.1) then
    fluxups=pors*(vs+vscap)/2/retard*(c(nunk-3))-1/retard*
      (dscap*porscap*c(nunk-1)-(ds+dscap)/2*pors*c(nunk-3))/dx
  elseif (cap.gt.1) then

```

```

fluxups=porscap*(vscap/retard*(c(nunk-3))-dscap/retard*
(c(nunk-1)-c(nunk-3))/dx)
endif
else
if (cap.eq.0) then
    fluxups=pors*(vs/retard*(c(nunk-1)+c(nunk-3))/2-ds/retard*(c(nunk-1)-
c(nunk-3))/dx)
elseif (cap.eq.1) then
    fluxups=1/retard*(vscap*porscap*c(nunk-1)+(vs+vscap)/2*pors*
c(nunk-3))/2-1/retard*(dscap*porscap*c(nunk-1)-
(ds+dscap)/2*pors*c(nunk-3))/dx
elseif (cap.gt.1) then
    fluxups=porscap*(vscap/retard*(c(nunk-1)+c(nunk-3))/2-
dscap/retard*(c(nunk-1)-c(nunk-3))/dx)
endif
endif
!
! ...Contaminant flux through lower boundary of sediment
!
fluxlos=pors*(-ds/retard*(c(3)-c(1))/dx)
!
! ...Contaminant flux through upper boundary of tube
!
ii=(nunk-2)/2
jj=(nunk)/2
fluxupt=((vt)*port(ii)*c(nunk-2)-dm*(port(jj)*c(nunk)-port(ii)*c(nunk-2))/dx)
!
! ...Contaminant flux through lower boundary (end of bioturbation zone)
!
b=xmax-biox
i=nint(b*2/dx)
j=i+2
ii=i/2
jj=j/2
fluxlot=(-dm*(port(jj)*c(j)-port(ii)*c(i))/dx)
!
! ...Sum of the mass flux to the upper and lower boudaries of sediment
!
sumups=sumups+dabs(fluxups)*area*dt
sumlos=sumlos+dabs(fluxlos)*area*dt
!
! ...Sum of the mass flux to the upper and lower boudaries of tube
!
sumupt=sumupt+dabs(fluxupt)*area*dt
sumlot=sumlot+dabs(fluxlot)*area*dt
!
```

```

! ...Contaminant flux exchanged between tube and sediment
!
    sumex = 0.0d0
    do 76 i=1,nn-1
        j=2*i-1
        n=2*i
        b = xmax - x(i)
        if(b.le.biox) then
            sumex=sumex+alfa(i)*(c(j)-c(n))*area*dx*dt
        endif
    76 continue
    mex = mex+sumex
!
! ...Contaminant mass "created" by source in the bioturbated zone
!
    sumdiss = 0.0d0
    do 78 i=1,nn-1
        n=2*i
        b = xmax - x(i)
        if(b.le.biox) then
            sumdiss=sumdiss+gamma*(1.0d3*(k1*cfes(i)+k2)-c(n))*dx*area*dt
        endif
    78 continue
    mdiss = mdiss+sumdiss
!
! ...check if ttime is desired for output
!
    nprint=0
    do 80 i=1,ntwant
        tcheck=twant(i)-ttime
        tcheck=dabs(tcheck)
        if (tcheck.lt.1.0d-4) nprint=1
    80 continue
!
! ...print the depths at which the concentrations are evaluated
!
    if(nprint.eq.1) then
        write(5,419)
419        format(/,24x,'X(m):',4x,\)
        do 82 i=1,nn
            write(5,420) x(i)
82        continue
420        format(4x,d12.5,\)
!
! ... print the time and the concentrations in the sediment
!
```

```

        write(5,434) ttime
434      format(/'Time(day):',d8.3,6x,'Cs:',6x,\)
        do 84 i=1,nunk-1,2
          write(5,435) c(i)
84        continue
435      format(4x,d12.5,\)
!
! ...print the concentrations in the tube
!
        write (5,436)
436      format (/,24x,'Ct:',6x,\)
        do 86 i=2,nunk,2
          write(5,437) c(i)
86        continue
437      format(4x,d12.5,\)
      end if
!
! ...Go back to beginning of time loop
!
      goto 500
!
! ...Print mass fluxes for sediment and tubes
!
999 write(5,440) sumups, sumlos, sumupt, sumlot
440 format(//,5x,'Mass leaving from the upper boundary of the sed.(ug):',t70,d12.5, &
           /,5x,'Mass leaving from the lower boundary of the sed.(ug):',t70,d12.5, &
           /,5x,'Mass leaving from the upper boundary of the tube (ug):',t70,d12.5, &
           /,5x,'Mass leaving from the lower boundary of the tube (ug):',t70,d12.5)
!
! ...Print mass flux that left from the upper bounadry at the end of the simulation
!
      sumup=sumups+sumupt
      write(4,446) sim, sumup
446      format(//,5x,'Simulation',t20 ,i4,                               &
           /,5x,'Mass leaving from the upper boundary (ug):',t70,d12.5)
!
! ...print surface concentration at the end of the simulation
!
      csurf=c(nunk-3)
      write(6,439)sim, csurf
439      format(//,5x,'Simulation',t20,i4,                               &
           /,5x,'Surface concentration in the sediment (ug/m3):',t70,d12.5)
!
! Mass balance
!
! ...Mass leaving the sediment by the boundaries

```

```

!
mouts=sumlos+sumups
!
! ...Mass leaving the tubes by the boundaries
!
moutt=sumlot+sumupt
!
! ...Mass      inside the column after simulation
!
mends=0.0d0
mendt=0.0d0
do 88 i=1, nunk-1,2
  n=(i+1)/2
  nc=ucap-n
  if (nc.ge.0.0d0) then
    mends=mends+c(i)*pors*area*dx
  else
    mends=mends+c(i)*porscap*area*dx
  endif
88 continue
do 90 i=2, nunk,2
  j=i/2
  mendt=mendt+c(i)*port(j)*area*dx
90 continue
balsed=min-s-mex-mouts-mends
baltub=mint+mdiss+mex-moutt-mendt
!
! ...Print the mass balance for sediment
!
write(5,442) mins, mends, mouts, mex, balsed
442 format(//,5x,'Diss mass of contaminant in sed. before simulation (ug):',t70,d12.5, &
           /,5x,'Diss mass inside the sediment after simulation (ug):',t70,d12.5,      &
           /,5x,'Diss mass which crossed the sediment boundaries (ug):',t70,d12.5,      &
           /,5x,'Diss mass exchanged with tube (ug):',t70,d12.5,                      &
           /,5x,'Balance for sediment:',t70,d12.5)
!
! ...Print the mass balance for sediment
!
write(5,444) mint, mendt, moutt, mex, mdiss, baltub
444 format(//,5x,'Diss mass of contaminant in tubes before simulation (ug):',t70,d12.5, &
           /,5x,'Diss mass inside the tubes after simulation (ug):',t70,d12.5,      &
           /,5x,'Diss mass which crossed the tubes boundaries (ug):',t70,d12.5,      &
           /,5x,'Diss mass exchanged with sediment (ug):',t70,d12.5,                  &
           /,5x,'Mass dissolved in the tube through oxigenation:',t70,d12.5,        &
           /,5x,'Balance for tube:',t70,d12.5)
!
```

```

        write(*,*) ''
        whatimeisit = CLOCK ()
        write(*,448) sim
448 format(1x,'Simulation ',i5,' endet at ')
        write(*,*) whatimeisit
        write(*,*) ''
        return
        end

!
!*****...SUBROUTINE Thomas, solves the block tridiagonal matrix.
!
!*****SUBROUTINE Thomas(a,b,c,d,unew,neq,nn,nunk,nunk2)
implicit none
double precision sum
double precision a, b, c, d, unew, w, qq, wtemp, g, z
integer i, ii, ia, ic, icc, icc2, ivar1, ivar2, j, k, kcc,
kk, neq2, neq, nn, nunk, nunk2
parameter (neq2=4)
dimension a(nunk2), b(nunk2), c(nunk2), d(nunk), unew(nunk),
w(nunk2), qq(nunk2), wtemp(neq2), g(nunk), z(neq2)
!
!...First, perform decomposition
!
DO 11 i=1,neq2
    w(i)=a(i)
11 CONTINUE
!
!...Invert w
!
DO 31 ic=2,nn
    icc=(ic-2)*neq2
    CALL Invert(w,wtemp,neq,icc,nunk2)
!
DO 27 i=1,neq
    ii=(i-1)*neq
    DO 25 j=1,neq
        sum=0.0d0
        DO 23 k=1,neq
            kk=(k-1)*neq
            sum=sum+ wtemp(ii+k)*b(icc+j+kk)
23    CONTINUE
            qq(icc+ii+j)=sum
25    CONTINUE

```

```

27    CONTINUE
!
    DO 37 i=1,neq
        ii=(i-1)*neq
        DO 35 j=1,neq
            sum=0.0d0
            DO 33 k=1,neq
                kk=(k-1)*neq
                sum=sum+ c(icc+neq2+ii+k)*qq(icc+j+kk)
33    CONTINUE
        w(icc+neq2+ii+j)=a(icc+neq2+ii+j)-sum
35    CONTINUE
37    CONTINUE
31    CONTINUE
!
!      ...Perform forward substitution
!
!      ...Invert the first w block.
!
    icc=0
    CALL Invert(w,wtemp,neq,icc,nunk2)
    DO 45 i=1,neq
        ii=(i-1)*neq
        sum=0.0d0
        DO 43 k=1,neq
            sum=sum+ wtemp(ii+k)*d(k)
43    CONTINUE
        g(i)=sum
45    CONTINUE
        DO 131 ic=2,nn
            icc=(ic-2)*neq
            kcc=(ic-1)*neq2
!
!      ...Invert w
!
    CALL Invert(w,wtemp,neq,kcc,nunk2)
!
    DO 55 i=1,neq
        ii=(i-1)*neq
        sum=0.0d0
        DO 53 k=1,neq
            sum=sum+ c(kcc+ii+k)*g(icc+k)
53    CONTINUE
        z(i)=d(icc+neq+i)-sum
55    CONTINUE
        DO 65 i=1,neq

```

```

ii=(i-1)*neq
sum=0.0d0
DO 63 k=1,neq
    sum=sum+ wtemp(ii+k)*z(k)
63      CONTINUE
        g(icc+neq+i)=sum
65      CONTINUE
131 CONTINUE
!
! ...Perform backward substitution
!
ia=(nn-1)*neq+1
DO 71 i=ia,nn*neq
    unew(i)=g(i)
71 CONTINUE
    ivar1=(nn-1)*neq
    ivar2=(nn-1)*neq2
    DO 231 ic=1,nn-1
        icc=ivar1-ic*neq
        icc2=ivar2-ic*neq2
    DO 95 i=1,neq
        ii=(i-1)*neq
        sum=0.0d0
        DO 93 k=1,neq
            sum=sum+ qq(icc2+ii+k)*unew(icc+neq+k)
93      CONTINUE
        unew(icc+i)=g(icc+i)-sum
95      CONTINUE
231 CONTINUE
    RETURN
END
*****
!
! ...SUBROUTINE for matrix inversion
!
*****
SUBROUTINE Invert(w,ainv,neq,icc,nunk2)
implicit none
    double precision aa,ainv, w, u, vi, y, l
    double precision sum
    integer i, ic, ii, in, in1, j, jj, k, kk, neq, neq2, icc, nunk2
    parameter    (neq2=4)
    dimension    aa(neq2), ainv(neq2), w(nunk2), u(neq2), vi(neq),
                y(neq), l(neq2)
!
! ...Set aa equal to part of w to invert

```

```

!
DO 5 i=1,neq*neq
  aa(i)=w(icc+i)
5 CONTINUE
!
!      ...Initialize upper part of l and lower part of u to zero.
!      and diagonal of u to one.
!
DO 9 i=1,neq
  ii=(i-1)*neq
  DO 7 j=1,neq
    IF(i.EQ.j) u(ii+j)=1.0d0
    IF(i.LT.j) l(ii+j)=0.0d0
    IF(i.GT.j) u(ii+j)=0.0d0
7   CONTINUE
9 CONTINUE
!
!      ...Find matrices l and u.
!
DO 121 j=1,neq
  jj=(j-1)*neq
  DO 113 i=j,neq
    sum=0.0d0
    ii=(i-1)*neq
    IF(j.EQ.1) THEN
      l(ii+j)=aa(ii+j)
    ELSE
      DO 111 k=1,j-1
        kk=k-1
        sum=sum + l(ii+k)*u(kk*neq+j)
111    CONTINUE
      l(ii+j)=aa(ii+j) - sum
    END IF
113  CONTINUE
    IF(j.LT.neq) THEN
      DO 117 i=j+1,neq
        sum=0.0d0
        ii=i-1
        IF(j.EQ.1) THEN
          u(i)=aa(i)/l(1)
        ELSE
          DO 115 k=1,j-1
            kk=k-1
            sum=sum + l(jj+k)*u(kk*neq+i)
115    CONTINUE
          u(jj+i)=(aa(jj+i)-sum)/l(jj+j)
        END IF
      END DO
    END IF
  END DO
121

```

```

        END IF
117  CONTINUE
        END IF
121  CONTINUE
!
!      ...Find inverse of aa.
!
!      Use vector of identity matrix as r.h.s to find
!      consecutive columns of aa'.
!      l u a' = i
!      l y = vi
!      u va' = y
!      where va' is a column of aa'.
!
!      DO 101 ic=1,neq
!
!      ...Initialize vector of i.
!
DO 135 j=1,neq
  IF(ic.EQ.j) THEN
    vi(j)=1.0d0
  ELSE
    vi(j)=0.0d0
  END IF
135 CONTINUE
!
!      ...Perform forward substitution
!
y(1)=vi(1)/l(1)
  DO 151 i=2,neq
    ii=i-1
    sum=0.0d0
    DO 145 k=1,ii-1
      sum=sum+ l(ii*neq+k)*y(k)
145    CONTINUE
    y(i)=(vi(i)-sum)/l(ii*neq+i)
151    CONTINUE
!
!      ...Perform backward substitution
!
ainv(neq*neq-neq+ic)=y(neq)
  DO 161 i=2,neq
    in=neq-i+1
    ii=(neq-i)*neq
    sum=0.0d0
    DO 155 k=in+1,neq

```



```

!*****
!
!      Framework for Monte Carlo simulation using TRANSCAP-1D
!
!*****
!
!
!
!      Arrays
!
!
!      cfes : vector of concentration of FeS (umol/g)
!      twant : vector of desired time(s) for output
!      x : vector of nodal coordinates (m)
!
!
!      Variables
!
!
!      Real
!
!
!      alfa1, alfa2: irrigation coefficients (1/day & 1/m)
!          alfa = alfa1*exp(alfa2*(x-xmax))
!      area : column area (m**2)
!      biox : maximum depth of bioturbation (m) (has to be a multiple of dx!)
!      k1, k2 : coefficients of linear dissolution equation
!      conc : concentration at the water/sediment interface (ug/m**3)
!      diff : effective diffusion coefficient (m**2/day)
!      dm : molecular diffusion
!      disp : dispersivity (m)
!      dt : time increment (day)
!      dx : distance increment (m)      (homogeneous grid!)
!      epsil : time weighting factor (normally =1)
!      gamma : cinetic coefficient for dissolution reaction
!      pors : sediment porosity
!      porscap : cap sediment porosity
!      port0 : tube porosity at the surface of the sediment
!          port=port0*exp(alfa2*(x-xmax))
!      qs : advective flow in sediment (m**3/day)
!      retard : retardation coefficient           retard = 1+rho*xkd/pors
!      tmax : maximum simulation time (day)
!      vt : average water velocity in tube (m/day)
!      xmax : lenght of column (m)
!      r1 : inner radius of tubes/burrows
!      r2 : half the distance between two tubes/burrows
!      dp : depth of bioturbation
!      d : distance from the burrow axis to the point where the concentration equals
!          the horizontally integrated value
!
```

```

!
! Distribution parameters:
!           ..dist(1)  ..dist(2)
!   if ..distyp=1=UNIFORM      minimum    maximum
!   if ..distyp=2=NORMAL       mean       variance
!   if ..distyp=3=EXPONENTIAL mean       translation
!
!
! Integer
!
! ntub :      number of tubes pro square meter
! nn : number of nodes
! neq : number of equations per node (tube + sediment)
! nunk : number of unknowns
! ntwant : number of desired time output
! nsim : number of desired montecarlo simualtions
! mc : if mc=0 then perform only one deterministic simulation
!       if mc>0 then perform montecarlo simulation
!
!
! Input parameters
!
! line 1 : tmax, dt, xmax, dx, capdx
! line 2 : area, qs, pors, porscap
! line 3 : disp, diff, dm, epsilon,
! line 4 : gamma, k1, k2, r1
! line 5 : ntwant
! line 6 : twant (1) --> twant(ntwant)
! line 7 : conc
! line 8 : cs(1) --> cs(nn)
! line 9 : ct(1) --> ct(nn)
! line 10 : cfes(1) à cfes (nn)
! line 11 : mc
! line 12 : nsim
!
!     if montecarlo = 1
!
! line 13 : vt -> disttyp, dist(2), iseed
! line 14 : rt -> disttyp, dist(2), iseed
! line 15 : ntub -> disttyp, dist(2), iseed
! line 16 : dp -> disttyp, dist(2), iseed
!
!     if montecarlo = 0
!
! line 13 : vt
! line 14 : retard

```

```

! line 15 : alfa1, port0
! line 16 : alfa2, biox
!
!
!*****
!
program montecarlo
!
! ...define global variables
!
common alfa1, alfa2, area, biox, capdx, &
      k1, k2, conc, dm, disp, diff, dp, dt, dx, epsil, &
      gamma, pors, porscap, port0, qs, retard, &
      tmax, vt, xmax
double precision alfa1, alfa2, area, biox, capdx, &
      k1, k2, conc, dm, disp, diff, dp, dt, dx, epsil, &
      gamma, pors, porscap, port0, qs, retard, &
      tmax, vt, xmax
common sim, nsim, ntwant, nn, AllocateStatus, mc
      integer sim, nsim, ntwant, nn, AllocateStatus, mc
common title
character *80 title
!
! ...define local variables
!
double precision r1, r2, bx, d, pi
double precision, dimension(:), allocatable :: x, cfes, &
      cs, ct, twant, vtran, rtran, ntran, dpran, ranvec
double precision dist(2)
integer i, j, ii, disttyp, iseed, ntub
parameter (d = 0.0026)
parameter (pi = 3.14159265358987)
!
! ...open the working files
!
open(3, file='mcinput.dat')
open(4, file='mcflux.out')
open(5, file='mcoutput.out')
open(6, file='mccsurf.out')
!
! ...read the input
!
read(3, 300) title
300 format(a80)
read(3,*) tmax, dt, xmax, dx, capdx
read(3,*) area, qs, porscap

```

```

read(3,*) disp, diff, dm, epsil
read(3,*) gamma, k1, k2, r1
!
! ...calculate number of nodes
!
nn = int(xmax/dx)
!
! ...read number for desired output(s)
!
read(3,*) ntwant
!
! ...allocate the memory for the arrays
!
allocate(x(nn), cs(nn), ct(nn), cfs(nn), stat = AllocateStatus)
  if (AllocateStatus /= 0) stop "***Not enough memory***"
allocate(twant(ntwant), stat = AllocateStatus)
  if (AllocateStatus /= 0) stop "***Not enough memory***"
!
! ...read time(s) for desired output(s)
!
read(3,*) (twant(i), i=1,ntwant)
!
! ...assign the first nodal x-coordinates
!
x(1)= dx/2
!
! ...assign nodal coordinates
!
do 10 i=1,nn-1
  x(i+1)=x(i)+dx
10 continue
!
! ...read value of concentration at the sediment-water interface
!
read(3,*) conc
!
! ...read initial concentrations for sediment
!
read(3,*) (cs(i), i=1,nn)
!
! ...read initial concentrations for tube
!
read(3,*) (ct(i), i=1,nn)
!
! ...read concentration of FeS at each node
!
```

```

    read(3,*) (cfes(i), i=1,nn)
!
! ...choose wheather or not want to do a montecarlo simulation
!
    read(3,*) mc
!
! ...read number of desired simulations
!
    read(3,*) nsim
!
! ...if not montecarlo simulation then nsim=1
!
    if (mc.eq.0) then
        nsim=1
    endif
!
! ...allocate the memory for the arrays containing random numbers
!
    allocate(ranvec(nsim), vtran(nsim), rtran(nsim),
             ntran(nsim), dpran(nsim), stat = AllocateStatus) &
    if (AllocateStatus /= 0) stop "***Not enough memory***"
!
! ...Write title of the simulation
!
    write(4,404) title
    write(5,404) title
    write(6,404) title
404 format(//,60('*'),/5x,'1D finite volume solution of the ', &
           'transport equation',/5x, a80,/60('*'),//)
!
! ... if montecarlo simulation then...
!
    if (mc.gt.0) then
!
! ...read distribution parameters
!
        do 12 i= 1,4
            read (3,*) disttyp
            read (3,*) dist(1), dist(2)
            read (3,*) iseed
            do 14 j=1,nsim
                ranvec(j)= 0.0d0
14        continue
!
! ...calculate random numbers for the distribution

```

```

!      and put them in different vectors
!
!      call randist(disttyp,dist,iseed,nsim,ranvec)
        if (i.eq.1) then
          vtran=ranvec
        elseif (i.eq.2) then
          rtran=ranvec
        elseif (i.eq.3) then
          ntran=ranvec
        elseif (i.eq.4) then
          dpran=ranvec
        endif
12    continue
!
! ...do montecarlo simulations with random parameters
!
!
!      do 10000 sim=1,nsim
        vt=vtran(sim)
        retard=rtran(sim)
        ntub=NINT(ntran(sim))
        dp=dpran(sim)
!
        r2=1/sqrt(REAL(ntub))/2
        alfa1=2*diff*r1/((r2**2-r1**2)*(d-r1))
        port0=pi*(r1**2)*dx*ntub
        bx=dp/dx
        biox=NINT(bx)*dx
        if (biox.le.0) then
          biox=dx
        endif
        alfa2=-DLOG(alfa1/100)/biox
!
        call solution(x, cfe, cs, ct,twant)
10000 continue
!
! ..if the user doesn't choose montecarlo carry out only one simulation
!
!
!      elseif (mc.eq.0) then
!
! ...read input
!
        read (3,*) vt
        read (3,*) retard
        read (3,*) alfa1, port0

```

```
    read (3,*) alfa2, biox
!
!      call solution(x, cfes, cs, ct,twant)
!
else
    write(*,*) 'Error: variable montecarlo must be a positive integer or 0'
    stop
endif
end
```

```

!*****
!
! This subroutine returns a vector containing a random variable
! with the given distribution type.
!
!*****
!
! subroutine randist(distyp,dist,iseed,nsim,ranvec)
!
! implicit real*8(a-h,o-z)
! implicit integer*4(i-n)
! double precision ranvec(nsim)
!
! ARGUMENTS:
!
! INPUT:
!
! type of distribution
!
! integer*4 distyp
!
! distribution parameters:
!
! real*8 dist(2)
!           dist(1)      dist(2)
!           if distyp=1=UNIFORM   minimum   maximum
!           if distyp=2=NORMAL    mean      variance
!           if distyp=3=EXPONENTIAL mean      translation
!
!*****
!
! LOCAL DECLARATIONS:
!
!
! real*8 ran3
! real*8 p
! integer*4 i, j
!
!*****
!
! ...read the input
!
do 10 j=1,nsim
  if(distyp .eq. 1) then
    ranum=dist(1)+(dist(2)-dist(1))*dble(ran3(iseed))
!was    ranum=dist(1)+(dist(2)-dist(1))*dble(rand())

```

```

!cc      ranum=dist(1)+(dist(2)-dist(1))*ran1(iseed)
elseif(distyp .eq. 2) then
    p=0.0d0
    do 100 i=1,12
        p=p+dble(ran3(iseed))
!cc      p=p+ran1(iseed)
!was    p=p+dble(rand())
100    continue
        ranum=dsqrt(dist(2))*(p-6.0d0)+dist(1)
elseif(distyp .eq. 3) then
    p=-dabs(dist(1)-dist(2))*dlog(1.0d0-dble(ran3(iseed)))
!was    p=-dabs(dist(1)-dist(2))*dlog(1.0d0-dble(rand()))
!cc      p=-dabs(dist(1)-dist(2))*dlog(1.0d0-ran1(iseed))
    if(dist(1) .gt. dist(2)) then
        ranum=dist(2)+p
    else
        ranum=dist(2)-p
    endif
endif
ranvec(j)=ranum
!
!      If you don't want the random number to be negative
!
!      ranvec(j)= dabs(ranum)
!
10    continue
      return
end

```

```

!*****
!
! This function returns a random variable
!
!*****
real*8 FUNCTION RAN3(IDUM)
implicit real*8(a-h,o-z)
integer*4 MA(55)
real*8 fac
integer*4 mbig,mseed,iff,mz,mj,mk,ii,inext,inextp,idum
save inext,inextp,ma
DATA IFF /0/
MBIG=1000000000
MSEED=161803398
MZ=0
FAC=1.E-9
IF(IDUM.LT.0.OR.IFF.EQ.0)THEN
  IFF=1
  MJ=MSEED-IABS(IDUM)
  MJ=MOD(MJ,MBIG)
  MA(55)=MJ
  MK=1
  DO 11 I=1,54
    II=MOD(21*I,55)
    MA(II)=MK
    MK=MJ-MK
    IF(MK.LT.MZ)MK=MK+MBIG
    MJ=MA(II)
11  CONTINUE
DO 13 K=1,4
  DO 12 I=1,55
    MA(I)=MA(I)-MA(1+MOD(I+30,55))
    IF(MA(I).LT.MZ)MA(I)=MA(I)+MBIG
12  CONTINUE
13  CONTINUE
INEXT=0
INEXTP=31
IDUM=1
ENDIF
INEXT=INEXT+1
IF(INEXT.EQ.56)INEXT=1
INEXTP=INEXTP+1
IF(INEXTP.EQ.56)INEXTP=1
MJ=MA(INEXT)-MA(INEXTP)
IF(MJ.LT.MZ)MJ=MJ+MBIG
MA(INEXT)=MJ

```

```
RAN3=MJ*FAC  
RETURN  
end
```